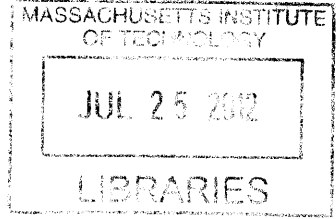


**Nuclear-Renewables Energy System for Hydrogen
and Electricity Production**

ARCHIVES



by

Geoffrey Haratyk

Ingénieur de l'Ecole Polytechnique (2009)

Submitted to the Department of Nuclear Science and Engineering
in partial fulfillment of the requirements for the degree of

Master of Science in Nuclear Science and Engineering

at the

MASSACHUSETTS INSTITUTE OF TECHNOLOGY

June 2011

© Massachusetts Institute of Technology 2011. All rights reserved.

Author
Department of Nuclear Science and Engineering
May 6th, 2011

Certified by
Charles W. Forsberg
Research Scientist
Thesis Supervisor

Certified by
Michael J. Driscoll
Professor Emeritus of Nuclear Engineering
Thesis Reader

Accepted by
Mujid S. Kazimi
TEPCO Professor of Nuclear Engineering
Chair, Department Committee on Graduate Students

Nuclear-Renewables Energy System for Hydrogen and Electricity Production

by

Geoffrey Haratyk

Submitted to the Department of Nuclear Science and Engineering
on May 6th, 2011, in partial fulfillment of the requirements for the degree of
Master of Science in Nuclear Science and Engineering

Abstract

Climate change concerns and expensive oil call for a different mix of energy technologies. Nuclear and renewables attract attention because of their ability to produce electricity while cutting carbon emissions. However their output does not match demand. This thesis introduces a nuclear-renewables energy system, that would produce electricity and hydrogen on a large scale while meeting the load demand.

The system involves efficient high temperature electrolysis (HTE) for hydrogen production, with heat provided by nuclear and electricity by the grid (nuclear and/or renewables). Hydrogen production would be variable, typically at time of low demand for electricity and large power generation from renewables. Hydrogen would be stored underground on site for later shipping to industrial hydrogen users by long-distance pipeline or for peak power production in fuel cells.

A hydrogen plant was designed, and the economics of the system were evaluated by simulating the introduction of the system in the Dakotas region of the United States in both a regulated and a deregulated electricity market. The analysis shows that the system is economically competitive for a high price of natural gas (\$12-13 MMBtu) and a capital cost reduction (33%) of wind turbines. The hydrogen production is sufficient to supply the current demand of the Great Lakes refineries. With today's electricity prices, a competitive production cost of \$1.5 /kg hydrogen is achievable.

The analysis indicates large economic incentives to develop HTE systems that operate efficiently in reverse as fuel cells to displace the gas turbines that operate only a few hundred hours per year and thus have high capital cost charges. The capital cost of the HTE system has a significant impact on system economics, with large incentives to develop reversible HTE/ FC systems to reduce those costs.

Such a system would expand the use of nuclear beyond electricity generation, and allows a larger penetration of renewables by providing an energy storage media and bringing flexibility to the grid operators.

Thesis Supervisor: Charles W. Forsberg
Title: Research Scientist

Acknowledgments

I would like to thank my advisor Dr Charles W. Forsberg for all his support during this research project. The main idea behind this thesis is from him and he completely trusted me to implement it. He pushed me beyond what I thought I could do, for example to write scientific papers. Always available and very knowledgeable, he could not have been better advisor.

It is an honor to have Dr Michael J. Driscoll as my thesis' reader, and I'm glad he accepted. It was always a pleasure to discuss with him and thank him for his advice.

I am also thankful to people who helped me at different moments: Dr Stephen Herring and the high temperature electrolysis team from Idaho National Laboratory, Dr Mujid Kazimi (MIT), Dr Carlos Battle (MIT), Dr Ruth Knibbe (Risø National Laboratory) and Dr Bilge Yildiz (MIT).

More generally I would like to thank MIT and the department of NSE for having me during these two years. I learned a lot in contact with prestigious professors and friendly students from all around the world. I have a special thought for Dr Mujid Kazimi, my academic advisor.

This research was partly funded by AREVA, which we acknowledge for their financial support.

I would not be here without having attended Ecole Polytechnique, and am very grateful to France for the excellent education it provided to me.

Finally I'd like to cite my parents and my sister Laurene for their support. It was hard for them to see me leave France, but they always respected my choices.

Table of Contents

Abstract	3
Acknowledgments	5
Table of Contents	7
List of Figures	11
List of Tables	15
Introduction	17
0.1 Motivation	17
0.2 Objectives	20
0.3 Outline of the thesis	22
1 Description of the system	23
1.1 Location and Markets	23
1.2 High Temperature Electrolysis / Fuel Cell	26
1.3 Wind Power	29
1.4 Nuclear Reactor	31
1.5 Hydrogen Underground Storage Facility	32
1.6 Hydrogen Pipeline	34
1.7 Comparison with other energy storage technologies	35
2 Hydrogen plant	37

2.1	Hydrogen Plant Design	37
2.1.1	General layout	38
2.1.2	Tritium contamination	40
2.1.3	Water requirements	41
2.1.4	Oxygen sales	42
2.2	Hydrogen Production Performance	43
2.2.1	Electrolysis cell model	43
2.2.2	Overload mode	48
2.2.3	Hydrogen plant model	48
2.2.4	Results	50
3	Economic analysis - regulated market	57
3.1	Methodology and assumptions	57
3.1.1	Electricity demand and wind data	58
3.1.2	Electricity generation technologies	60
3.1.3	Generation dispatch modelling	61
3.2	Example	62
3.3	Preliminary study - no hydrogen generation	64
3.3.1	Wind power capacity	64
3.3.2	Cost of fossil fuel (natural gas)	67
3.3.3	Carbon emission	70
3.4	Parametric studies with nuclear-hydrogen system	70
3.4.1	New assumptions	71
3.4.2	Results	80
3.5	Summary	89
4	Economic analysis - deregulated market	93
4.1	Methodology	94
4.2	Results	96
4.2.1	Hydrogen production	96
4.2.2	Electricity production	98

4.3	Sensitivity analyses	99
4.3.1	Cost of hydrogen	99
4.3.2	Electricity production	100
4.4	Perspectives	101
4.5	Summary	102
	Conclusion	105
	Appendix A: MATLAB code for electrolyzer performance calculation	111
	Appendix B: Statoil alkaline electrolyzers	135
	References and Bibliography	137

List of Figures

0-1	Example of mismatch between electricity demand and wind power generation (Week of August 2010, Midwest ISO grid)	18
0-2	The wind resources in the US are far from the energy consumption areas of the East- and West coasts	18
0-3	A possible location of the nuclear-wind energy system: the Dakotas, between Alberta and the Great Lakes region	20
0-4	The energy system in both modes of operation	21
1-1	US wind resource map	24
1-2	The reliability region of MISO	26
1-3	Energy requirements to electrolyze water decreases with the steam temperature	27
1-4	A cross section view of a Solid Oxide Electrolysis Cell (courtesy of Idaho National Laboratory)	27
1-5	Example of high temperature electrolysis modules (courtesy of INL) .	28
1-6	Operating hours per year for electricity peaking plants in MISO (2009)	29
1-7	Capacity factor of Dakotas wind turbines, 2008-2009	30
1-8	Direct coupling between the nuclear reactor's secondary loop and the hydrogen plant (Areva EPR operating conditions)	32
1-9	Chevron-Phillips Clemens Terminal	33
1-10	Location of the major salt deposits in the US	34
1-11	Energy storage options capabilities (after [33])	36
2-1	Hydrogen plant diagram - HTE mode only	39

2-2	Schematic of the 1-D cell model	43
2-3	Molar fractions desired in the cells	46
2-4	Qualitative degradation rate of the cells vs current density, for <i>ASR</i> = 0.25 $\Omega\cdot\text{cm}^2$	49
2-5	Flowsheet in a hydrogen plant coupled to a 300 MWe PWR - Normal mode of production	51
2-6	Heat and energy balance in normal mode - example of a 300 MWe nuclear-hydrogen plant	52
2-7	Flowsheet in a hydrogen plant coupled to a 300 MWe PWR - Overload mode of production	54
2-8	Heat and energy balance in overload mode - example of a 300 MWe nuclear-hydrogen plant	55
2-9	Hydrogen production performance of the plant (300 MWe nuclear re- actor size)	55
3-1	Hourly load of the MISO grid in 2009 (in GW)	58
3-2	Hourly wind power output (MW) of a 1MW wind turbine in North Dakota (2009)	59
3-3	Example of generation dispatch, last week of June 2009	62
3-4	Electricity generation breakdown for the reference case	64
3-5	Excess electricity vs wind power capacity	65
3-6	Global LCOE vs wind power capacity	66
3-7	Effect of wind subsidies on global LCOE	67
3-8	Effect of wind power cost reduction on global LCOE	68
3-9	Equivalence between natural gas price and carbon cost	69
3-10	Effect of natural gas price on the global LCOE	69
3-11	Carbon emission by the grid vs wind power capacity	70
3-12	Flowsheet of the hybrid system while producing hydrogen	71
3-13	Typical LCOH breakdown	73
3-14	LCOH vs electricity price and degradation rate	74

3-15 LCOH vs electricity price and capital cost	75
3-16 LCOE vs hybrid nuclear capacity and price of excess electricity . . .	76
3-17 LCOE vs wind capacity and price of excess electricity	76
3-18 Generation dispatch with hydrogen plant - example of the last week of June 2009	78
3-19 Power converted for hydrogen production - example of the last week of June 2009	79
3-20 Excess wind electricity (GW-year) without hydrogen production . . .	80
3-21 Residual excess wind electricity (GW-year) with hydrogen production	81
3-22 Total hydrogen production (million MT /yr)	82
3-23 Fuel cell operation time (hours /yr)	83
3-24 Net hydrogen production (million MT /yr)	84
3-25 LCOH (\$ /kg) vs wind power and hybrid nuclear capacity	85
3-26 Correlation between NG price and hydrogen production cost (in 2010 US \$)	86
3-27 LCOE (\$ /MWh) vs wind power and hybrid nuclear capacity	87
3-28 Relative total profit (billion \$ /yr)	88
3-29 Electricity generation breakdown	90
3-30 Hydrogen production cost breakdown	91
4-1 Operation modes of the hydrogen plant in a liberalized electricity market	95
4-2 Hydrogen production by a 300MWe nuclear-hydrogen plant in a liber- alized market	97
4-3 LCOH breakdown for the optimized case in a liberalized market . . .	97
4-4 Impact of natural gas price on hydrogen production cost (steam methane reforming process)	98
4-5 Sensitivity of the hydrogen cost to the assumptions as compared to the base case (\$1.51/kg)	100
4-6 Fuel cell electricity cost and operation time for a price of hydrogen of \$1.7/kg	101

4-7	Fuel cell electricity cost and operation time for a price of hydrogen of \$1.5/kg	101
5-1	300-MWe nuclear-hydrogen plant performance	106
B-1	Statoil alkaline electrolyzer (courtesy of Statoil Hydrogen)	136

List of Tables

1.1	Monthly relative net hydrogen production - example	33
2.1	1-D electrolysis cell model summary	47
2.2	Assumptions used for the calculation of hydrogen plant performance .	50
2.3	HTE cell operating conditions	53
3.1	Main features of the MISO load in 2009	59
3.2	Cost of generating electricity (2010 US \$)	60
3.3	LCOE formulas (2010 US \$)	61
3.4	Power capacities in the reference case	63
3.5	Fuel cost for CCGT in the reference case	63
3.6	Results of the reference case dispatch	63
3.7	Power capacities for the preliminary study	64
3.8	Fuel cost for CCGT for the preliminary study	65
3.9	Hydrogen production by hybrid nuclear system	71
3.10	Assumptions for LCOH calculation	72
3.11	Hydrogen storage and transportation cost assumptions	72
3.12	Assumptions relative to fuel cells	77
3.13	Summary - system benefits	90
4.1	Assumption for LCOH calculation	96
4.2	Assumptions for p_s calculation	99

Introduction

0.1 Motivation

Climate change concerns and expensive prices of oil may restrict fossil fuel use in the mid- and long-term future. Fossil fuels are however the main source of energy production today, and by far. They are easy to store, and the capital costs of equipment to convert fossil fuel to heat, hydrogen, or electricity are low. These characteristics enable the use of fossil fuel to economically produce energy at variable rates to match demand.

In a low-carbon world, all the major alternative energy technologies (fossil with carbon dioxide sequestration, nuclear, solar, wind, hydro) have high capital costs and low operating costs, which favors operation of such plants at maximum output to be economical. Among these technologies, renewable energy sources, namely wind and solar, have variable or intermittent generation pattern that does not match demand (Figure 0-1). Moreover, the best location for large-scale, long-term viable renewables are far from major energy consumption areas (Figure 0-2).

These observations call for energy storage technologies, that would fully utilize capital intensive generating technologies and intermittent energy sources while meeting variable energy outputs. At the scale of an electrical grid, large amounts of storage capacity are required to account for the seasonal, daily, and hourly variations in demand as well as intermittent generation.

On the other hand hydrogen demand is likely to increase dramatically in the future - independent of whether it is used to directly fuel vehicles. The primary uses of hydrogen today are (1) the upgrading of heavy oils and oil sands to gasoline and

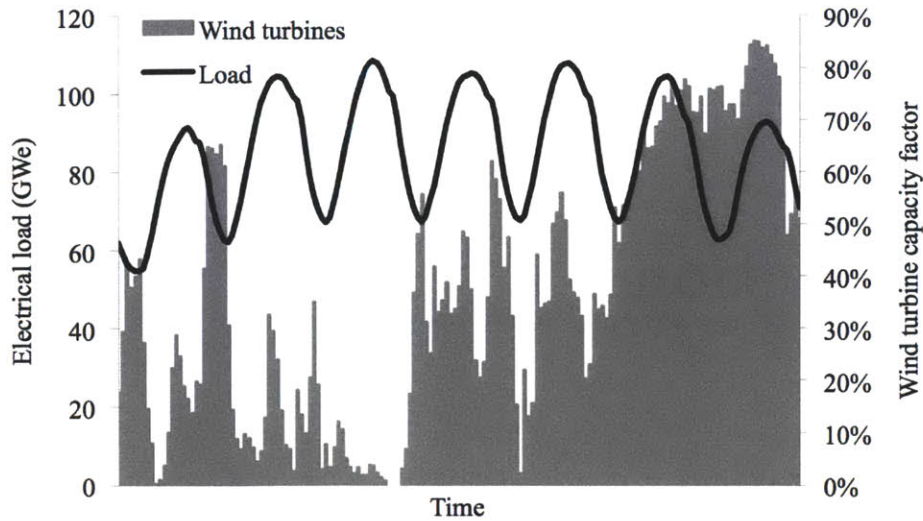


Figure 0-1: Example of mismatch between electricity demand and wind power generation (Week of August 2010, Midwest ISO grid)

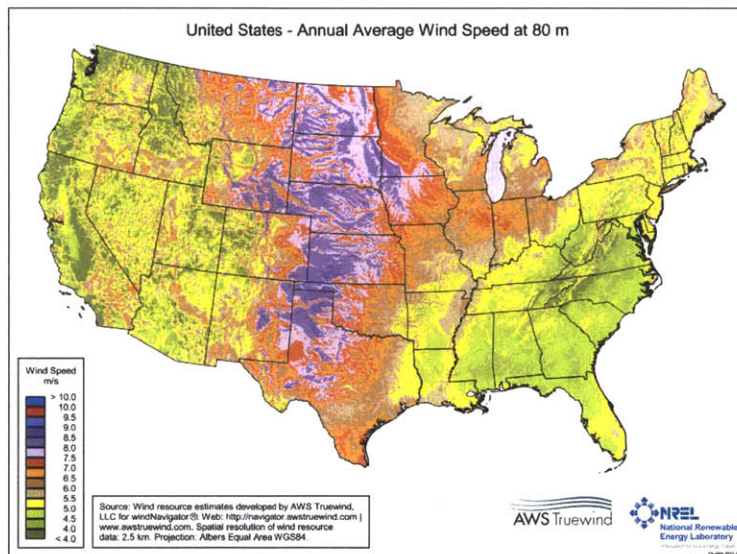


Figure 0-2: The wind resources in the US are far from the energy consumption areas of the East- and West coasts

diesel fuels (~50%) and (2) fertilizer production (~33%). Future large-scale hydrogen markets may include liquid fuels production from biomass and conversion of metal ores to metals. These applications imply large hydrogen demands in a few specific locations and markets for pipeline transport of hydrogen from areas where hydrogen can be produced inexpensively.

The recent and promising development of High-Temperature Electrolysis (HTE), a carbon-free process producing hydrogen and oxygen out of steam/ water at high temperature, motivates us to consider it in the big picture described previously. It might be the key technology to manage the issues previously described. A HTE hydrogen plant, coupled to a nearby nuclear unit and to the grid, would indeed:

- enable operation of the nuclear unit at base-load capacity with the steam used to produce variable amounts of electricity and hydrogen. Depending upon the local electricity demand, the steam would be sent to the turbine to produce electricity or to the hydrogen plant to produce hydrogen.
- regulate the intermittent and unpredictable generation of power from renewables so that power supply equals demand. The excess electricity from renewables at times of large output and/or low demand for electricity would be converted by the HTE cells into hydrogen. The renewables energy source would operate at full capacity at all times.
- provide a dense energy carrier in the form of hydrogen. Pipelines could ship hydrogen from the best places for renewable electricity (high Great Plains in the Dakotas for wind) to major electricity markets or major hydrogen markets (Oil sands of Alberta [Canada], refineries in Chicago and Houston, and future biorefineries in the central Midwest).
- create an opportunity for electricity storage. Hydrogen, stored on site, could be used in the HTE cells used in reverse as fuel cells to generate electricity. The hydrogen plant would hence become a power production unit at time of peak demand.

The different technologies considered, i.e. nuclear, wind, HTE and hydrogen storage and transportation, combine attractively to offer a large energy system that is sustainable, carbon-free and flexible for grid operators. The concern is now to assess

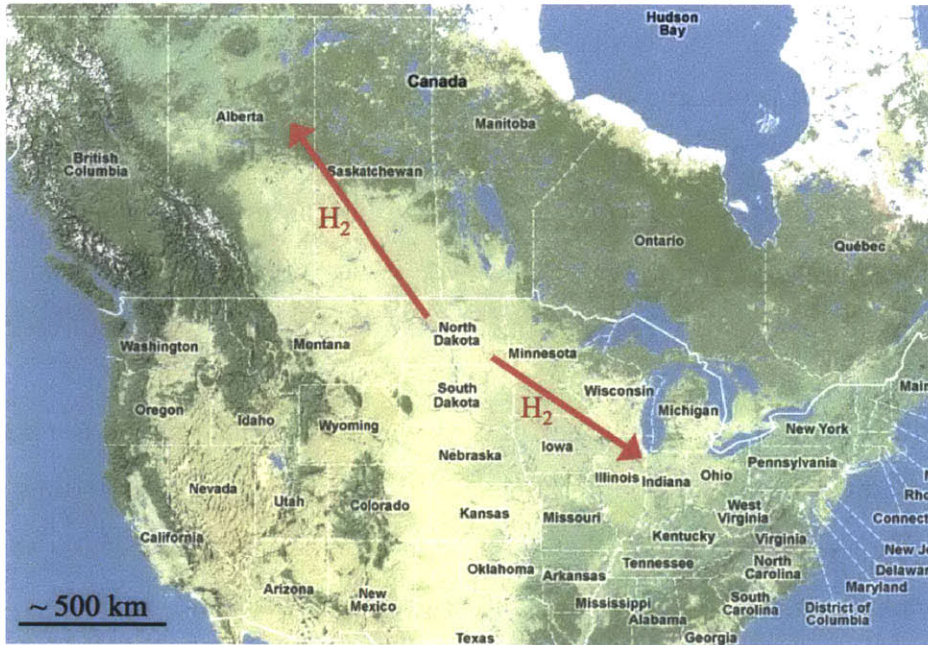


Figure 0-3: A possible location of the nuclear-wind energy system: the Dakotas, between Alberta and the Great Lakes region

the economic viability of the system and identify the key conditions for its future construction in the mid-term.

0.2 Objectives

This thesis constitutes a technico-economic study of a nuclear-renewable energy system for electricity and hydrogen production. This large system would fit in an electrical grid and industrialized region. It is both a production and a storage system for electricity.

As can be seen in Figure 0-4, the facility includes several major components: a hydrogen plant, a nuclear reactor and a hydrogen storage system. It operates in two different modes: hydrogen production mode and electricity production mode.

The hydrogen production mode occurs at time of low demand for electricity and large power supply from renewables (for example during a windy night in Spring). The nuclear reactor supplies all its steam (heat) to the HTE cells of the hydrogen

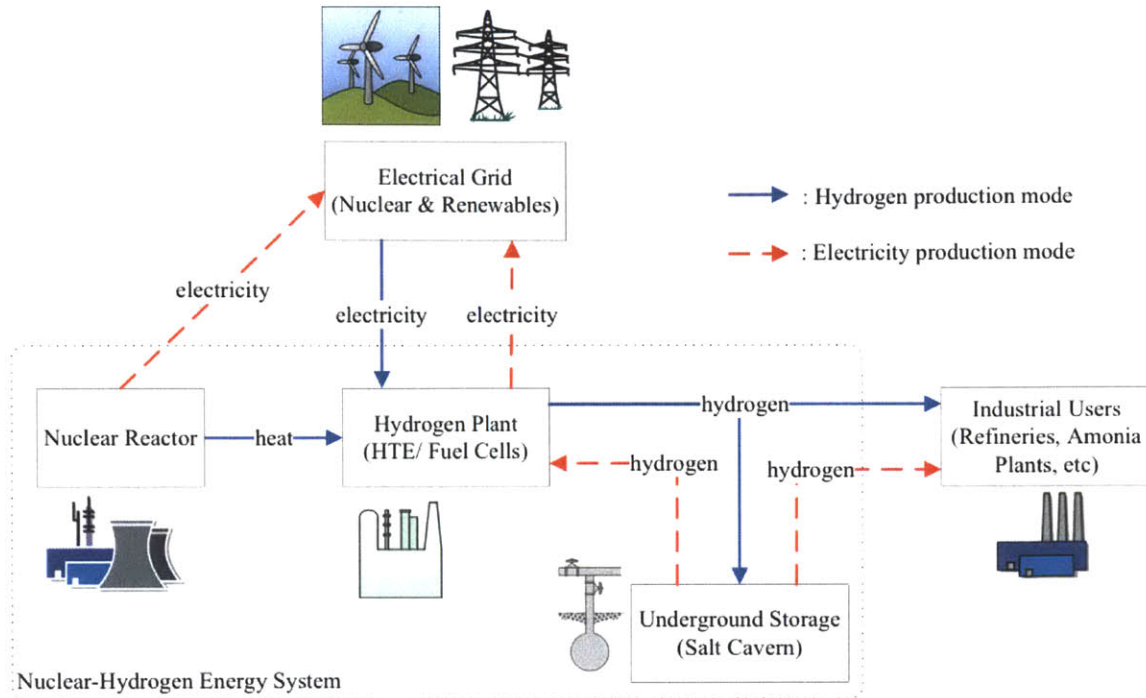


Figure 0-4: The energy system in both modes of operation

plant, while electricity is provided by the grid (the renewable energy sources are connected to the grid). Hydrogen - and possibly oxygen - is produced and stored on site in a large underground facility.

In the electricity production mode, which takes place during peak demand for electricity, the nuclear reactor generates electricity for the grid. The hydrogen plant becomes a power generation unit, with the electrolysis cells used in reverse to produce electricity out of stored hydrogen.

At all times hydrogen may be exported to the industrial users by pipeline.

The system is hence an actor in two markets: the electricity market and the hydrogen market. The flexibility of the plant takes advantage of both. If electricity prices are low, and/or if there is an excess power generation from renewables that can not be absorbed by the grid, the system buys electricity and produces hydrogen. If electricity prices are high and hydrogen prices low, hydrogen generates electricity in fuel cells for the grid; otherwise, hydrogen is sold. The important storage capacity enables decision making on a large scale and on a long time frame. The system is

however quite nimble, being able to switch from one mode of production to another in one hour.

0.3 Outline of the thesis

The thesis first identifies the possible locations and markets for the system. It then describes the different technologies involved in the system, the reason for their specific choice and their characteristics: hydrogen plant, wind farm, nuclear reactor, hydrogen underground storage and pipeline.

The second chapter evaluates the technical performances of the hydrogen plant coupled to the nuclear reactor. A model is presented to simulate the needs of the hydrogen production and the results are summarized to serve as an input for the following economic analysis.

A reference case is chosen to study the economic potential. The operation of the hydrogen plant is simulated over one year on a hourly basis as if it were included in the Dakotas region of the United States. The economic assumptions are modified to see under which conditions the system is competitive. Two approaches are selected for the economic analysis. The first one simulates the situation of a regulated electricity market, in which a vertically integrated utility would own the entire generation capacity and would minimize its cost to meet the demand. Several prospective scenarios of generation mix are considered. The second approach considers a deregulated market, where private investors face variable electricity prices, with the goal to maximize their profit. It predicts the economic performance of the system with today's prices.

The main results are summarized in the conclusion chapter. Recommendations and thoughts are expressed for future implementation of the system in an electricity and hydrogen market.

Chapter 1

Description of the system

The objective is to develop an economic system that can utilize geographically-stranded low-cost but intermittent electricity provided by renewables. Nuclear energy with HTE is proposed as the enabling technology to utilize stranded renewables while matching local electricity demand with supply and converting excess low-cost energy into exportable hydrogen. The nuclear reactor is a constant-output heat source where that heat can be used for variable electricity or hydrogen production. Hydrogen can be shipped directly to industrial users or/and be converted back to electricity using the electrolysis cells as fuel cells at time of peak power demand.

We provide in this chapter a detailed description of the system.

1.1 Location and Markets

Renewable resources in the United States and much of the world are located in remote areas. For example, on- shore wind is abundant in the upper Great Plains, hundreds of miles away from the major industrial hydrogen users (Figure 1-1). The biggest hydrogen consumer, the oil industry, requires large quantities of hydrogen for its refineries. In this situation there is a strong incentive to concentrate the production of hydrogen as well, in order to ship it by pipelines and achieve low transportation costs. A plant composed of a nuclear reactor and a hydrogen production unit fulfills these requirements. By adding large-scale hydrogen storage at production sites, we

obtain a concentrated production of hydrogen with the capability to absorb the seasonal, weekly, and daily variation in hydrogen production while enabling the pipeline to be continuously filled (and the refineries to get the constant hydrogen delivery they demand).

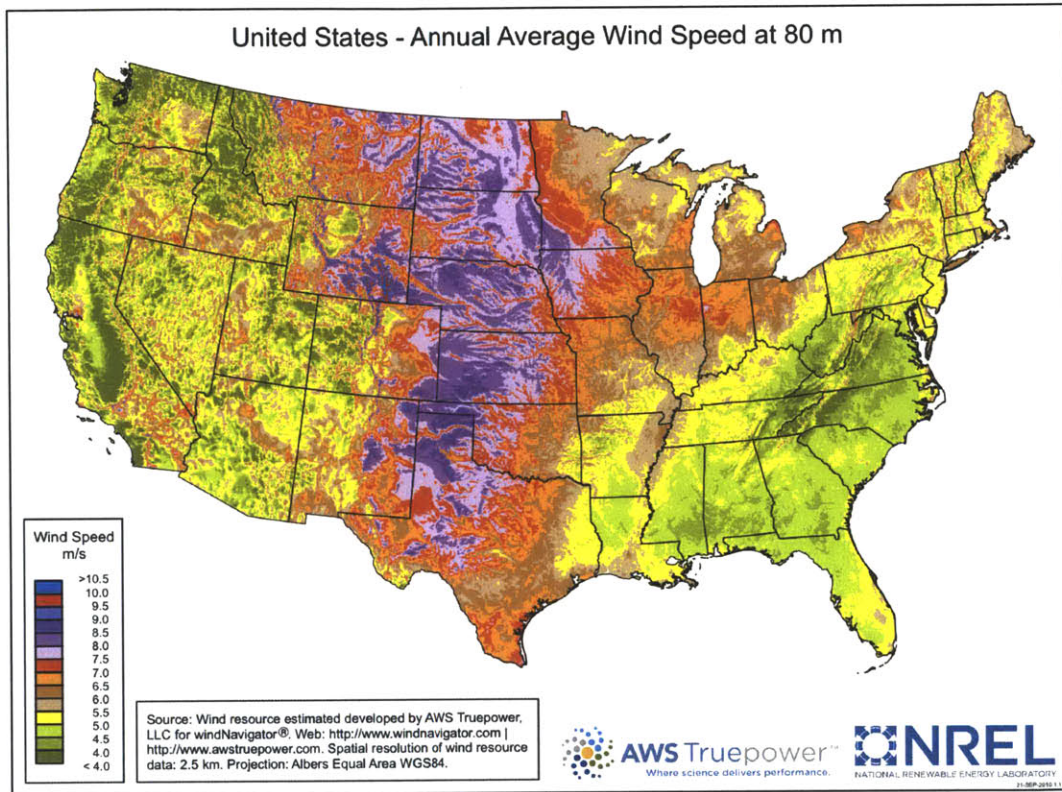


Figure 1-1: US wind resource map

To provide a realistic case for analysis, we assumed a nuclear-wind facility in North Dakota. Some of the best and most concentrated North American wind resources are in North and South Dakota. North Dakota wind generation data, collected over one year on a hourly basis, show an annual capacity factor of 37.4% [?], which is one of the highest in the country. North Dakota is about halfway between Chicago and Alberta (Canada). These two regions are large hydrogen consumers. Illinois has a refining capacity of 916,000 barrels /day and neighboring Indiana has a capacity of 432, 000 barrels per day. Alberta oil sands are a major source of oil supply that is expected to

significantly expand if prices remain higher than \$80 per barrel. Illinois (1000 km) is closer to North Dakota. In addition, the low population densities and flat land make transport of large components (windmill blades, reactor vessels, steam generators, turbines) easy and reduce the cost of pipeline construction to either market.

37,044 million cubic feet of natural gas were used as feedstock for hydrogen production by the US refineries in the PAD District II (Midwest and Great Lakes) in 2008. Converted into hydrogen by methane steam reforming ($\text{CH}_4 + 2\text{H}_2\text{O} \rightarrow \text{CO}_2 + 4\text{H}_2$), it amounts to about 433,000 MT of hydrogen annually. Therefore an annual hydrogen demand in the Great Lakes area between 200,000 and 400,000 MT/year is a realistic assumption. Those values represent respectively 2.2 and 4.4% of the total US hydrogen production in 2009. The constant flow rate of hydrogen that is required through the pipeline ranges from 550MT to 1100MT per day, a capacity achievable with a standard 20in-diameter pipeline (see section dedicated to pipeline in this chapter). The electricity required is in the gigawatt range, and heat in the megawatt range. This scale of hydrogen production implies large facilities, large capital investments, and large economies of scale.

This is a picture of today's hydrogen markets; however, if there were major constraints on emissions of greenhouse gases to the atmosphere, the hydrogen markets could be several orders of magnitude larger to serve two Midwest markets: conversion of biomass to diesel and gasoline and conversion of iron ore to iron. The Midwest has the largest resources of concentrated biomass (corn stover). Northern Minnesota is the primary producer of iron ore in North America. Currently that iron ore is shipped to markets where coal is used to reduce the iron oxides to iron. The alternative process, used for about 5% of world iron production, is direct hydrogen reduction. Both are highly centralized markets for hydrogen.

The electricity market, the Midwest Independent System Operator (MISO) market, is a large market, with about 137 GWe capacity installed [5]. Most of the generation (75%) comes from coal. More than 10,000 GWe of wind power capacity are expected to be built in the next several years, which confirms the wind potential of the region.

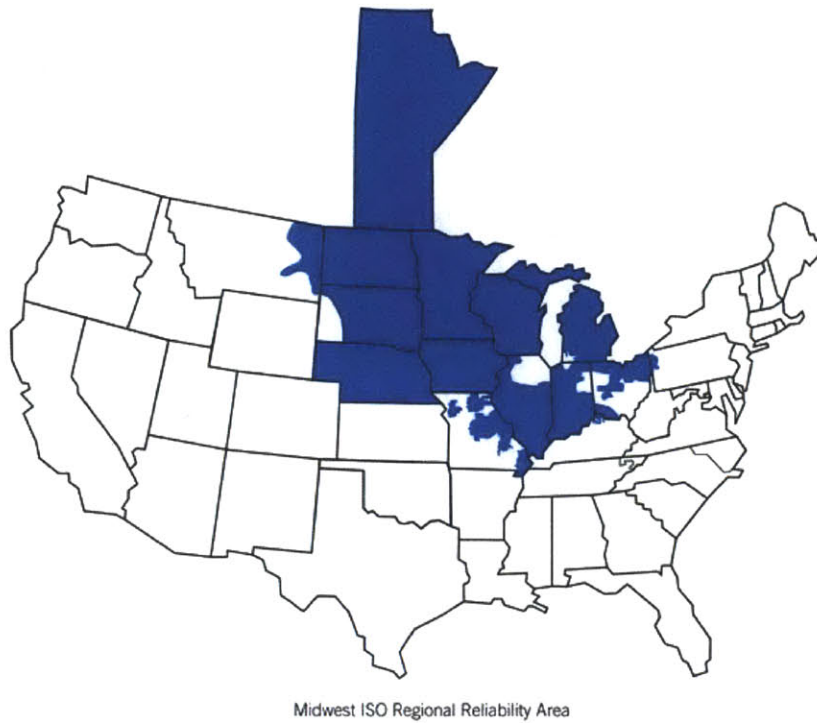


Figure 1-2: The reliability region of MISO

1.2 High Temperature Electrolysis / Fuel Cell

High-temperature electrolysis (steam electrolysis) is being developed as a next generation method for hydrogen production. HTE is more efficient than traditional electrolysis because heat can partly substitute for electricity (Figure 1-3). When water is converted to hydrogen and oxygen, energy is required to convert the liquid to a gas and to break the chemical bonds. Heat is used to convert water to steam and raise the temperature. At higher temperatures the electricity required to break water bonds is less. The cost of heat from a nuclear reactor is about one-third the cost of electricity, making this hydrogen production process potentially very economical. HTE has operating temperatures near 800-850°C but the heat source can be either an LWR or a high-temperature reactor. If an LWR is used, steam is fed to counter-current heat exchangers that heat the steam to high temperatures while cooling product hydrogen and oxygen from the electrolyzer. Additional heaters (electrical or fossil fuel fired) can compensate for heat losses and accurately adjust the temperature to the desired one.

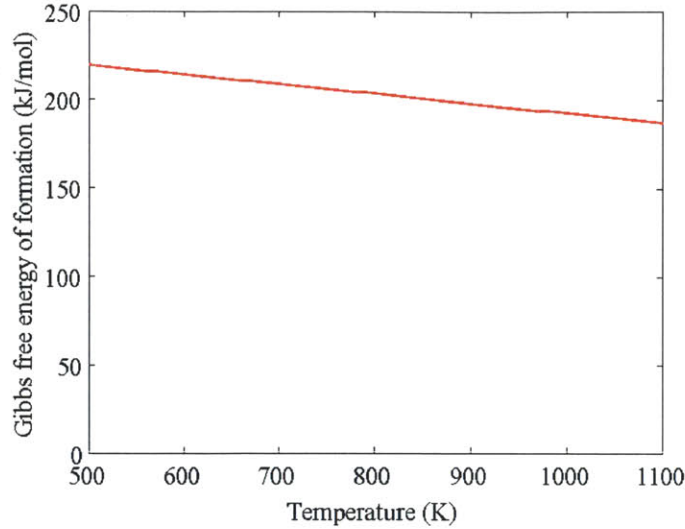


Figure 1-3: Energy requirements to electrolyze water decreases with the steam temperature

Idaho National Laboratory is currently the leading laboratory for high-temperature electrolysis development, followed by Risø National Laboratory in Denmark. Both work on Solid Oxide Electrolysis Cells (SOECs) and Solid Oxide Fuel Cells (SOFCs) to increase their longevity and performance.

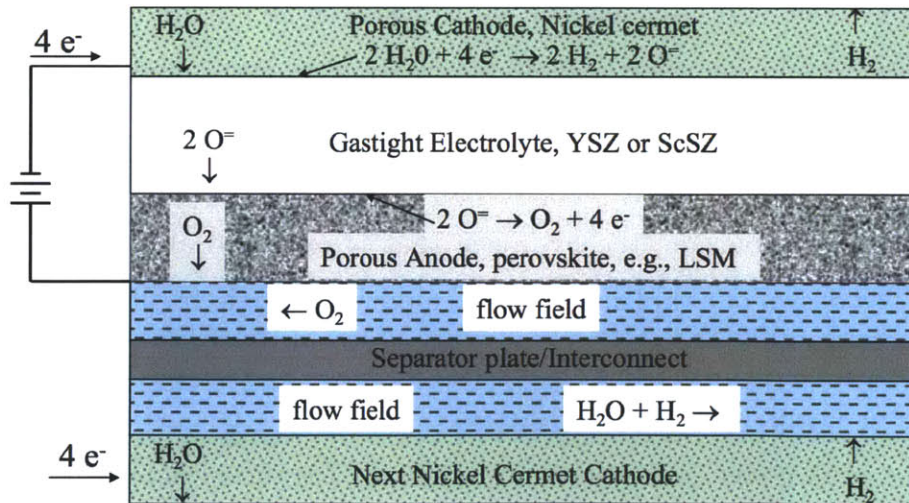


Figure 1-4: A cross section view of a Solid Oxide Electrolysis Cell (courtesy of Idaho National Laboratory)

The output of an HTE system, like a traditional electrolysis system, is dependent upon the energy input. If the steam input and voltage are increased, the current

flow is increased and more hydrogen is produced. For the system as a whole, there is a particular operating condition where the electricity/steam-to-hydrogen efficiency is greatest; however, more hydrogen can be produced with some decrease in system efficiency. This implies several modes of operation, as described in the next chapter.

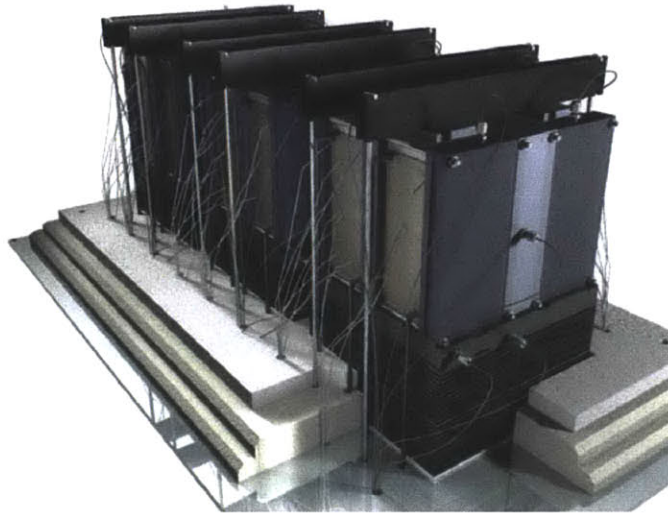


Figure 1-5: Example of high temperature electrolysis modules (courtesy of INL)

It is economically important that the cells used to produce hydrogen and oxygen out of water steam and electricity by electrolysis can be used in reverse as fuel cells (FCs) as well, producing water and electricity out of hydrogen and oxygen (air). The hydrogen production facility operates part time only: at time of low power demand and high wind power production. The hydrogen plant can therefore become a power generation unit by burning the hydrogen that is produced at times of low power demand. The design of the plant should be modified though, to allow for the streams to go in the reverse direction. The electricity production can take place at time of peak power demand, provided that the cost of electricity is competitive. This is likely: the existing peak power generation units, typically gas turbines, have high electricity cost because they are used a very limited time per year, as shown in figure 1-6. The capital cost of many gas turbines is spread over a relatively small electrical output. Some gas turbines are used a few hours per year only, leading to electricity costs exceeding thousands of dollars per megawatt hour electric. If the peak electricity is produced by the fuel cells of the hydrogen plant instead of the gas turbines, even at

a few hundred dollars per megawatt hour of FC generation cost, large savings can be achieved. Chapter 3 assesses the potential economics of such change in the grid structure.

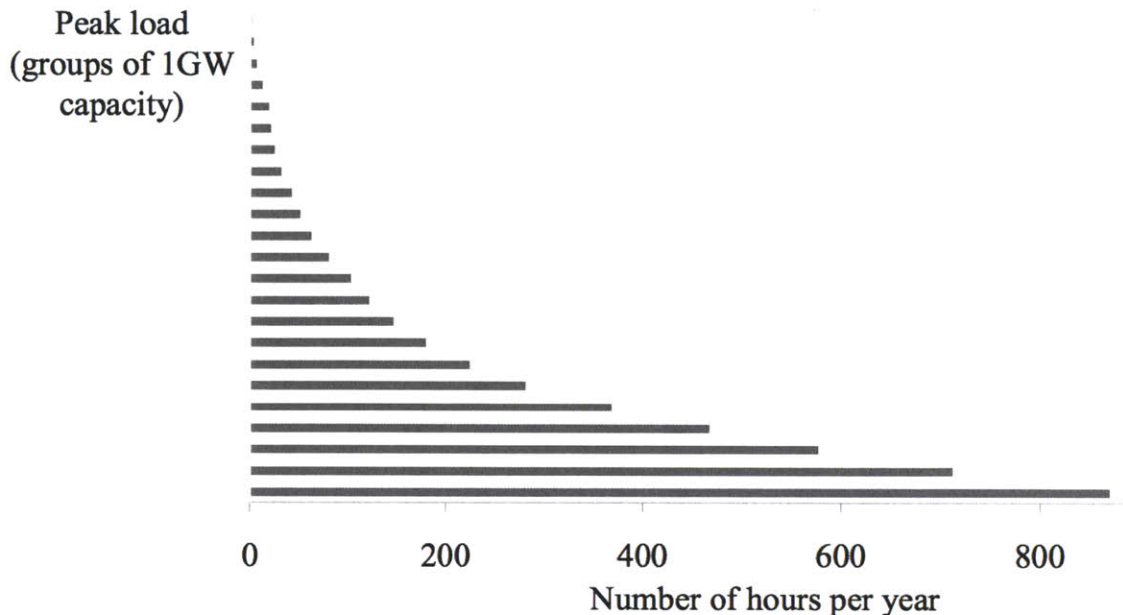


Figure 1-6: Operating hours per year for electricity peaking plants in MISO (2009)

Operating the cells in reverse, i.e. fuel cells instead of electrolysis cells, also provides an advantage in terms of reducing cell degradation. Performance is improved over a longer period of time [34].

These system characteristics imply the potential to fully utilize wind and nuclear energy production over large variations in both electricity demand and wind energy inputs. The HTE/FC facility both absorbs the excess wind electricity and backs up the electricity supply at time of high demand. While HTE/FC technology is not fully developed, understanding potential markets defines both the incentives to commercialize the technology and the ultimate requirements for the technology.

1.3 Wind Power

As will be demonstrated later, the wind farm can be at a gigawatts-scale because the hydrogen plant can absorb such quantities of power. With wind turbines in the

megawatt range, several hundred turbines are required. As a comparison, the largest existing wind farm in the United States (Roscoe Wind Farm, TX) has 781 MWe capacity with 627 wind turbines. It covers an area of nearly 400 kilometers square. The increase in wind turbine size should allow both cost reduction and more compact wind farms for the same capacity in the near term.

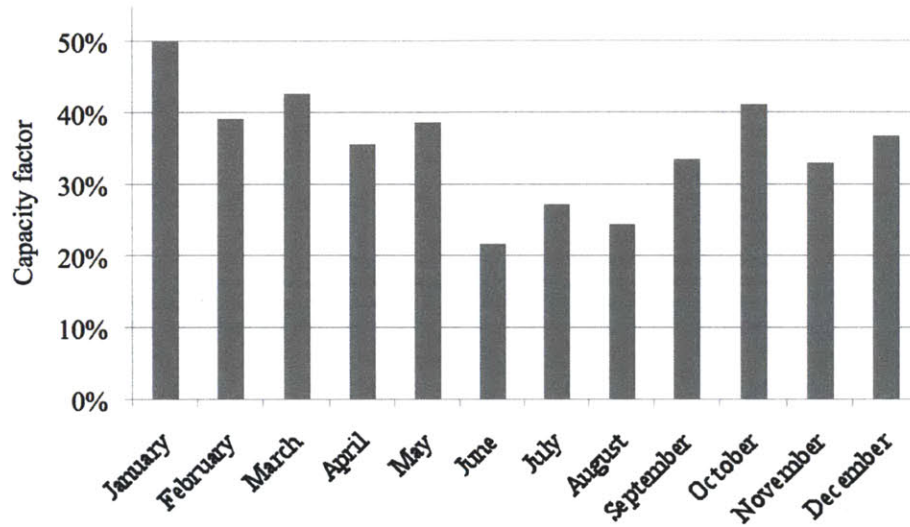


Figure 1-7: Capacity factor of Dakotas wind turbines, 2008-2009

The monthly mean capacity factors of North Dakota wind turbines (Figure 1-7) in 2009 show large variations in output over the seasons [17]. June, July and August are the less productive months, whereas the electricity consumption is high. On the other hand spring is windy, whereas electricity demand is at the lowest level. There are also large hourly variations in output. The annual capacity factor of 37.4%, the advances in technology and the economies of mass production enable one to reasonably forecast a wind electricity cost below \$40/MWh - but production not matching demand even in locations with highly favorable wind conditions.

Note that predictability of wind power generation (thanks to accurate forecasts) improves with wind farm size [2]. Large wind farms, because they are spread over a large area, have a total generation pattern which is a somewhat smoother.

1.4 Nuclear Reactor

The nuclear reactor provides heat for the HTE process, but it can also normally produce electricity at times of low wind production. The heat takes the form of steam that directly feeds the HTE process. The process becomes more efficient as the steam temperature increases. Several reactor types with secondary loops can be considered: pressurized water reactors (PWRs), sodium-cooled fast reactors, and high-temperature reactors (HTR). The HTR produces hotter steam but the technology is not fully developed, so that the analysis herein is based on using existing PWR technology. A 2008 techno-economic study [32] describes these options and concludes that there are small differences in final hydrogen cost among them.

Steam is directly accessible from the steam generator (see figure 1-8). Instead of supplying the turbine, a part of the steam is bypassed to the electrolyzer, while new feed water enters the loop to replace it. A number of nuclear reactors have been built to supply electricity and variable amounts of steam to industrial users. Fossil plants have been built where all of the steam can be diverted to industrial users - an option also applicable to nuclear plants. If a large fraction of the steam will sometimes be diverted to hydrogen production, there is the option of building the reactor with multiple steam turbines and shutting down a turbine during times of high hydrogen production. Many nuclear reactors have been built with multiple turbines. For example, the Loviisa power plant in Finland has two turbines per reactor (510 MWe). For this application, the economics require that the nuclear reactor operates at maximum output at all times but the associated secondary steam system can be designed to vary steam to the turbines and the HTE units. Given the variability of the wind, the response time for the secondary steam system to divert steam from one application or the other will be measured in tens of minutes.

For our analysis we used the steam conditions that are provided by the Areva EPR. Thus the nominal heat and electricity balances for an HTE system with the Areva EPR steam temperature and pressure are computed. Note that a 1-GW plant could be one dedicated plant or several plants where a fraction of each plant is used

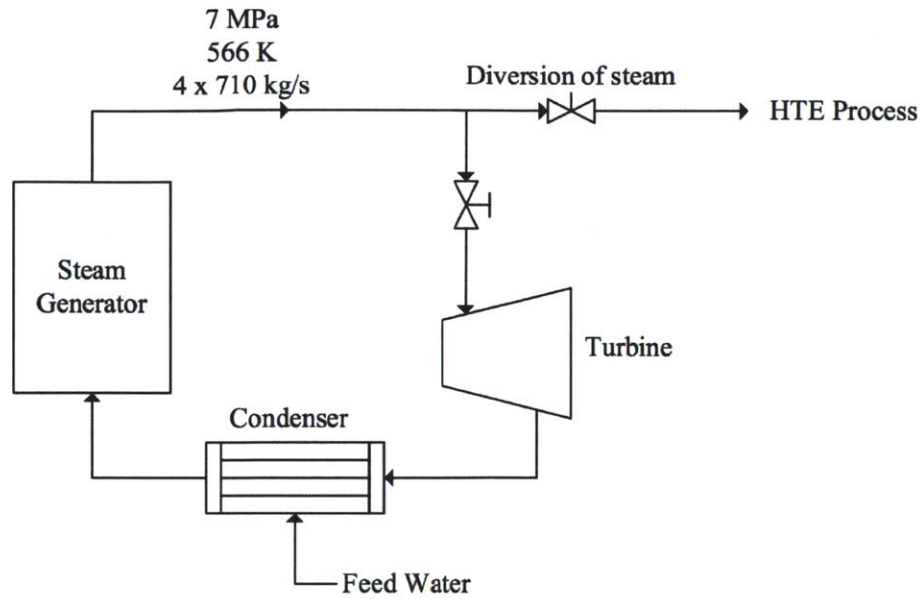


Figure 1-8: Direct coupling between the nuclear reactor's secondary loop and the hydrogen plant (Areva EPR operating conditions)

for the production (one or two steam generators for example).

A detailed study of the possible coupling between the nuclear reactor and the hydrogen plant can be found in the next chapter.

1.5 Hydrogen Underground Storage Facility

The storage of hydrogen is required if we desire not only to reuse that hydrogen to produce electricity later, but also to fill the pipeline continuously, so that the flow through the pipeline is constant (thus eliminates fluid flow instabilities), the user is always supplied, and transport costs are minimized. Large storage facilities are required because it is necessary to absorb seasonal variations in the production of hydrogen.

This hydrogen production depends both on the wind electricity generation and the electricity demand. Table 1.1 shows the relative monthly hydrogen production, for a utilization factor of the electrolyzer of 16% (thus corresponds to the optimized case identified in the following economic analysis). Hydrogen production occurs when the

electricity demand is low and the wind electricity abundant. As a consequence, we observe a net maximal production in spring and fall, whereas the winter and summer production is very low or even negative. This calls for a seasonal storage of hydrogen.

Table 1.1: Monthly relative net hydrogen production - example

Jan	Feb	Mar	Apr	May	June	July	Aug	Sep	Oct	Nov	Dec
0.94	0.91	1.50	1.39	1.79	-0.06	0.48	-0.06	0.86	1.41	0.92	0.26

The storage capacity is determined by the amount of hydrogen stored for summer, when the demand for electricity is high and the net hydrogen production, as a consequence, low. For those four months, referring to Table 1.1¹, about 277% of the monthly average production of hydrogen has to be stored. This corresponds to a storage capacity of 230,000 MT of hydrogen if the annual production is 1,000,000 MT.



Figure 1-9: Chevron-Phillips Clemens Terminal

Such quantities of hydrogen can only be stored underground if we want to achieve good economics - using the same technology used for storage of natural gas. Underground storage of hydrogen is a commercial technology. For example, in Texas the Chevron-Phillips Clemens Terminal (Figure 1-9) has a working capacity of 2,500 MT, and uses a salt cavern. The same geology exists in North Dakota (Figure 1-10), so that caverns of the same type can be built close to the hydrogen production facility.

¹Annual average = 1.00 per month.

Other possible geologies in North Dakota could also be used (aquifers, oil and gas fields), but the cost would be higher and the existing experience much less.



Figure 1-10: Location of the major salt deposits in the US

Assuming a pressure of hydrogen close to 7 MPa at the outlet of the electrolyzer, an extra pressurizer, a very expensive item, could be avoided to fill the cavern (Clemens Terminal authorizes pressures up to 15 MPa). Cavern filling and drain could take place during 20 years with very frequent cycles without major losses [22].

1.6 Hydrogen Pipeline

Between 2,000 and 3,000 kilometers of hydrogen pipeline exist worldwide, mostly in the United States and in Europe. Standard pipes are 50- and 91-cm diameter (20 and 36 in). Hydrogen pipelines have specific problems compared to natural gas pipelines, in particular hydrogen embrittlement, which can cause the rupture of the pressurized pipe. These issues are tackled by proper material selection, thicker pipes and by limiting the number of load cycles for instance [22]. In our case the pipelines would operate at steady state, which limits fatigue and accommodates the industrial users.

A distance of about 1,000 km divides the storage facility from the hydrogen users - the Great Lakes refineries for example. Assuming a pipeline diameter of 50 cm and

an inlet pressure of 7 MPa, one can express the mass flow rate of hydrogen through it using the pressure drop equation:

$$\Delta P_{friction} = \bar{f} \frac{\dot{m}^2 L}{2\rho A^2 D} \quad (1.1)$$

Assuming a turbulent flow regime, \bar{f} equals (Mc Adams correlation):

$$\bar{f} = 0.184 Re^{-0.2} \quad (1.2)$$

With a pressure drop of 4MPa over 1,000km, the hydrogen mass flow rate equals 696.2 MT/day, or 217,600 MT/yr. To decrease the flow rate, the pressure at the customer end of the pipeline is allowed to rise. There is significant storage capacity in the pipeline by varying pressure - an option that allows for short-term variations in production or consumption without use of storage systems. To increase flow rates, an extra compressor on the pipeline, a costly device, or a larger diameter pipe is needed.

1.7 Comparison with other energy storage technologies

The system aims to provide electricity and hydrogen on a large scale, because of the large size of the components (nuclear reactor, underground storage facility). The normal power production is in the gigawatt range, as well as the additional peak power generation. The hydrogen production can supply a significant amount (several percent) of the national demand.

The storage capacity is very large. Several months of hydrogen production are stored underground at low cost. The facility can store this hydrogen as long as desired and release it very quickly (the pressure is 7 MPa), in a matter of minutes.

On the other hand the response time for peak power production is less than one

hour. It is a reasonable estimate of the time required to start-up the fuel cells (several minutes [3]), but also to start-up the components of the plant (pumps, heat exchangers, compressors; several tens of minutes), and reach steady-state power production.

The nuclear-hydrogen system as an energy storage technology has a large field of application. It can be used not only to accommodate the seasonal and monthly variation in electricity demand and supply, but also the weekly and daily variations. It is very flexible and this flexibility is likely to bring extra revenue when introduced in a liberalized market, as discussed in chapter four.

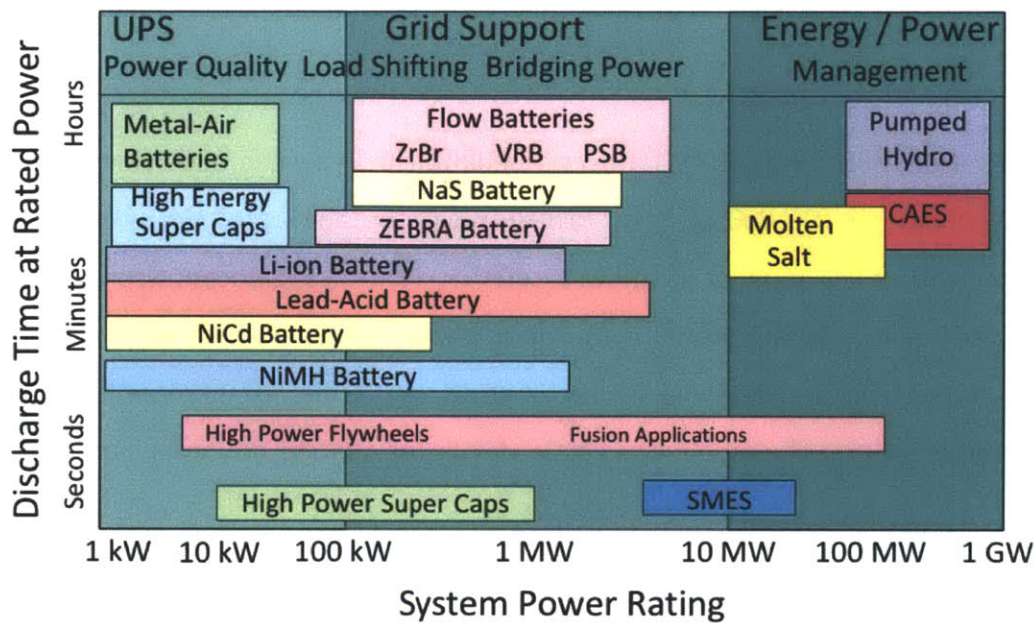


Figure 1-11: Energy storage options capabilities (after [33])

The American Physical Society classes energy storage technology options in three categories [2]: (1) base load bulk power management, (2) grid support in the form of distributed or load leveling storage, and (3) power quality and peak power storage, including uninterruptable power supply applications. Figure 1-11 shows where the current options are located in this classification. Our system, with a power rating ranging from the megawatt up to the gigawatt, and a discharge time at rated power from minutes to days, is able to both support the grid to level the load and help manage the base load power production. In this regard the nuclear-hydrogen system has unique capabilities.

Chapter 2

Hydrogen plant

This chapter focuses on the design of the hydrogen production facility that would be linked to the nuclear reactor. The objective is to assess, with reasonable accuracy, the water, heat and electricity requirements to perform the electrolysis in a variable way.

A conceptual design of the plant is proposed in this chapter, which can be seen as a baseline to derive the efficiency of the process with a reasonable accuracy, and enable us to compare the performance of the plant to classical electrolysis. The objective here is not to perform a detailed design but rather to provide a reference to derive the flowsheets for the later economic analysis.

Finally the chapter focuses on the reversibility of the hydrogen plant, that is using it as a peak power generation unit, with HTE cells used as fuel cells.

2.1 Hydrogen Plant Design

Hydrogen is produced in a hydrogen production facility in the vicinity of the nuclear reactor. A distance of a few hundred meters between the nuclear island and the hydrogen plant should ensure safety without affecting the heat losses much if the pipes are adequately insulated.

2.1.1 General layout

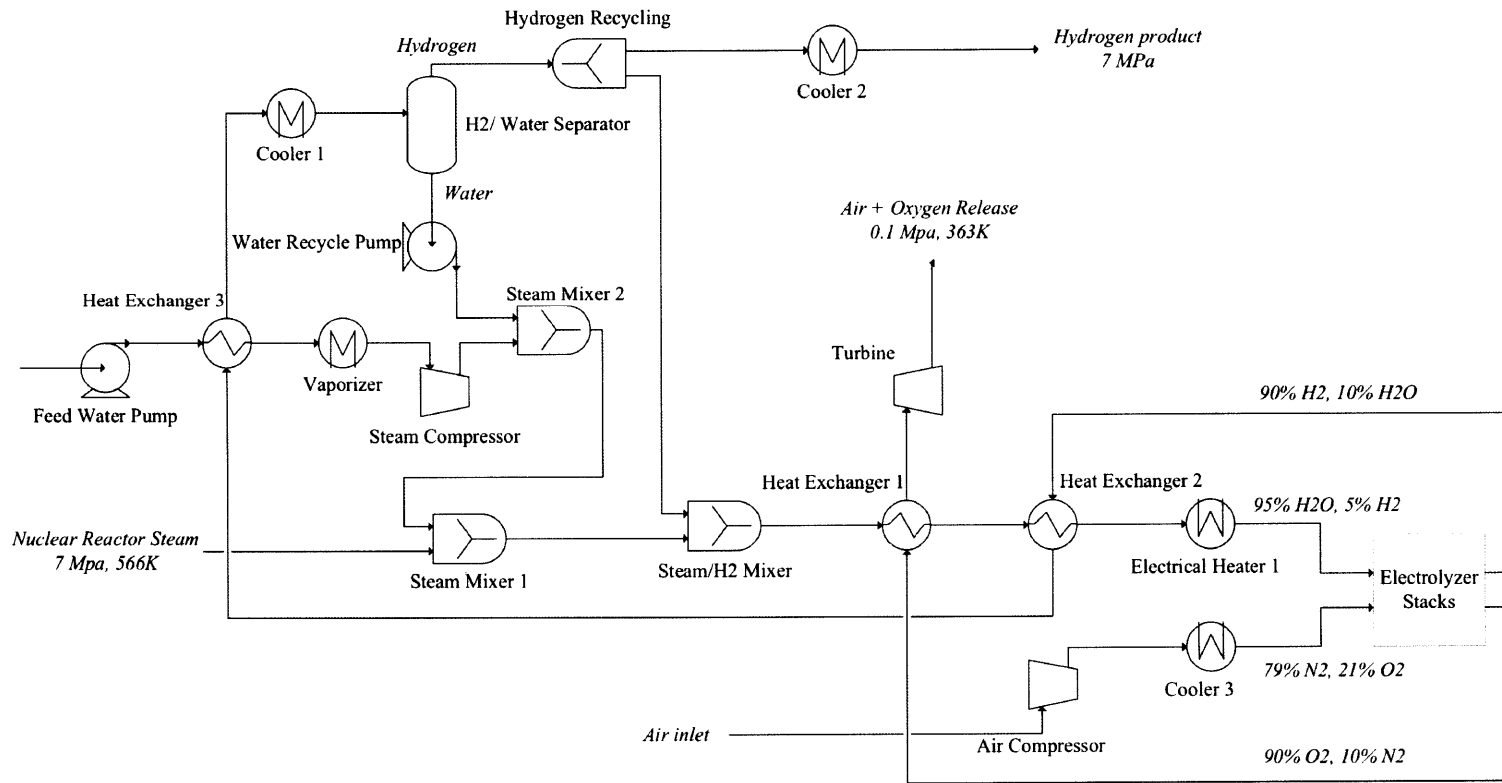
The selected design uses a direct coupling between a pressurized water reactor and the hydrogen production facility. The high quality, high purity steam produced in the steam generators is directly used as feedstock for electrolysis.

A set of heat exchangers pre-heats the steam (mixed with 5% hydrogen to get reducing conditions) up to the desired operating temperature (near 850C) before it enters the electrolyzer stacks. Additional heaters (electrical) are required because of the heat losses in the system. Electrolysis is performed and the hydrogen product is cooled down and separated from the residual water steam (10% of the output stream) that is recycled. Air is swept through the other channel of the stack to convey the oxygen, by-product of the process. That oxygen can be stored for later sale or vented to the atmosphere. Pure oxygen is a hazardous material; thus, any oxygen that is released will be released at temperatures significantly above local temperatures to provide buoyancy and assure fast mixing with air and no risk of a ground-hugging gas. A diagram of the system is shown in Figure 2-1.

Because of the direct coupling option, the hydrogen production process takes place at the nuclear secondary side steam pressure, which is 7 MPa. Operating at 7 MPa instead of atmospheric pressure as commonly done raises some safety concerns, but it has several major advantages. First hydrogen is produced at 7 MPa, and hence can readily be stored and/or shipped while minimizing the need for hydrogen compressor. Compression of hydrogen at low pressure is indeed very expensive. Second the cell degradation rate is lowered. The first results obtained at 1 MPa by Risø National Laboratory in this domain are encouraging. They show that the HTE cells performance improves significantly at high pressure [18].

Since the hydrogen production is inherently variable, the plant is designed to be flexible in terms of hydrogen output. Electrical heaters provide additional heat during start-ups. They also enable boosting the hydrogen production by vaporizing fresh water in addition to the nuclear reactor in very particular situations: when wind output is so high and the electricity demand so low that the excess wind power is

Figure 2-1: Hydrogen plant diagram - HTE mode only



beyond the nominal power capacity of the electrolysis cells. In that case, one can still absorb an important excess of electricity by overloading the HTE cells, which means increasing the power supply, although efficiency is lowered and the temperature rises within the stacks. It should remain a special case, limited in time per year, because of accelerated cell degradation. Few studies have been performed about the effect of high current densities on cell degradation : the degradation rate increases and the cell performance drops rapidly [20].

2.1.2 Tritium contamination

The secondary loop of the nuclear reactor contains Tritium, a radioactive element. If we directly couple this loop with the hydrogen production plant, the hydrogen produced might contain some tritium, and will be radioactive.

However, proper material selection of the steel constituting the tubes of the steam generator should limit the transport of heavy water and tritium from the primary loop to the secondary loop. For example in the case of a PWR, the use of Inconel 690 allows the secondary loop contamination to be as low as 3,000 pCi/L, whereas the use of Inconel 600 allows 20,000 pCi/L. That feature must be kept in mind in the design of the PWR linked to hydrogen production.

In addition, performing electrolysis on water including tritium separates tritium. Tritium remains in the aqueous phase, in the same way deuterium stays in the aqueous phase during heavy water production. In this process, water electrolysis at low temperature is performed to increase the ratio $^2\text{H}/^1\text{H}$ in natural water (it originally equals 1/6400). Lewis and Macdonald [23], who first developed the technique, find that the electrolysis involved five times less deuterium atoms than hydrogen atoms, yielding to an increase of deuterium concentration in the remaining water. Additional stages enable one to produce pure heavy water.

Literature about tritium production (more precisely separation from water or heavy water) by electrolysis is much less abundant and precise, presumably because tritium is used for military purposes. We can expect the electrolysis to involve even

less tritiated water than heavy water, hence very few tritium atoms would be in T-H or T₂ form as a by-product of the hydrogen process. The contamination by tritium in the steam being already very low (3,000 pCi/L), the concentration of tritium would be even lower in the hydrogen produced and sold to the industrial users; seven times less at least when the hydrogen will be finally used and converted to water, that is 430 pCi/L. The contaminant level for drinking water is set at 20,000 pCi/L (NRC). We are far from this level.

On the other side, this means that tritiated water builds up in the water stream of the hydrogen plant. It is then necessary to monitor the tritium concentration and replace that water when the radioactivity is too high.

2.1.3 Water requirements

In the hydrogen production mode, a significant amount of water is used as feedstock for the electrolysis process. It is legitimate to evaluate the water consumption since it might affect the decision to build the plant in a certain location (for example in an arid and dry area such as the South West of the United States).

Consider a 1 GWe nuclear-hydrogen plant. It generates 120.81 kg hydrogen per second (see calculation in the next section), or 434,916 kg of hydrogen per hour. The water feedstock for such production is then 3,914,244 liters per hour.

One can compare these water requirements with the water demanded by the same nuclear unit in "normal" operation, that is electricity production. Assuming a cooling tower equipment, the plant consumes about 700 gal per MWh net generation, that is 2,650,000 liters per hour¹ [1]. The water requirements of the nuclear-hydrogen plant are hence increased by 50% in the hydrogen production mode as opposed to the electricity production mode.

Water is thus an important factor to take into consideration when building the nuclear-hydrogen plant. One should make sure that an abundant and reliable source of water is located near the plant. Furthermore, the water treatment unit should

¹This number, given by the reference, can be easily checked by assuming the vaporization of 20 °C water due to the heat rejection of a 33%-efficient PWR.

be sized to process (clean up) a high flow rate of water, because this water will go through the steam generators and needs to be clean of impurities.

2.1.4 Oxygen sales

As in every water electrolysis process, oxygen is produced at the same time as hydrogen. Oxygen is a valuable product that can be sold to industrial users in the same way as hydrogen.

In particular, a possibly important use of oxygen in the mid-term could be its use as oxidizing agent for "clean coal". Indeed, in the hypothesis carbon capture and storage is implemented for coal power plants, the use of pure oxygen instead of air to burn coal makes the capture of pure CO₂ much easier. There is no production of nitrogen oxides, and the gas produced from the combustion is pure enough to be directly stored. Using imported oxygen is profitable for the coal power plant because separation of oxygen from air, or separation of CO₂ from the combustion exhaust gas requires a considerable amount of energy. In addition, coal power plants represent today the major source of electricity of the Dakotas region. The distance between the production site of oxygen (nuclear-hydrogen plant) and these sites is expected to be short, facilitating transportation.

Again here, the nuclear-hydrogen plant combines very well with technologies of a low-carbon world and generates profitable synergies.

E. A. Harvego, from Idaho National Laboratory [12], evaluates the additional revenue due to oxygen sales to be 20 cts per kg of hydrogen produced. It is not negligible and that is the reason why several designs of the hydrogen plant from INL suggest oxygen storage and shipping [30].

However, the design proposed in this report does not try to recover oxygen product. The first reason is that it complicates the design, with additional stages to get a pure oxygen stream instead of a mix of nitrogen-oxygen at the outlet. The goal here is only to approximate the performance, sufficiently to derive the economics. Secondly oxygen is more dangerous than hydrogen to handle, especially when it is pressurized and at high temperature. Oxygen is a strong oxidizer that is likely to

damage ordinary metals. An oxygen pipeline (using copper-based alloy for example) is thus uneconomical.

The release of the oxygen product into the atmosphere² is thus chosen instead of sales, for safety and simplicity reasons. One can consider it as a conservatism for the later economic analysis.

2.2 Hydrogen Production Performance

2.2.1 Electrolysis cell model

A model has been developed to compute the voltage and outlet temperature of an electrolysis cell according to the inlet temperature, pressure, gas compositions and current density applied to the cell. That 1-D model, using MATLAB software, is inspired by a similar model developed by INL . It computes the Nernst potential while ensuring energy and mass conservation at every point of the cells (1-D mesh).

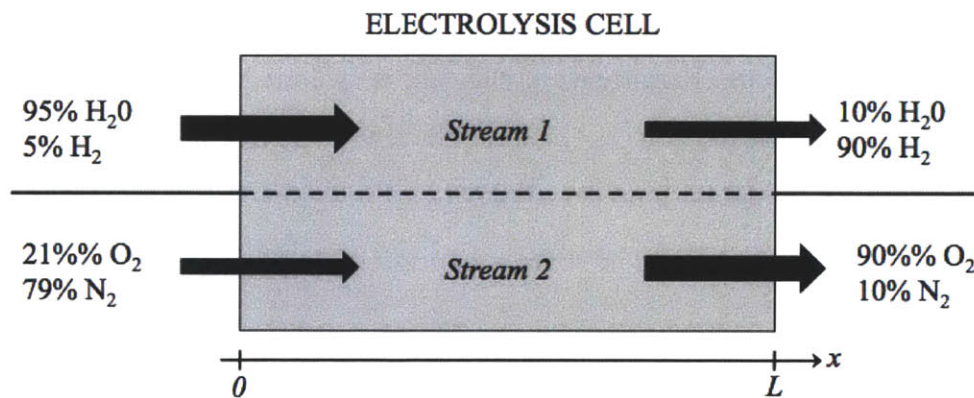


Figure 2-2: Schematic of the 1-D cell model

A schematic of such a cell is shown in Figure 2-2. One can see two streams: the first stream, entering the cell with mainly hot (water) steam and exiting with mainly hydrogen, and the second stream, entering with air and exiting with mainly oxygen.

²at low pressure and medium temperature

The electrolysis reaction is



The current density is fixed by the desired hydrogen production. Two electrons are required to produce one molecule of hydrogen. Hence the total molar flow rate of hydrogen \dot{N}_{H_2} produced in the plant is related to the total current I per cell by:

$$\dot{N}_{H_2} = \dot{N}_{H_2O} = \frac{I}{2F}N_{cells} = \frac{iA_{cell}}{2F}N_{cells} , \quad (2.2)$$

where i is the current density in one cell and A_{cell} and N_{cells} the area and number of cells respectively. F is the Faraday constant.

The operating voltage V_{op} of one cell is the sum of two contributions: the Nernst potential V_{Nernst} , responsible for the water splitting, and an additional voltage due to internal resistance of the cell (Joule effect).

$$V_{op}(T) = V_{Nernst}(T) + i \times ASR(T) \quad (2.3)$$

$ASR(T)$, the Area Specific Resistance of the cell, is an indicator of the performance of the cell, because it greatly affects the final efficiency. ASR_{1100K} equals $1.25 \Omega.cm^2$ today. The long term goal is to achieve $0.25 \Omega.cm^2$.

The temperature dependence of ASR is expressed by

$$ASR(T) = ASR_{1100K} - 0.463 + 3.973 \times 10^{-5} \exp \frac{10300}{T(K)} \quad (2.4)$$

This expression was developed experimentally [31].

The Nernst potential is accord with the reaction equation:

$$V_{Nernst}(T) = \frac{\Delta_R G^0(T)}{2F} - \frac{RT}{2F} \ln \left(\frac{P_{H_2} P_{O_2}^{1/2}}{P_{H_2O}} \right) \quad (2.5)$$

P_i is the partial pressure of i , and $\Delta_R G^0(T)$ is the standard Gibbs free energy of

the reaction. It can be calculated according to:

$$\Delta_R G^0(T) = \Delta_R H^0(T) - T \times \Delta_R S^0 = \sum_i \nu_i G_{f,i}(T) = \sum_i \nu_i (H_{f,i}^0(T) - T \times S_i^0) \quad (2.6)$$

$\Delta H_{f,i}^0$ and S_i^0 are tabulated for each chemical molecule (in NIST Chemistry Webbook [4] for example).

Difficulty arises because the partial pressures are not constant along the cell (indeed, hydrogen is made and water consumed). The temperature might also vary because of the Joule effect. The spatial variations of the parameters must be considered when deriving V_{op} to be accurate. Thus,

$$V_{op} = \bar{V}_{Nernst} + i \times \overline{ASR}, \quad (2.7)$$

with

$$\bar{V}_{Nernst} = \frac{1}{(T_{out} - T_{in})(P_{H_2,out} - P_{H_2,in})(P_{O_2,out} - P_{O_2,in})(P_{H_2O,out} - P_{H_2O,in})} \times \int_{T_{in}}^{T_{out}} \int_{P_{H_2,in}}^{P_{H_2,out}} \int_{P_{O_2,in}}^{P_{O_2,out}} \int_{P_{H_2O,in}}^{P_{H_2O,out}} V_{Nernst}(T, P_{H_2}, P_{O_2}, P_{H_2O}) dT dP_{H_2} dP_{O_2} dP_{H_2O} \quad (2.8)$$

and

$$\overline{ASR} = \frac{1}{(T_{out} - T_{in})} \int_{T_{in}}^{T_{out}} ASR(T) dT \quad (2.9)$$

For simplicity, assume the temperature and partial pressure vary linearly across the cell. For example, if x is the space variable and L the length of the cell,

$$\begin{aligned} P_{H_2}(x) &= \frac{P}{P^0} \times \frac{\dot{N}_{H_2}(x)}{\dot{N}_{tot}} = \frac{P}{P^0} \times y_{H_2}(x) \\ &= \frac{P}{P^0} \times \left(y_{H_2,in} + \frac{y_{H_2,out} - y_{H_2,in}}{L} x \right) \end{aligned} \quad (2.10)$$

The following molar fractions at the inlet and outlet of the cells (Table 2-3):

Figure 2-3: Molar fractions desired in the cells

	Inlet	Outlet
Stream 1	$y_{H_2} = 0.05, y_{H_2O} = 0.95$	$y_{H_2} = 0.90, y_{H_2O} = 0.10$
Stream 2	$y_{O_2} = 0.21, y_{N_2} = 0.79$	$y_{O_2} = 0.90, y_{N_2} = 0.10$

Some hydrogen is introduced in the first stream because it is a reducing agent that prevents corrosion in the high pressure and high temperature pipes.

What about the temperature? The inlet temperature is known. However, the outlet temperature is an unknown that depends on the mass and energy balance in the cell. One can not predict what will be the outlet temperature at first sight. The energy conservation equation across the cell is:

$$\dot{Q} - \dot{W} = \sum_{\text{products } i} \dot{N}_i \times H_i(T_{out}) - \sum_{\text{reactants } j} \dot{N}_j \times H_j(T_{in}), \quad (2.11)$$

where \dot{W} is the electrical work supplied by the cell (negative value) and \dot{Q} the heat transfer to the cell. The cell is considered adiabatic (no external gain or loss of heat across the cell) so

$$\dot{Q} = 0 \quad (2.12)$$

The electrical work supplied by the cell is simply

$$\dot{W} = -\bar{V}_{op} \times I = -\bar{V}_{op} \times i A_{cell} \quad (2.13)$$

$H_i(T) = \Delta H_{f,i}^0 + H_{f,i}(T) - H_i^0$ can be obtained from tables.

Since V_{op} and the right handside of equation 2.11 both depend on T_{out} , an iterative process is required to converge towards a solution. Practically, one starts with a guess for T_{out} , which is adjusted by the numerical code to give a solution to the problem.

The solution is carried out using MATLAB software. The code is documented in Appendix A. The inputs and the outputs of the model are summarized in Table 2.1.

Table 2.1: 1-D electrolysis cell model summary

Inputs	Cells parameter: $A_{cell}, L, N_{cells}, ASR_{1100K}$
	Hydrogen production desired: \dot{m}_{H_2}
	Operating pressure: P
	Inlet temperature: T_{in}
	Molar fractions at the inlet and outlet of the cells: $y_{i,in}, y_{i,out}$
Output	Operating voltage: V_{op}
	Outlet temperature: T_{out}

It is theoretically possible to run the cells at any temperature. However, it is not desirable to have a temperature gradient across the cells. Temperature gradients induce mechanical stresses, increase cell degradation, and create heterogeneities. For this reason one tries to operate under isothermal conditions: at T_{in} such that $T_{in} = T_{out}$. Such temperature a exists. In the present example, it is around 800-850°C, which, as expected, is high. The corresponding voltage is called thermal neutral voltage [30].

The hydrogen production for a given cell is limited by a maximal current density. The phenomenon is investigated in the next section of this chapter called "overload mode".

Model validation

To validate the model, results were compared with the ones obtained by Idaho National Laboratory [30]. The model developed by INL was validated with experimental data, and is considered "exact" here.

At a pressure of 0.1 MPa and inlet temperature of $T_{in} = 1073K$, inlet mole fraction of oxygen equal to 5%, $ASR = 0.5 \text{ A/cm}^2$, one finds $V_{Nernst} = 0.772 \text{ V}$, which is identical to the INL result. To achieve a current density of 0.25A/cm^2 , the operating voltage is 0.928, whereas the INL report gets 0.897 (3% difference). The thermal neutral voltage obtained by our model is the same as in the report: 1.287 V.

It is therefore considered that the model is correct, with an accuracy of 5%.

2.2.2 Overload mode

It is possible to increase the voltage and current density in the cells to increase the hydrogen production. However, it becomes difficult to keep isothermal conditions because the outlet temperature rises rapidly. In this regard, INL reports a maximal current density that depends on ASR : 0.6 A/cm² for $ASR = 0.25 \Omega \cdot \text{cm}^2$ and 0.25 A/cm² for $ASR = 1.25 \Omega \cdot \text{cm}^2$ [31].

[Figure: $(T_{out} - T_{in})$ and hydrogen production vs power supplied for high current densities]

However, there are situations in practice where large excess electricity is available, and where it becomes economical to push the cells beyond these limits to produce more hydrogen, even if we lose some efficiency and degrade the cells more rapidly.

Few investigations have been made on the HTSE process at high current densities. Risø National Laboratory in Denmark started a deeper study on this mode of operation [20]. Based on this first study, the degradation rate of the cells is plotted vs the current density of the cells in Figure 2-4. The accuracy of this curve is possibly low due to the lack of data since we don't have many material to rely on. Therefore, the following results should be taken with care.

2.2.3 Hydrogen plant model

The electrolysis cell model computes the electrical power requirements for a given hydrogen production and gives the desired operating temperature of the electrolyzer (inlet and outlet temperatures are equal, as explained before). This temperature, in the 800-850°C range, is however much higher than the temperature of the steam provided by the nuclear reactor. This problem is partly solved by recycling the heat of the hydrogen product through heat exchangers (see diagram of Figure 2-1), but

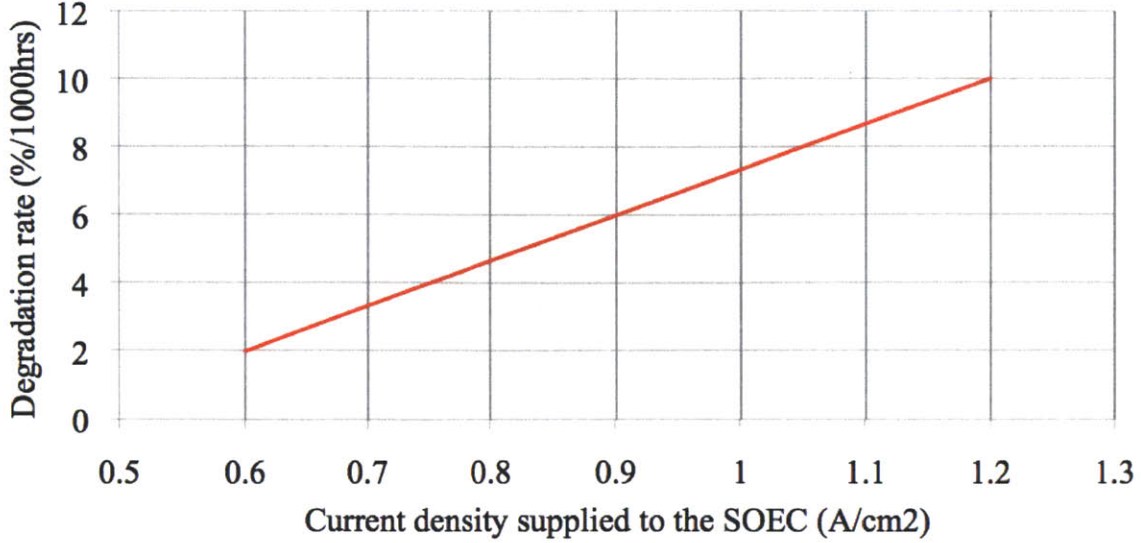


Figure 2-4: Qualitative degradation rate of the cells vs current density, for $ASR = 0.25 \Omega \cdot \text{cm}^2$

one still has to deal with heat losses through the pipes and components. Furthermore, compressors and turbines are used in the plant, which affects the power consumption. This section aims to model the plant as a whole to arrive at a reasonable estimate of the total heat and power balance for a given hydrogen production.

The components that are likely to affect the energy balance and hence the efficiency of the hydrogen production plant are:

- the heat exchangers. Their efficiency is defined by

$$\eta_{HE} = \frac{|\dot{m} (h_{out} - h_{in})|_2}{|\dot{m} (h_{out} - h_{in})|_1}, \quad (2.14)$$

where 1 and 2 refer to the heating and heated streams that exchange heat respectively, and h to the enthalpy.

- the compressor. It is used to compress the air intake before it enters the electrolyzer to carry the oxygen product. Its efficiency is defined by

$$\eta_{comp} = \frac{|\dot{m} (h_{out} - h_{in})|}{|\dot{W}|}, \quad (2.15)$$

where \dot{W} is the electrical power supplied.

- the turbine. It is used to recuperate some power while decompressing the oxygen product before release into the atmosphere. Its efficiency is defined by

$$\eta_{turb} = \frac{|\dot{W}|}{|\dot{m}(h_{out} - h_{in})|}, \quad (2.16)$$

where \dot{W} is the electrical power supplied.

- the electrical heaters. They are used to heat the steam up to the desired temperature just before the electrolyzer and compensate for the heat losses in the plant. Their efficiency is defined by

$$\eta_{heater} = \frac{|\dot{m}(h_{out} - h_{in})|}{|\dot{W}|}, \quad (2.17)$$

where \dot{W} is the electrical power supplied.

The pipes and other components (mixers, pumps, separator) are considered not to yield any additional energy losses. In the same way, no pressure losses are considered in the pipes.

A MATLAB model was implemented to derive the temperatures and energy losses at every point of the plant. The code can be seen in Appendix A.

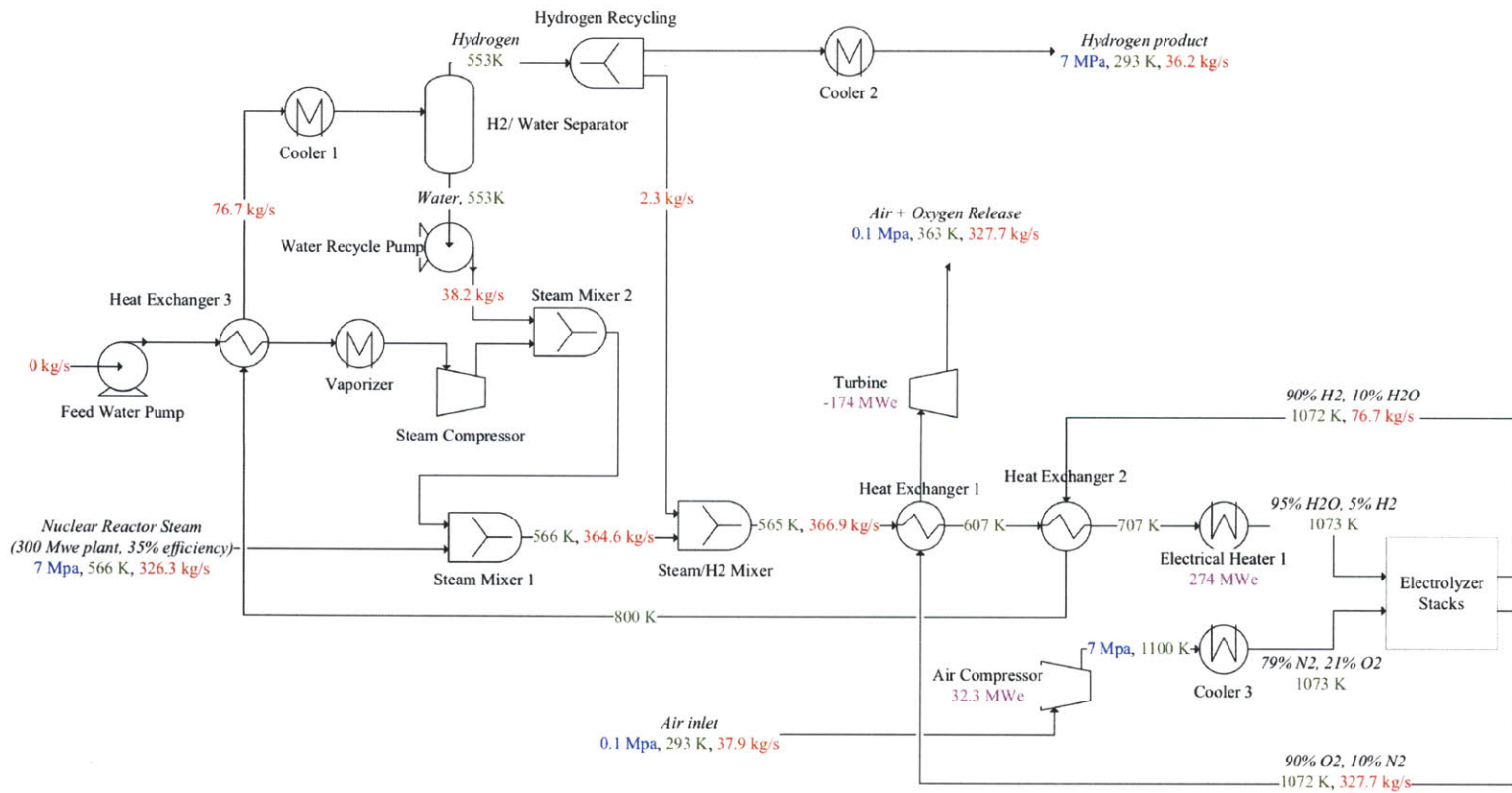
2.2.4 Results

The power and heat balance for a given hydrogen production were calculated according to the assumptions listed in Table 2.2.

Table 2.2: Assumptions used for the calculation of hydrogen plant performance

<i>ASR</i>		0.25 $\Omega \cdot \text{cm}^2$
Thermodynamic efficiencies	Turbine & compressor	85%
	Heat exchangers	90%
	Electrical heaters	95%

Figure 2-5: Flowsheet in a hydrogen plant coupled to a 300 MWe PWR - Normal mode of production



Electrolyzers only

ASR = 0.25 Ω.cm²
 i = 0.6 A/cm²
 V_{op} = 1.287 V
 N_{cells} = 25.9 millions
 Welectrol = 4,500 MWe

Nuclear-hydrogen system

Welectrol = 4,500 MWe
 Whydplant = 4,631 MWe
 Wnuclear = 300 MWe
 Hydrogen prod = 36.2 kg/s

=> Electricity-to-hydrogen efficiency = 88.1%

The process flowsheets, as well as the temperature and pressure have been computed according to the previous assumptions in normal hydrogen production mode (see Figure 2-5). The calculations are done for the case where the hydrogen plant is directly linked to a 300 MWe³ pressurized water nuclear reactor, from which the maximum amount of steam is diverted. It means that 326 kg/s of water as steam enters the plant and is converted to hydrogen and oxygen. The EPR temperature and pressure of the secondary loop are retained for this steam, which are respectively 566 K and 7 MPa.

The results of the simulations are given in Figure 2-6. It gives the power and heat balance for a given hydrogen production. A very significant amount of power can be absorbed by a 300-MWe nuclear-hydrogen system at time of low demand. It allows the penetration of tens of gigawatts of wind power capacity since their excess electricity production can be used to make hydrogen.

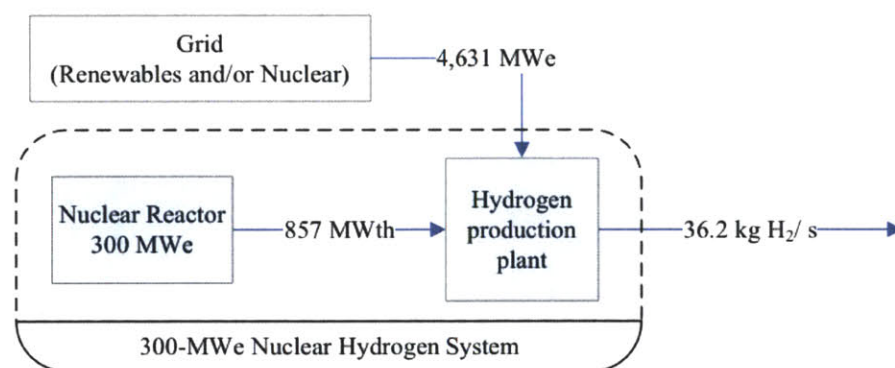


Figure 2-6: Heat and energy balance in normal mode - example of a 300 MWe nuclear-hydrogen plant

If a large excess of electricity is still available (from wind), the overload mode can be used; the electrolyzer characteristics are given for this mode of operation (Figure 2-8⁴) as compared to the normal mode. The temperature difference between the inlet and outlet of the electrolyzer cells is the limiting factor in this mode, as can be noticed in Table 2.3. The process flowsheets for a doubling of the hydrogen production are

³equivalent to 860 MWth, assuming 35% efficiency.

⁴The numbers given correspond to twice the hydrogen output of the normal mode of hydrogen production.

shown in Figure 2-7.

The temperature difference limit was set to 100C, which results in a maximal power input of 17.7 GWe for a nuclear-hydrogen plant size of 300 MWe (857 MW of heat). This limit appears in figure 2-9.

Table 2.3: HTE cell operating conditions

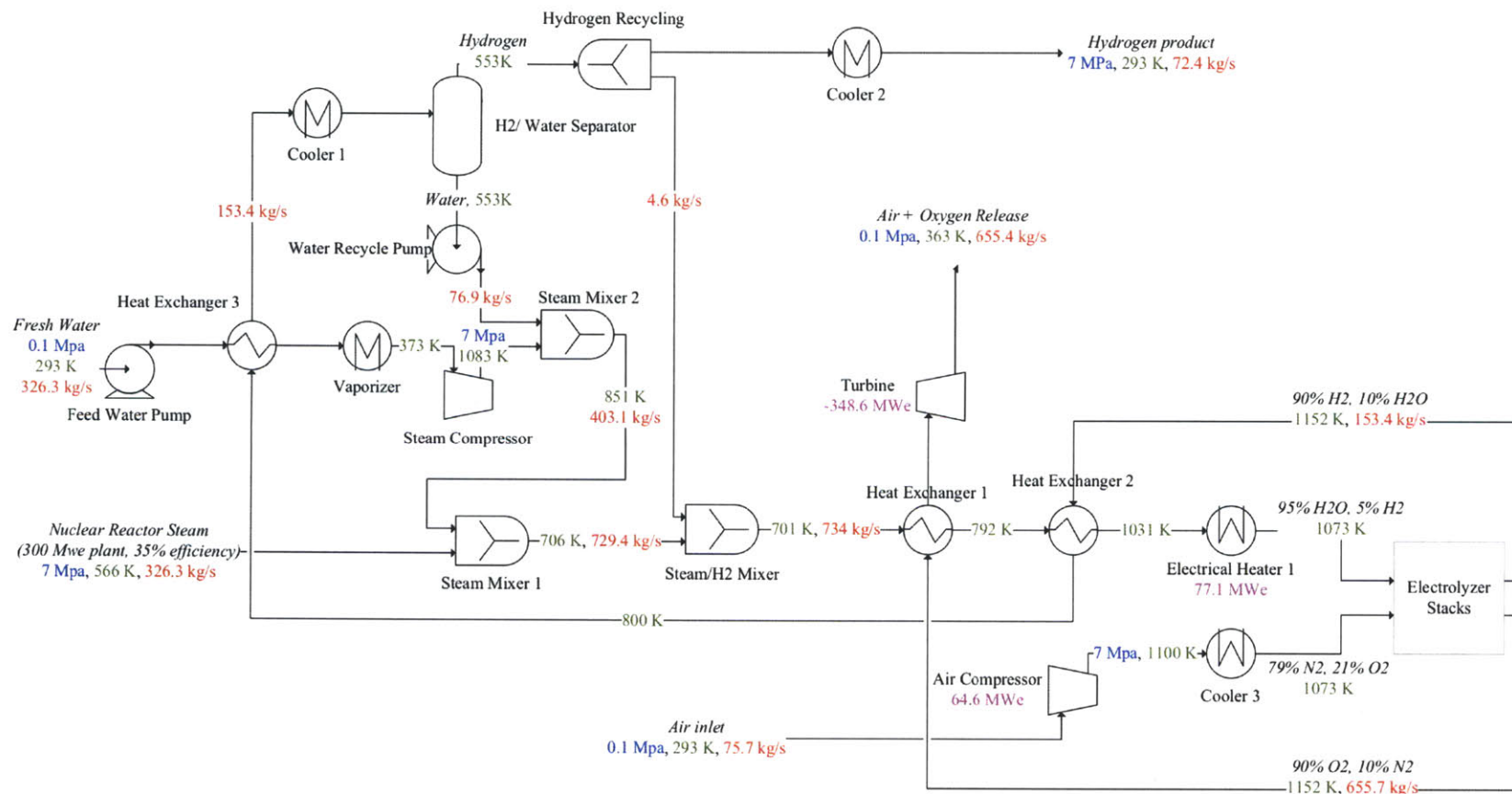
	Normal mode	Overload mode (example)
i_{cell}	0.6 A/cm ²	1.2 A/cm ²
V_{op}	1.287 V	1.310 V
$T_{out} - T_{in}$	1 K	79 K

The efficiency of the hydrogen production process, defined as

$$\eta_H = \frac{\dot{Q}_H}{W_{elec} + \dot{Q}_{heat} \times \eta_{reactor}} , \quad (2.18)$$

where \dot{Q}_H is the low heating value of the hydrogen produced per unit time, is plotted in figure 2-9. The efficiency, ranging from 80 to 89%, is much better than the efficiency of classic alkaline electrolysis, which is about 70% (NorskHydro electrolyzers, see Appendix B). Surprisingly, the efficiency is not affected much by operating in overload mode. This is explained by the fact that the heat is regenerated efficiently in the heat exchangers (the heat exchangers are assumed to have 90% efficiency). However, even if the impact on the grid management could be important by providing an extra absorption capacity in the grid, we chose not to operate in overload mode in our case study because the extent of the damage caused by that mode of operation is uncertain and it is difficult to model. Further research and development should provide more knowledge in this area soon.

Figure 2-7: Flowsheet in a hydrogen plant coupled to a 300 MWe PWR - Overload mode of production



Electrolyzers only

ASR = 0.25 Ω.cm²
 i = 1.2 A/cm²
 V_{op} = 1.3103 V
 N_{cells} = 25.9 millions
 W_{electrol} = 9,163 MWe

Nuclear-hydrogen system

W_{electrol} = 9,163 MWe
 W_{hydroplant} = 10,094 MWe
 W_{nuclear} = 300 MWe
 Hydrogen prod = 72.4 kg/s

=> **Electricity-to-hydrogen efficiency = 83.6%**

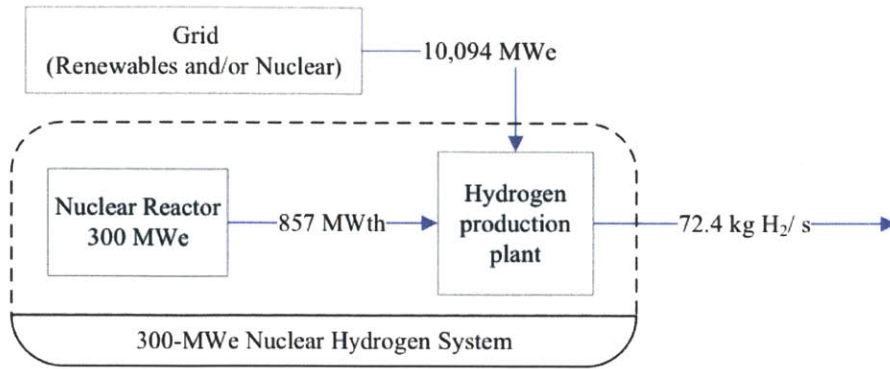


Figure 2-8: Heat and energy balance in overload mode - example of a 300 MWe nuclear-hydrogen plant

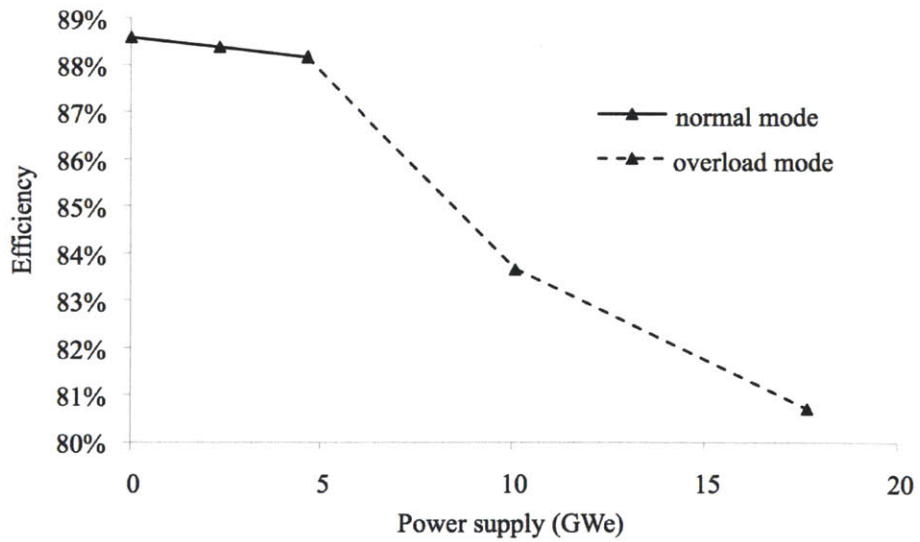


Figure 2-9: Hydrogen production performance of the plant (300 MWe nuclear reactor size)

Chapter 3

Economic analysis - regulated market

This chapter simulates the introduction of the nuclear-renewable energy system in an electricity market to analyze the economics. The first approach is to consider a regulated market, where a utility would own the entire generation capacity and would try to minimize its cost while meeting the demand. It enables to investigate different scenarios of future generation mix, in particular a mix where CO₂-free technologies (nuclear, wind, fuel cells) are maximized and fossil fuel ones are minimized. The analysis provides a good understanding of the impact of the nuclear-hydrogen plant and tells us what is its optimal size.

3.1 Methodology and assumptions

The modeling of the electricity generation and hydrogen production in an electrical grid is based on electricity demand, wind data, electricity generation costs and hydrogen plant costs. We detail in this section these different assumptions, and the way the model works.

3.1.1 Electricity demand and wind data

The analysis is applied to the case of a real grid in order to get meaningful results. We chose the case of the Midwest Independent System Operator (MISO) grid for several reasons.

First the electrical load (demand) of that grid shows the main features of a continental grid, with high demand in winter and summer. Secondly, the Midwest region is a very favorable location for wind, and thus is likely to introduce a large share of wind power in its energy mix if the economical and political context enables it. Thirdly, the electrical power plants of this region are mainly coal power plants, which means that in a low carbon world they would be replaced by other technologies since the fuel cost of coal (with carbon sequestration or carbon tax / cap and trade system) would be much higher than today. Finally the Dakotas present favorable geology for underground storage of hydrogen (salt caverns in particular).

The demand over the year 2009 has been taken for the analysis (Figure 3-1). The year 2009 is considered as a "normal" year in terms of temperature and weather conditions, even though short temperature peaks occurred during the summer.

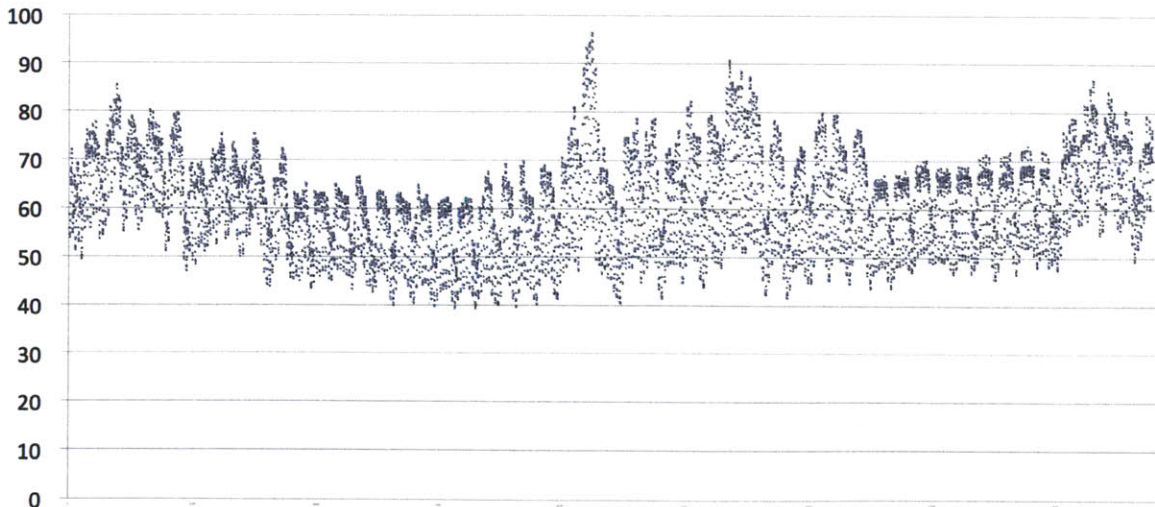


Figure 3-1: Hourly load of the MISO grid in 2009 (in GW)

The hourly data have been collected and processed [29]. The main features of the

load are presented in Table 3.1.

Table 3.1: Main features of the MISO load in 2009

Average load	Minimum load	Maximal load
61.82 GW	39.53 GW (on May 3rd)	96.51 GW (on June 26th)

For the modelling, assume that it is not possible to import or export electricity from this grid. It is isolated. This assumption is motivated by the goal of modelling a autonomous grid that does not rely on another one for meeting its demand or dumping its excess electricity.

The wind data refer to the same year¹. They come from the average wind power generation of wind turbines located in North Dakota [17]. The average capacity factor (CF) of these turbines is 37.4%, which is a very good performance. The hourly data are presented in Figure 3-2.

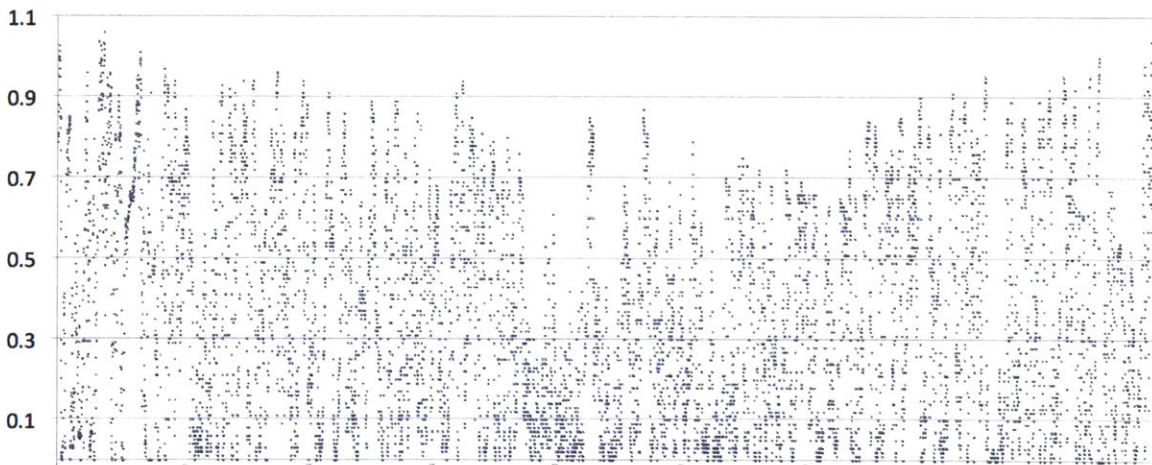


Figure 3-2: Hourly wind power output (MW) of a 1MW wind turbine in North Dakota (2009)

As one can notice, the wind power output is highly intermittent and unpredictable, with a lower output in summertime, which confirms the statement according which that it is difficult to integrate large amounts of wind power into the grid.

¹more precisely, data go from October 2008 to September 2009, because complete 2009 data were not available during the initial analysis

3.1.2 Electricity generation technologies

Three² electricity generation technologies were selected for the analysis. Nuclear power plants, wind turbines and Combined Cycle Gas Turbines (CCGT). Coal power plants were not retained in the grid, because it is assumed that they would release large amounts of greenhouse gases (GHG), which would make this technology uncompetitive with nuclear or CCGT because of a high generating cost of electricity (caused by the expected cost of carbon emission and/or the carbon sequestration cost).

CCGT, although being a GHG emissive technology, is expected to be a wide spread electricity generation technology in the short- or mid-run. The releases of carbon by methane combustion are lower than from coal, and natural gas resources are still large today [26].

The Levelized Cost Of Electricity (LCOE) for those three technologies have been collected, and are summarized in Table 3.2. The LCOE reflects the cost of generating electricity accounting for capital cost, operation and maintenance costs, fuel cost (including carbon cost), and a discount rate of return over the economic life of the generating unit. The data are from the 2010 report of the International Energy Agency on the projected costs of generating electricity [28].

Table 3.2: Cost of generating electricity (2010 US \$)

Technology	LCOE	Comments
Nuclear power plant	\$80/MWh	at 85% load factor
Wind turbines	\$117/MWh	at 26% load factor
Combined Cycle Gas Turbines	\$90/MWh	at 85% load factor, \$10/MMBtu natural gas cost and \$10/MT carbon cost

The discount rate is fixed for the rest of the analysis, equal to 7%.

The outage times of any production plant is neglected. Their availability is 100%. This assumption does not impact the results significantly as it modifies the cost of every technology in roughly the same way, and thus just offsets the global cost of

²four if we include fuel cells

electricity.

Depending on the installed capacity of each technology, the costs of generating electricity will be modified since the load factors³ will be modified. In the same way the fuel cost has a large impact on the cost of CCGT electricity.

The sensitivity analysis performed in the IEA report [28] enables derivation of simple expressions of the LCOE for each technology (Table 3.3).

Table 3.3: LCOE formulas (2010 US \$)

Technology	LCOE formula (\$/MWh)
Nuclear power plant	$20 + 60 \frac{0.85}{LoadFactor}$
Wind turbines	$23 + 94 \frac{0.27}{LoadFactor}$
Combined Cycle Gas Turbines	$4 + 16 \frac{0.85}{LoadFactor} + 60 \frac{NGcost}{\$10/MMBtu} + 10 \frac{CarbonCost}{\$30/MTCO_2}$

Again, more than the absolute values of costs, the relative costs of each technology for generation dispatch are of interest.

3.1.3 Generation dispatch modelling

Once every parameter of the problem has been specified (capacity installed, costs of fuel, etc), the modeling can take place. For every hour, a dispatch is allowed among the available generation technologies to meet the demand, as done in a real electrical grid.

Nuclear, with its high capital cost and low operating cost, first serves the demand. Then the wind turbines, with a higher marginal cost and a higher production uncertainty, come on line⁴. Finally, CCGT technology covers the residual demand, because

³actual electricity generation divided by theoretical maximal electricity generation

⁴Note that the wind power generation at that very hour is given by the wind data, and thus is very variable

it has a low capital cost, a high operating cost (fuel) and a maximal ability to follow the demand curve (short response time).

A classic dispatch is shown in Figure 3-3 during the last week of June 2009 (June 23rd to 29th, 2009). In that case the nuclear capacity is 40 GW, the wind power capacity 40 GW and the CCGT capacity 57 GW. Note the presence of excess wind electricity on Friday night.

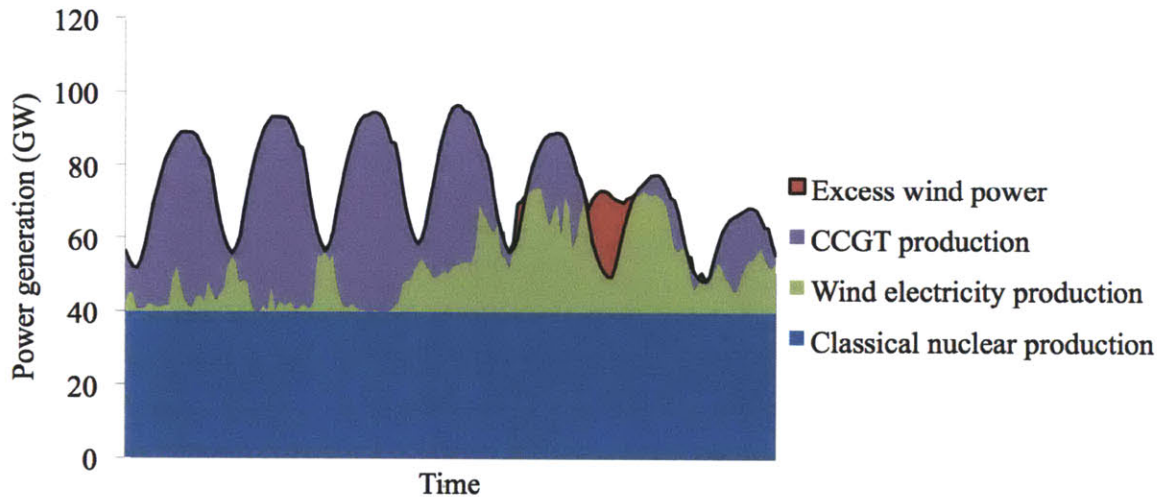


Figure 3-3: Example of generation dispatch, last week of June 2009

3.2 Example

The methodology is applied with a example as follows.

There are three technologies of electricity production: nuclear power plants, wind turbines, and combined cycle gas turbines (CCGT). There is no hybrid nuclear technology to produce hydrogen by high temperature steam electrolysis, and therefore no storage of electricity. It is considered that the excess wind electricity is lost, or dumped, without any cost of damage for the electric system.

Nuclear provides the base load electricity; therefore its capacity is equal to the minimal load of the demand over the year. The wind turbine capacity is set equal

to the maximal load minus the minimal load, so that when wind blows, it covers any potential demand. As a backup in case of low wind conditions, CCGTs substitute for the wind turbines. Hence it was decided that they have the same capacity.

Table 3.4: Power capacities in the reference case

Nuclear	Wind	CCGT
40 GW	57 GW	57 GW

The fuel cost assumptions are summarized in Table 3.5.

Table 3.5: Fuel cost for CCGT in the reference case

Natural gas cost	Carbon Cost
\$10/MMBtu	\$10/MT CO ₂

Once the generation dispatch is performed, the LCOE can be derived for each technology since the load factor is known. The global LCOE is defined as the average of the LCOEs for each technology weighted by their respective electricity generation. The results are in Table 3.6.

Table 3.6: Results of the reference case dispatch

	Nuclear	Wind	CCGT	Total
Electricity production ³ (GWyr)	40.00	13.04	8.78	61.82
Electricity Dumped (GWyr)	0	7.1	0	7.1
Load Factor (%)	100	22.9	15.4	
LCOE (\$/MWh)	71.0	133.9	162.3	97.2

The amount of excess wind electricity is very large, and represents several billions of dollars. That is why this energy mix is not sustainable and realistic. Nevertheless it gives a reference cost of electricity generation, which is equal to \$97.2/MWh.

The electricity generation breakdown is given in Figure 3-4⁵. Even if the installed

⁵The electricity production refers to the electricity produced and effectively used by the users. It does not include the excess wind electricity production.

capacity of wind power is 43% larger than the nuclear capacity, its share in the total electricity generation is just slightly over 20%, whereas the share of nuclear is 65%. It will be seen that increasing the capacity of wind power does not lead to a significant increase of this share, because above a certain threshold most of the power produced by wind is excess electricity.

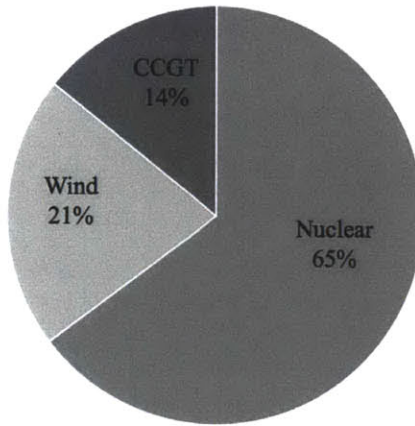


Figure 3-4: Electricity generation breakdown for the reference case

3.3 Preliminary study - no hydrogen generation

The purpose of this section is to identify the important parameters of the reference case assumptions for the cost of electricity, the electricity dumped and the carbon emissions.

3.3.1 Wind power capacity

First make the wind power capacity vary while keeping all the other parameters constant.

Table 3.7: Power capacities for the preliminary study

Nuclear	Wind	CCGT
40 GW	Variable	57 GW

Table 3.8: Fuel cost for CCGT for the preliminary study

Natural gas cost	Carbon Cost
\$10/MMBtu	\$10/MT CO ₂

After dispatch, notice in Figure 3-5 that there is almost no power dumped until the wind power capacity reaches 20 GW. At this point, wind represents 10.7% of the electricity generated in the grid, and the load factor of the wind turbines is almost maximal, equal to 33.1%.

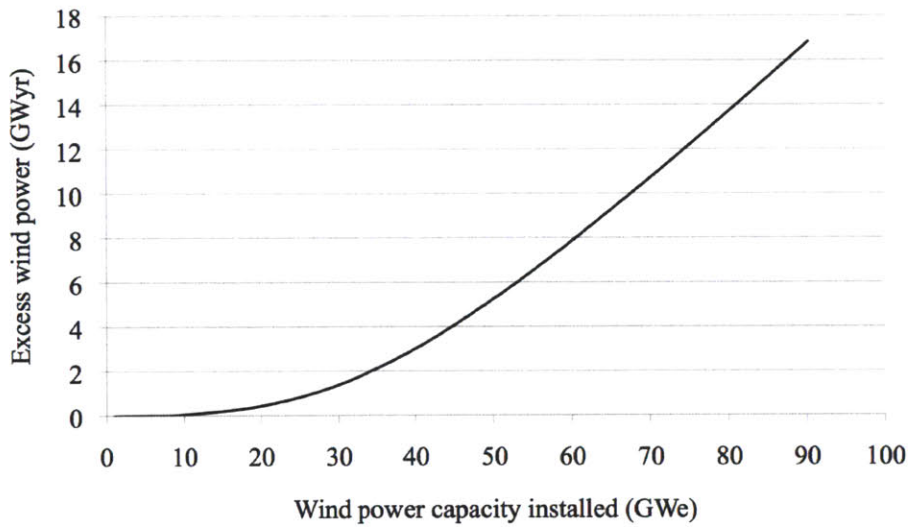


Figure 3-5: Excess electricity vs wind power capacity

The global LCOE does not decrease as more wind turbines are installed (Figure 3-6). That is explained by the fact that the load factor of both wind turbines and gas turbines decrease.

The immediate conclusion is that it is not economical to have wind turbines in the MISO grid with today's cost of generating electricity.

The first solution to justify wind power in the grid would be to have a lower cost of generating electricity by wind. It is studied next.

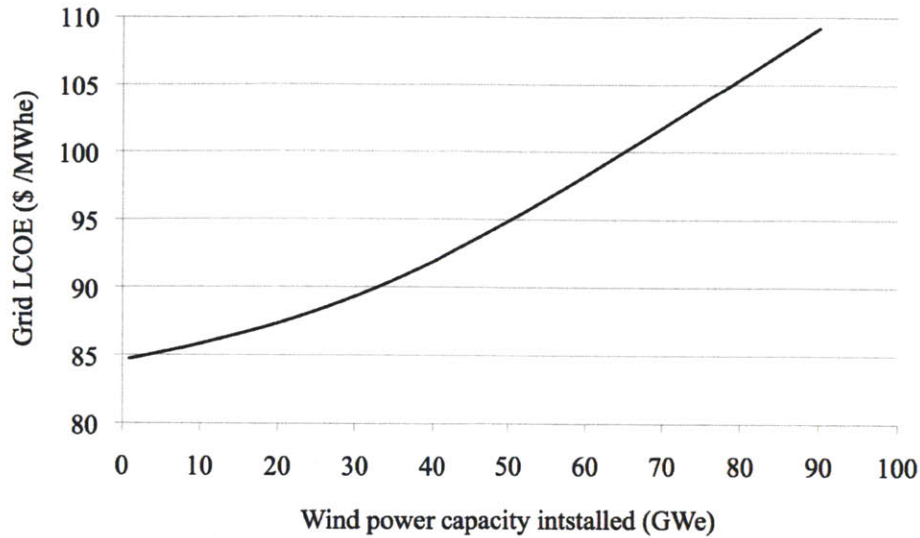


Figure 3-6: Global LCOE vs wind power capacity

Wind subsidies

One could provide subsidies to the wind power technology so that the LCOE of wind decreases artificially, as it is performed in many countries today.

Figure 3-7 shows that a minimal subsidy of \$30/MWh is required today to help the penetration of wind power in the grid. The optimal wind power capacity would be in this case 20 GW, generating 6.625 GWyr of electricity. The cost of such policy would then be 1,741 million dollars per year for the MISO grid. The bargain in terms of carbon emission (see further) is clearly not worth it. One could however use it in conjunction with other policies as a carbon tax to make wind more attractive.

Cost of wind power

The cost of wind power is expected to decrease within the next decades as larger wind turbines are developed and more wind turbines of the same type are installed [35], since we are still in the early ages of large wind power production.

The first effect is the economy of scale. In quantitative terms, the cost C_i depends on the size K_i as

$$\frac{C_i}{C_0} = \left(\frac{K_i}{K_0}\right)^n \quad (3.1)$$

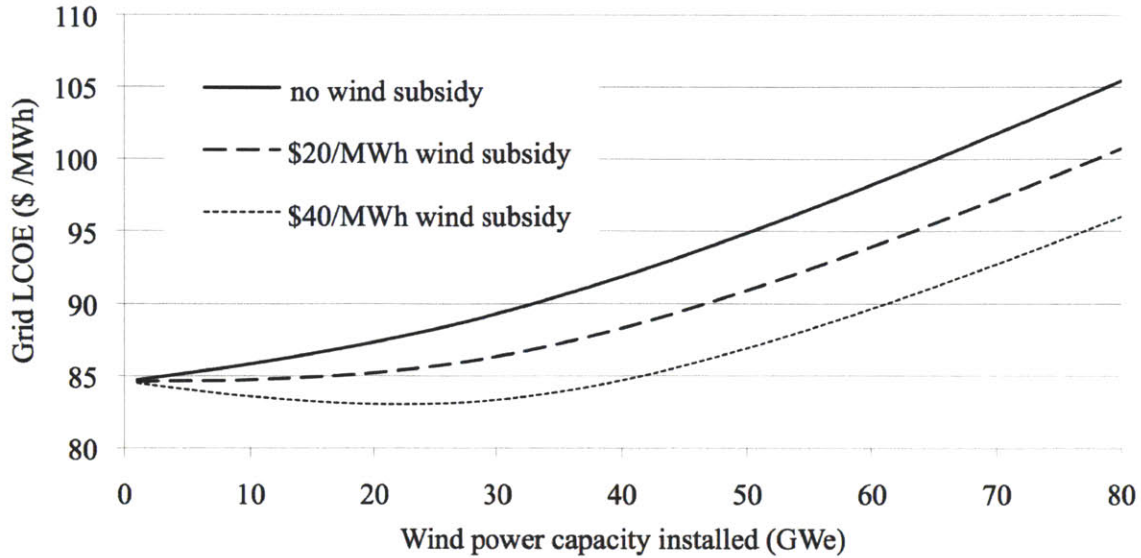


Figure 3-7: Effect of wind subsidies on global LCOE

n is a scale exponent, typically $2/3$. It reflects the idea that "bigger is cheaper". The current size of the wind turbines is 3.5 MW. 10 MW wind turbines are under development, which would lead to a reduction of the cost by a factor of 2.

The second effect is the learning curve effect. Experience shows that the cost of the N^{th} unit can be characterized as

$$C_n = C_1 N^{-\alpha} , \quad (3.2)$$

where $\alpha = -\frac{\ln 0.85}{\ln 2}$ for a 85% learning coefficient. The 100^{th} unit thus costs 3 times less than the first unit.

Notice in Figure 3-8 that a cost reduction by a factor 1.5 is sufficient for inducing a large wind penetration. It corresponds to a wind turbine rating twice as big as today, or to an expansion of wind power by a factor of five. Again, the optimal installed capacity is 20 GW.

3.3.2 Cost of fossil fuel (natural gas)

The cost of fuel is a very important parameter for CCGT, as it represents two thirds of the cost of generating electricity for this technology. Therefore, as wind

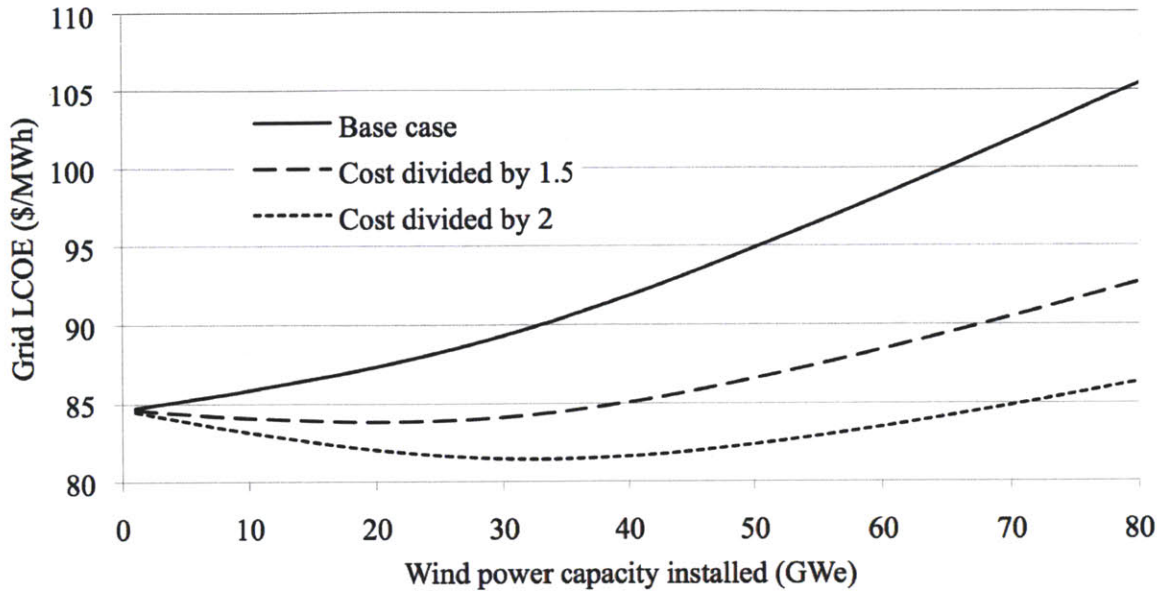


Figure 3-8: Effect of wind power cost reduction on global LCOE

competes with CCGT for electricity production, wind power penetration is indirectly affected by the fuel cost.

The fuel cost includes the cost of natural gas and the cost of carbon emission.

Equivalence between natural gas price and carbon cost

Based on our semi-empirical formula of the LCOE generated by CCGT (Figure 3.3), the equivalence between Natural Gas price and Carbon cost can be derived with regard to the effect on the LCOE generated by CCGT technology (Figure 3-9).

For the rest of the study, we will only refer to the "equivalent natural gas price", which includes the carbon cost.

Effect of natural gas price on global LCOE

The first effect of an increase of the fuel cost is to level the average cost of electricity produced in the grid, as expected. The second effect is to produce a new trend on the curve of LCOE vs wind capacity. As the cost of electricity produced by CCGT increases, wind power becomes more and more competitive economically, and its introduction makes the global cost of electricity decrease, as shown in Figure 3-10.

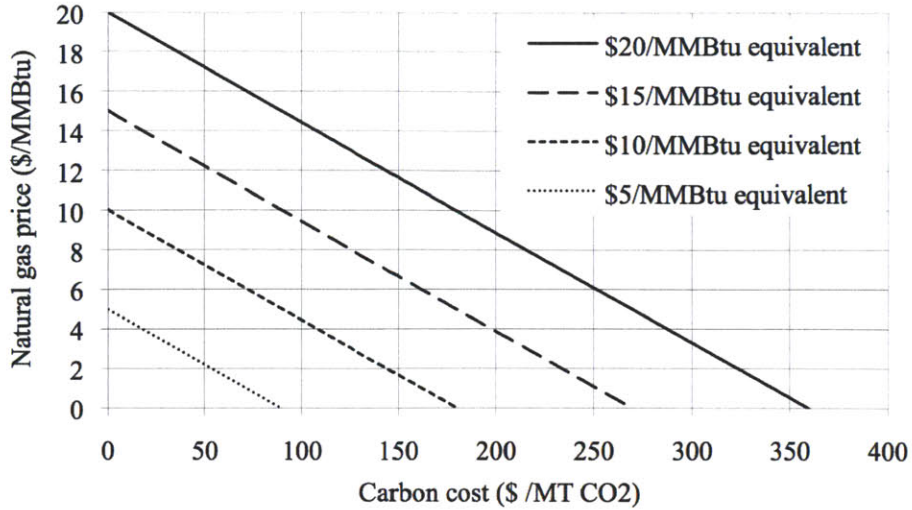


Figure 3-9: Equivalence between natural gas price and carbon cost

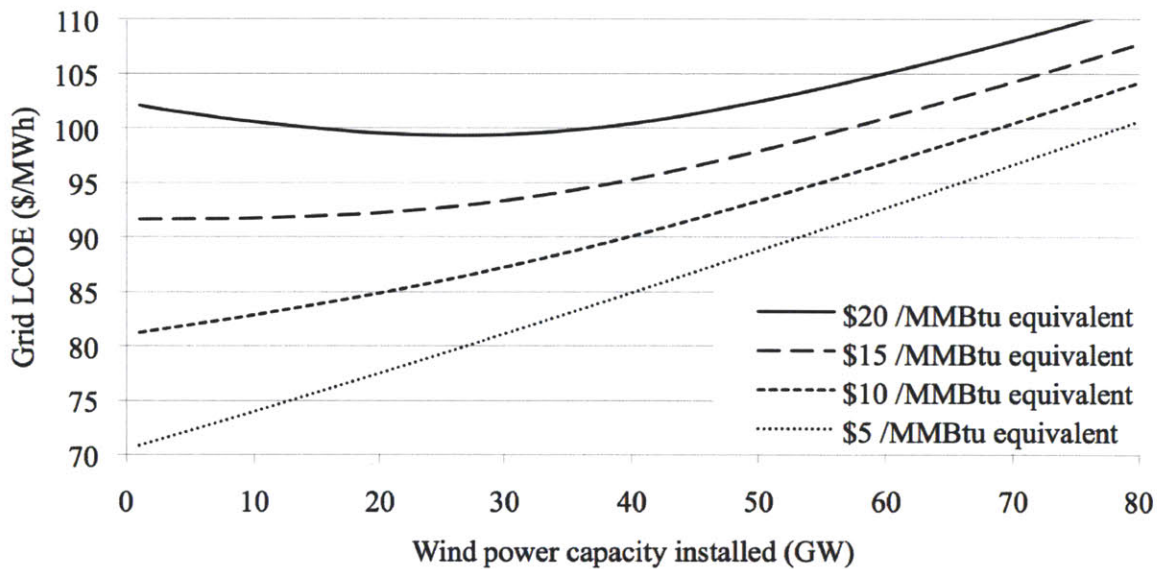


Figure 3-10: Effect of natural gas price on the global LCOE

An optimal share of wind power appears.

However, a bigger introduction of wind in the grid still makes the global cost of electricity increase, because the load factor drops as we dump more and more electricity.

Wind penetration is allowed for a fuel cost between \$15 and \$20/MMBtu equivalent. The optimal wind capacity is then around 25GW.

3.3.3 Carbon emission

One of the most outstanding features of the nuclear-renewables grid is its very low carbon emission level.

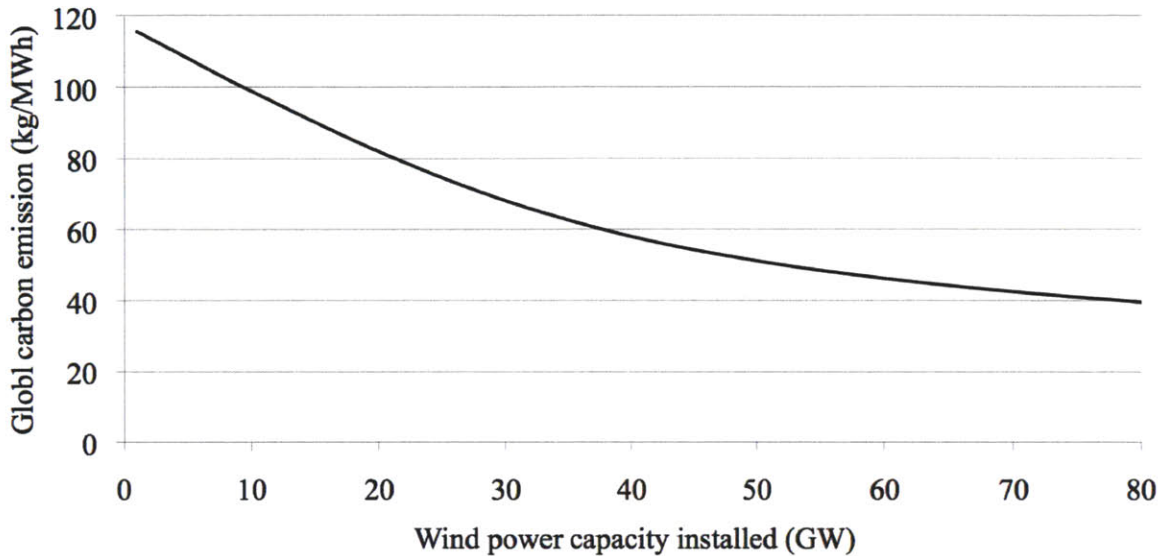


Figure 3-11: Carbon emission by the grid vs wind power capacity

A system including 40GW of nuclear, 57GW of wind and 57GW of CCGT capacity emits about 47 kg of carbon per MWh generated. As a comparison, the current emission rate is about 600 kg/ MWh in the US. Knowing that in the US, electricity generation counts for 40% of the total emissions, a great improvement can be achieved with such a new grid configuration.

3.4 Parametric studies with nuclear-hydrogen system

Next introduce nuclear-hydrogen systems in the grid, enabling the production of hydrogen from the excess wind power observed previously.

3.4.1 New assumptions

The size of the nuclear-hydrogen system (plant) is scaled on the size of the nuclear power plant. As calculated in chapter two, when all the power of a 1-GWe nuclear reactor (PWR) is used (diverted) for hydrogen production, 15.438GWe can be absorbed, or stored, to produce 120.810 kg of hydrogen per second. At times of high electric demand, the system provides electricity to the grid. This electricity comes from nuclear but also possibly from the HTE cells used in reverse as fuel cells.

Table 3.9: Hydrogen production by hybrid nuclear system

Nuclear power diverted	Maximal electricity converted	Corresponding hydrogen production rate
1,000 MWe (2857 MWth)	15.438 MWe	120.810 kg/s

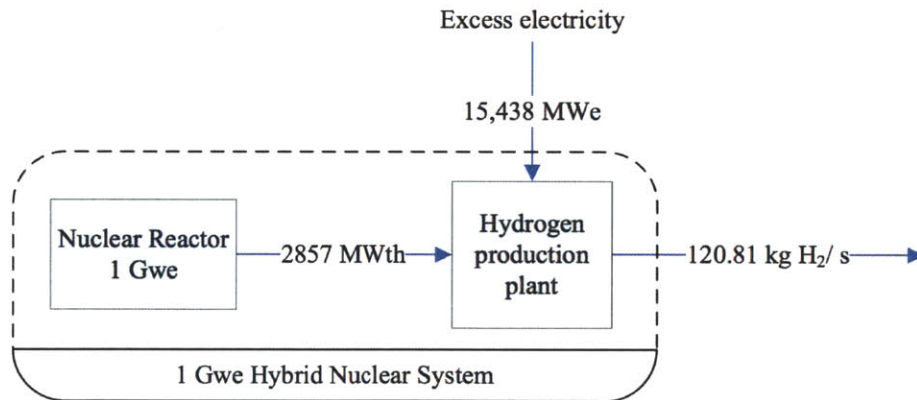


Figure 3-12: Flowsheet of the hybrid system while producing hydrogen

Levelized cost of hydrogen production

The levelized cost of hydrogen production (LCOH) is one of the most important parameters derived by the simulation. It accounts for all the costs over the lifetime of the hydrogen plant. It is expressed by

$$LCOH = \frac{\sum_{t=0}^{t=Te} \frac{CapitalCost(t)+OMCost(t)+ElectricityCost(t)+HeatCost(t)}{(1+r)^t}}{\sum_{t=0}^{t=Te} \frac{H_2Production(t)}{(1+r)^t}} \quad (3.3)$$

We start the analysis with the following assumptions (Table 3.10)

Table 3.10: Assumptions for LCOH calculation

Capital cost	\$400 /kWe electrolysis cell capacity
Degradation rate	2% /1000 hrs of operation (HTE as well as fuel cell mode)
Corresponding O&M cost	\$8 /MWh
Lifetime of the plant	30 years
Construction time	3 years
Purchase price of heat	Cost of nuclear electricity / η
Purchase price of electricity	\$40 /MWh (fixed)
Discount factor	7%

Table 3.11 reports the economic assumptions for the hydrogen storage and transportation cost.

Table 3.11: Hydrogen storage and transportation cost assumptions

	Capital Cost	O&M cost	Lifetime
Underground storage facility	\$8 per kg hydrogen of working capacity	neglected	20 yrs (+ 3 yrs construction)
Hydrogen pipeline	\$50 per m per in diameter	\$2.3 per m per yr	20 yrs (+ 3 yrs construction)

Price of electricity for hydrogen production

The price at which this excess wind electricity, which is also the price of electricity used for hydrogen production, is traded is of high importance, because it determines the cost of the hydrogen produced by HTSE. The electricity purchase is the major cost (with the cells capital cost) for the hydrogen producer, as shown in Figure 3-13.

In this example, for an electricity price of \$40/MWh, the hydrogen production cost is \$2.75/kg, and electricity represents more than the half of the production cost (40 GW of wind power and 1 GW of hybrid nuclear capacity installed, capital cost \$400/kW).

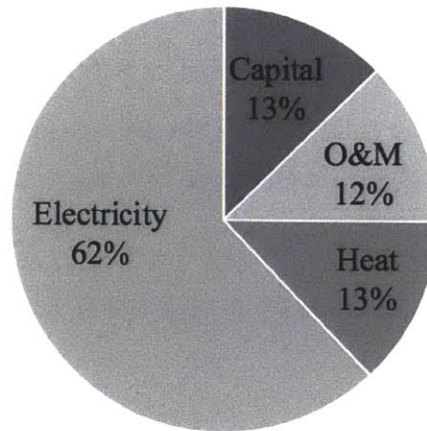


Figure 3-13: Typical LCOH breakdown

That said, it is very unlikely that the producer will purchase electricity at the average market price, for several reasons. Firstly, if so, the hydrogen would have a very high production cost, and would be totally uncompetitive with other hydrogen production processes (such as steam methane reforming). Secondly, the hydrogen producer will buy the electricity at time of low demand, during off peak periods. At that time electricity price is low, because the potential supply exceeds the demand. The lowest electricity generation technologies are online. Thirdly, in a grid that is significantly penetrated by renewables, the excess electricity generated at time of low demand must be absorbed (or cleared) by the grid, or exported. Wind producers and grid operators see hydrogen producers as a great bargain for them, because they facilitate the management of this excess electricity by consuming it.

For all those reasons (at least), it is very likely that an agreement (or a deal, contract) will be closed between wind and hydrogen producers, because they share common interests. It can be imagined that a contract will be signed that stipulates a fixed price of electricity, for minimal/maximal amounts of electricity traded per year, under specific conditions. However, it is difficult to assess all the details of the contract, partly because the situation has never occurred in practice since no hybrid system for hydrogen production has ever been built. The best one can do is to take the electricity exchange price between wind turbine holders and hydrogen producers as a parameter of the problem.

As an illustration plotted in figure 3-14 is the price of hydrogen production as a function of electricity price, for a capital cost of \$400/kWe. The O&M costs depend on the degradation rate of the cells. Today the cells degrade at a rate of 8%/1000hrs, but it is very likely that in the future that performance will be greatly improved.

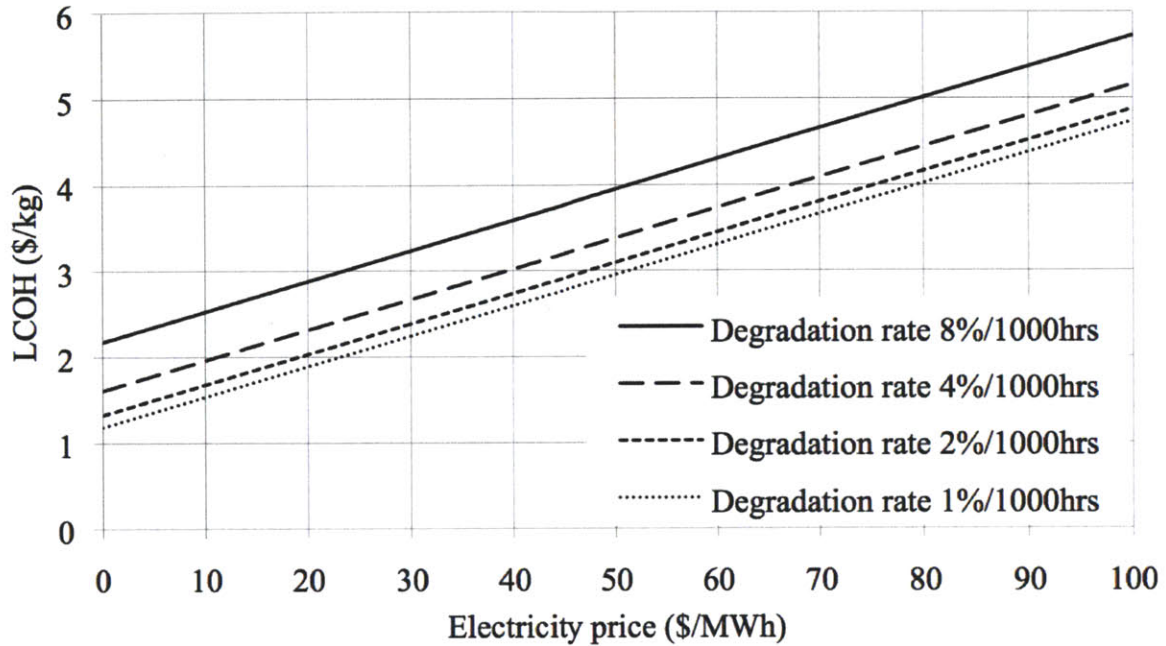


Figure 3-14: LCOH vs electricity price and degradation rate

Also plotted is the effect of the price of cells, for a degradation rate of 2%/1000hrs (Figure 3-15)

The correlated effect of a low price of electricity for hydrogen producers is that the income of the wind turbine holders is lowered. The selling price of wind excess electricity is below the LCOE level for this technology. In order to balance for this lower revenue on the hydrogen side, the generation cost of electricity from wind on the grid side must be increased. It results an increase of the global LCOE in the grid.

The profitability is expressed by the following expression, that gives the new LCOE for wind:

$$LCOE = \frac{\sum_{t=0}^{t=Te} \frac{CapitalCost(t)+OMCost(t)}{(1+r)^t} - \sum_{t=0}^{t=Te} \frac{ExcessElectricityPrice(t) \times Q_{elec-to-H_2}}{(1+r)^t}}{\sum_{t=0}^{t=Te} \frac{Q_{elec-to-grid}}{(1+r)^t}} \quad (3.4)$$

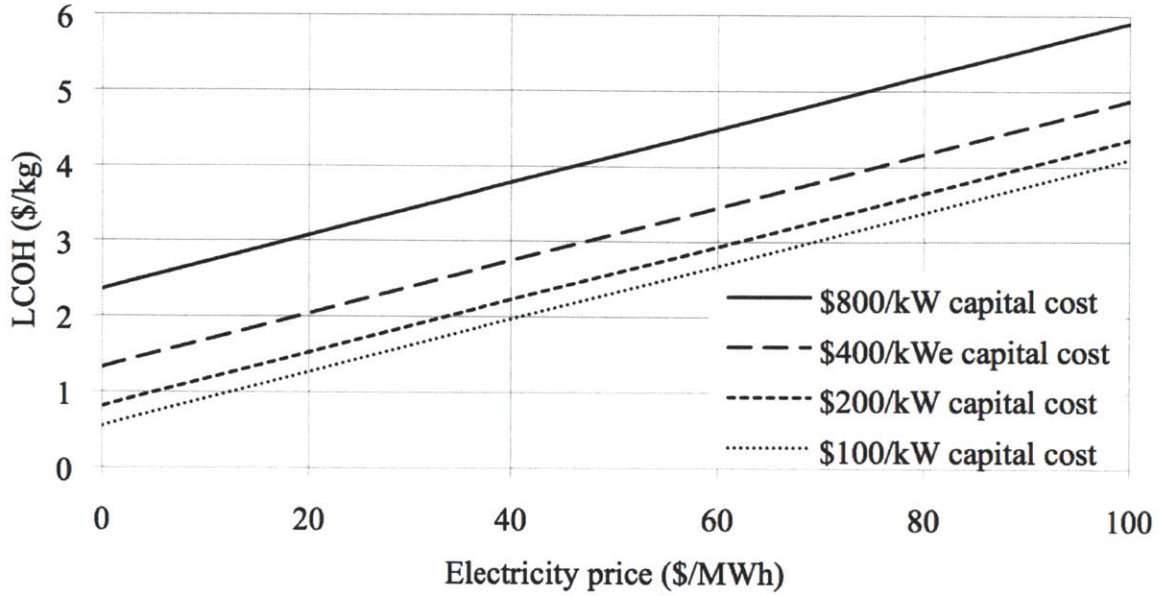


Figure 3-15: LCOH vs electricity price and capital cost

And based on our simple expression for wind LCOE, a simple expression resulted for the new LCOE (\$/MWh) for wind:

$$LCOE = \frac{Q_{tot}}{Q_{elec-to-grid}} \left(23 + 94 \frac{0.27}{LoadFactor} \right) - ExcessElectricityPrice \times \frac{Q_{elec-to-H_2}}{Q_{elec-to-grid}} \quad (3.5)$$

In Figure 3-16 are the variations of this new LCOE according to the installed hybrid nuclear and wind capacity for different trade prices of electricity between wind turbine holders and hydrogen producers (57 GW of wind capacity installed):

Free electricity delivered to hydrogen producers shrinks the income of the wind turbine holders. As a consequence they must increase the level of their bids to the grid operator as they sell more and more electricity to the hybrid nuclear plants. The green curve represents that trend. On the contrary, if the cost of electricity delivered to hydrogen producers is high, having more hydrogen producers increases the income of the wind power producers and decreases the marginal cost of selling electricity to the grid. The global cost of electricity on the grid decreases. In between those two situations, there is the case in which the global cost of electricity remains constant.

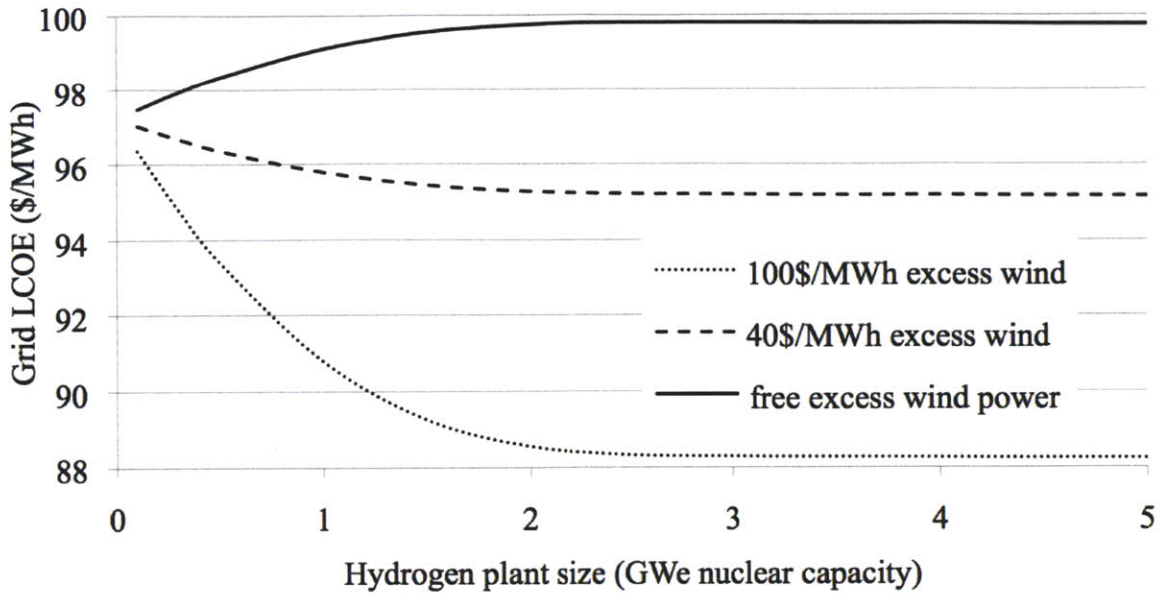


Figure 3-16: LCOE vs hybrid nuclear capacity and price of excess electricity

It is achieved for a selling price of \$20/MWh from the wind turbine holders to the hydrogen producers.

The same trend is observed for different wind power capacity (Figure 3-17)

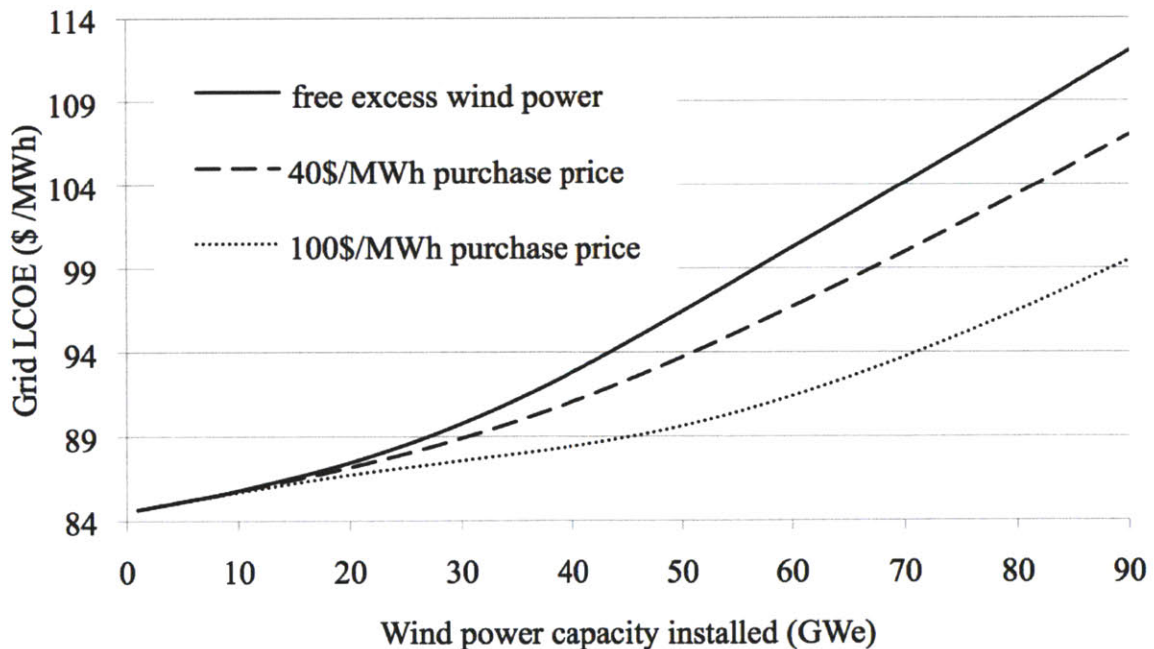


Figure 3-17: LCOE vs wind capacity and price of excess electricity

For the rest of the study, an intermediate price of electricity for hydrogen produc-

tion is chosen, equal to \$40 /MWh.

Electricity production by fuel cells

The key parameter for electricity production by the hydrogen plant is the efficiency of the fuel cells. For the analysis, a value of 40% was selected, which is conservative because the best fuel cells today achieve 60% efficiency. This conservatism makes sense because the cells are not designed primarily for electricity production. No added cost except the O&M costs are assumed. Again, this is conservative because recent experiments show an improvement of the cells lifetime when used in both directions instead of HTE mode only.

Table 3.12: Assumptions relative to fuel cells

Additional capital cost for modifying the hydrogen plant	Zero
Cell degradation	Same as in electrolysis mode (conservative)
Fuel cell efficiency	40% (conservative)

The fuel cell LCOE is related to the LCOH by:

$$LCOE_{FC} = \frac{LCOH}{\eta_{FC} \times LHV_{H_2}} \quad (3.6)$$

because the owner of the plant is indifferent to selling hydrogen or selling electricity produced with this hydrogen if both bring the same revenue to him. $\eta_{FC} \times LHV_{H_2} = 0.013$ MWh/kg is the energy value of one kilogram of hydrogen when it is used in 40%-efficiency fuel cells.

Summary of assumptions

In order to optimize the capacity of hydrogen production and the capacity of wind power for the MISO grid, a set of parametric studies were performed based on the realistic following assumptions:

- Price of CCGT fuel cost: \$13 /MMBtu equivalent

- Cost of wind turbines: 1.5 times lower than today's cost, hence \$78 / MWh at 26% load factor
- Capital cost of hydrogen production plant: \$400 /kw cell
- Degradation rate of the electrolyzer: 2% /1000hrs
- Price of excess electricity for the hydrogen producers and the wind turbine holders: \$40 /MWh
- Fuel cell efficiency 40%

The same set of assumptions as before concerning the grid demand and wind data was retained. The nuclear capacity and the CCGT capacity installed are still 40 GW and 57 GW, respectively. The parameters that vary are the wind power capacity and the size of the hydrogen plant.

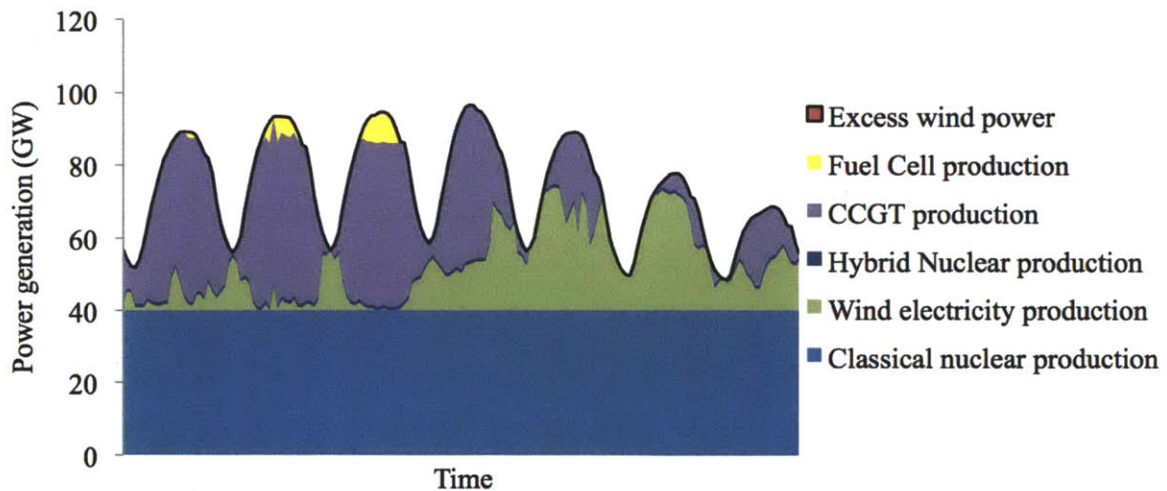


Figure 3-18: Generation dispatch with hydrogen plant - example of the last week of June 2009

Figure 3-18 is an example of generation dispatch in the last week of June 2009, for a hybrid nuclear capacity of 1 GW and 40 GW of wind turbines installed. Notice that there is no excess power anymore, since it is now used for hydrogen production (Figure 3-19). Fuel cells complete the power supply when the CCGT capacity is not large enough to meet the demand. As it will be seen, it is more economical to

produce power with fuel cells than with gas turbines when it comes to produce the last gigawatts of peak power.

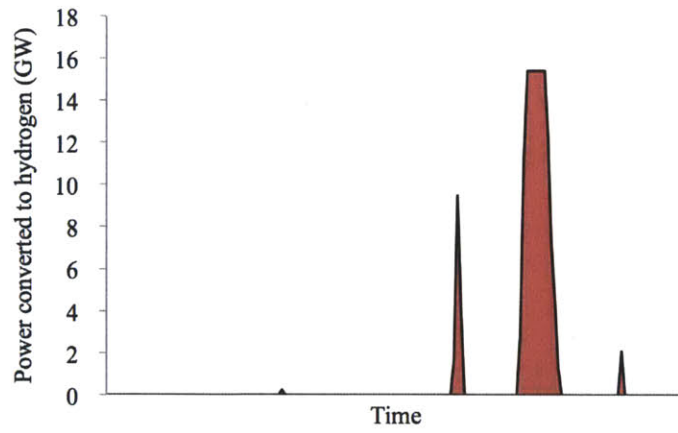


Figure 3-19: Power converted for hydrogen production - example of the last week of June 2009

It is nevertheless still possible to have excess electricity since the hydrogen production capacity is limited.

3.4.2 Results

Excess electricity

As expected, the excess wind electricity is large when a significant amount of wind energy penetrates the grid. It reaches several gigawatt-year when 30 GW capacity are added, which possibly represents hundreds of millions dollars in losses.

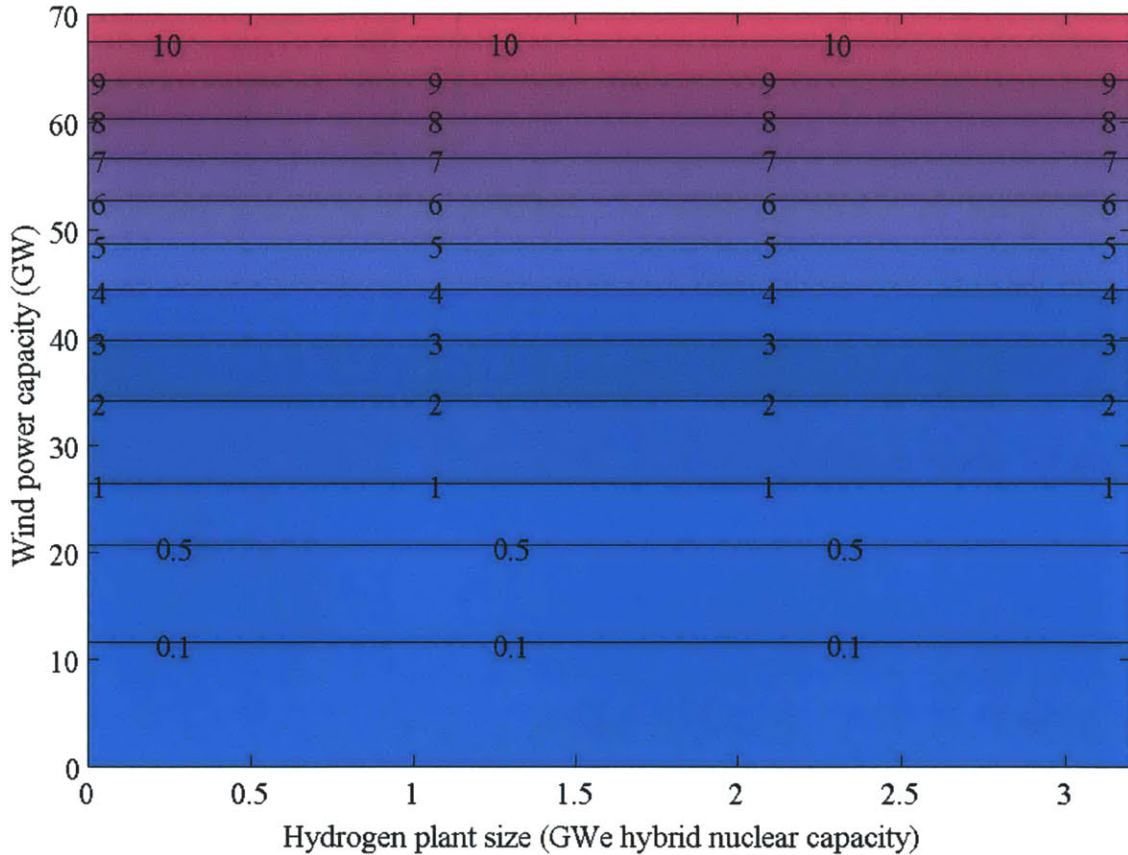


Figure 3-20: Excess wind electricity (GW-year) without hydrogen production

The introduction of hydrogen production shows a large reduction of the power generated in excess (Figures 3-20 and 3-21). The system absorbs the excess electricity and converts it into hydrogen, provided that the hydrogen facility is large enough. A small hydrogen facility can not absorb all the excess electricity produced by large wind farms, as seen on the top left corner of the figure.

Allowing a variable hydrogen production at time of excess electricity is a very important improvement from a grid operator point of view. The management of the

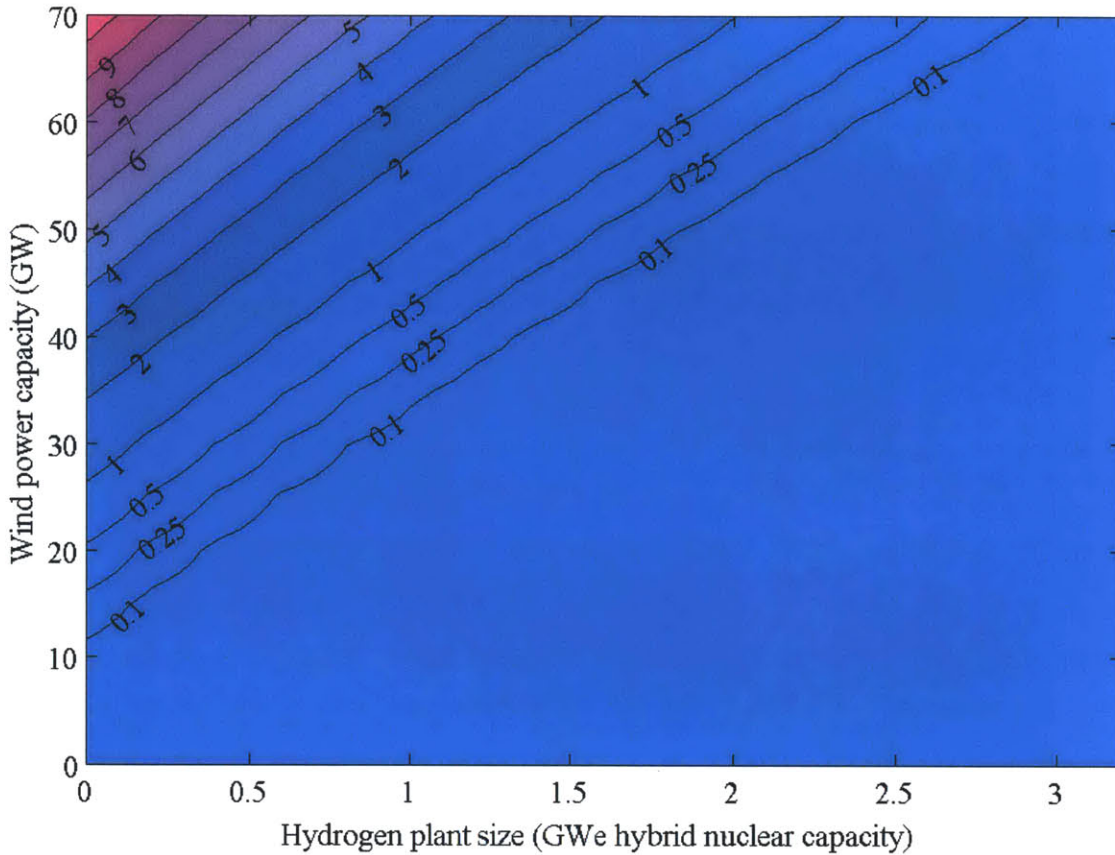


Figure 3-21: Residual excess wind electricity (GW-year) with hydrogen production

intermittent and unpredictable energy sources like wind turbines becomes feasible at a large scale, and enables their penetration in the grid.

Hydrogen Production

The amount of electricity converted to hydrogen gives the total hydrogen production, plotted in Figure 3-22. It grows with the size of the hydrogen plant but foremost with the wind power capacity, because it provides more excess wind electricity. Indeed, the electricity generation meets primarily the demand of the grid rather than the demand of the hydrogen plant owner. If there is no excess wind electricity, the hydrogen plant does not produce hydrogen. The nuclear units produce electricity for the grid, which is more economical for them.

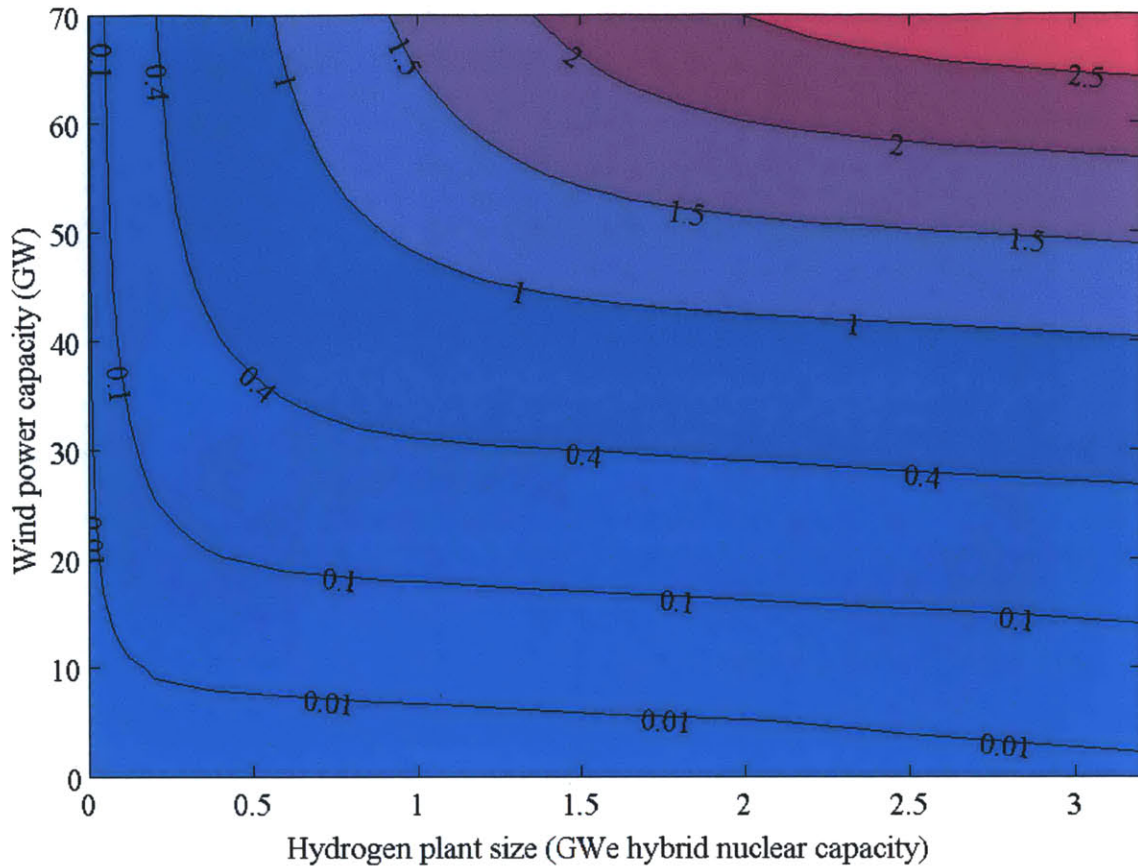


Figure 3-22: Total hydrogen production (million MT /yr)

Peak electricity- and net hydrogen production

As shown earlier, the hydrogen plant has the ability to produce peak power by using the electrolysis cells as fuel cells. The peak power generation capacity is directly proportional to the size of the hydrogen plant and to the efficiency of the fuel cells. Typically, the equivalent of a GW nuclear plant with high temperature electrolysis cells operated as 40%-efficient fuel cells has a generation capacity of 11.4 GW, which is enough to displace tens of gas turbine units. Those fuel cells come online in last resort, when the demand for electricity is high and when all the other generation units are at full power. It does not happen often, as shown by Figure 3-23 that plots the operation time of the fuel cells per year. It barely exceeds one thousand hours per year. This figure is a result of the specific wind characteristics of North Dakota and the electricity peak demand profile as shown earlier in Figure 1-6.

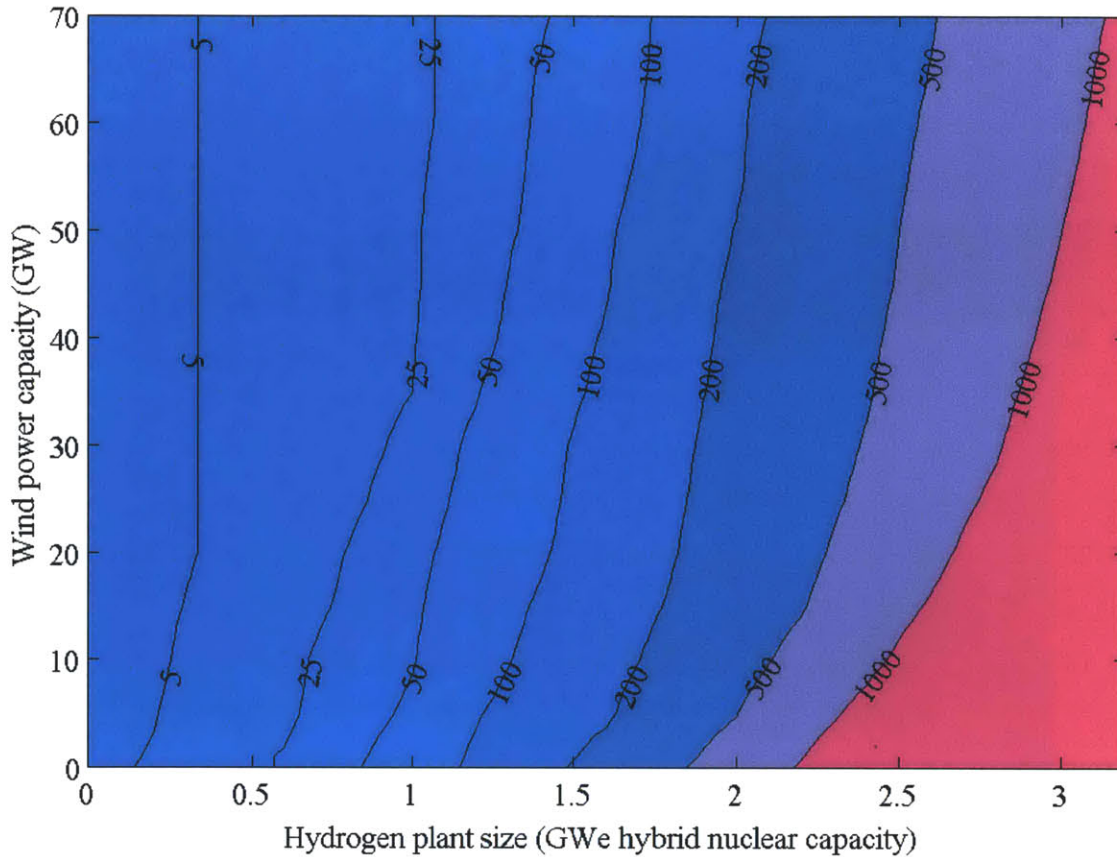


Figure 3-23: Fuel cell operation time (hours /yr)

The peak electricity generation by the hydrogen plant affects the net hydrogen production since hydrogen is consumed to produce electricity. The net hydrogen production (production minus consumption) can even become negative in the case where the hydrogen plant is very large and the wind power capacity small (resulting in limited excess electricity available for hydrogen production), as shown in Figure 3-24 in the right lower corner. With small hydrogen plant sizes, hydrogen plant capacity limits hydrogen production whereas with large plant capacities, availability of excess electricity limits hydrogen output. Net production of about one million MT hydrogen can still be achieved by a medium size nuclear hydrogen plant (1-2 GW), enough to supply by pipeline the hydrogen demand of a region like the Great Lakes or Alberta.

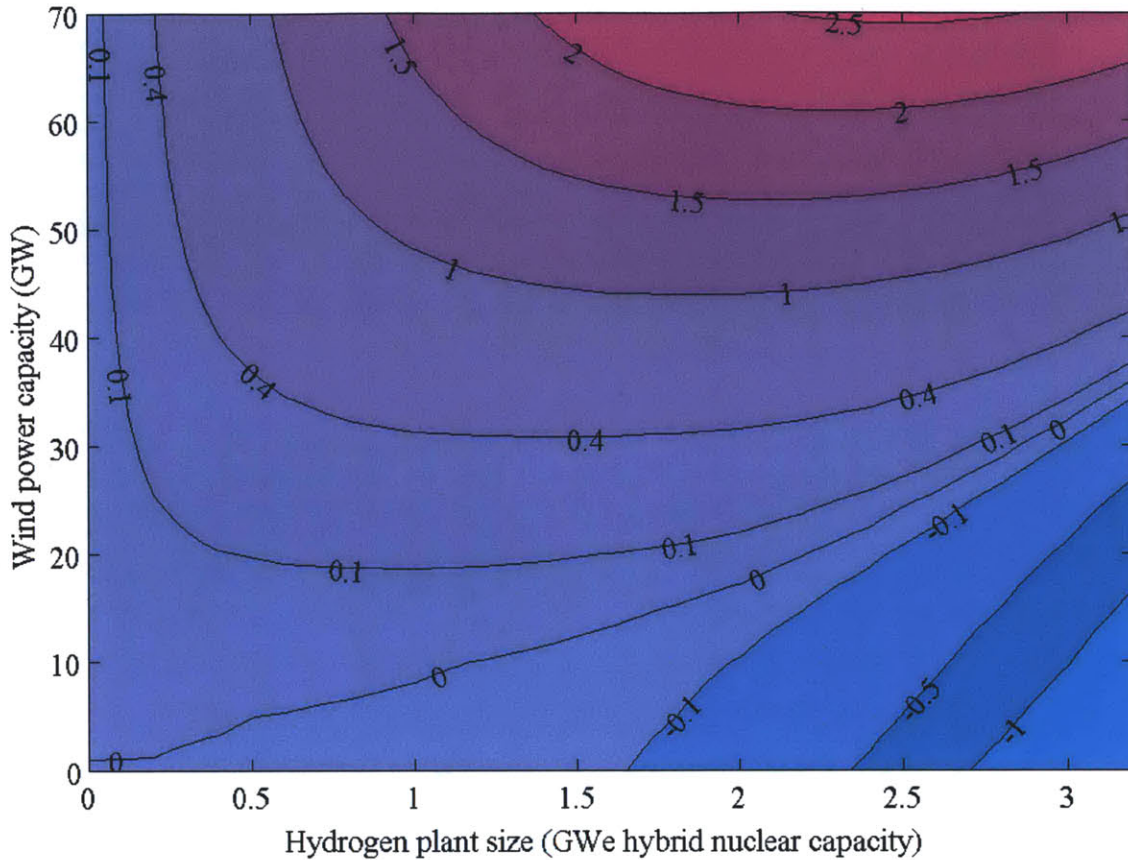


Figure 3-24: Net hydrogen production (million MT /yr)

Cost of hydrogen

The levelized cost of hydrogen (LCOH) is certainly the most interesting indicator for an investor in a hybrid nuclear plant. It is closely linked to the capacity factor of the electrolyzer cells, so that when we increase the hydrogen capacity (number of cells increases), the cost increases as well. On the contrary when more wind power capacity is installed, the electricity available for electrolysis is more important and the cost decreases.

One recalls that the LCOH calculated here does not account for a possible transportation cost (typically half a dollar per kg for a 1000km-long pipeline).

Depending on the cost of hydrogen produced by other technologies such as SMR, one can determine what is the size range that makes the plant competitive.

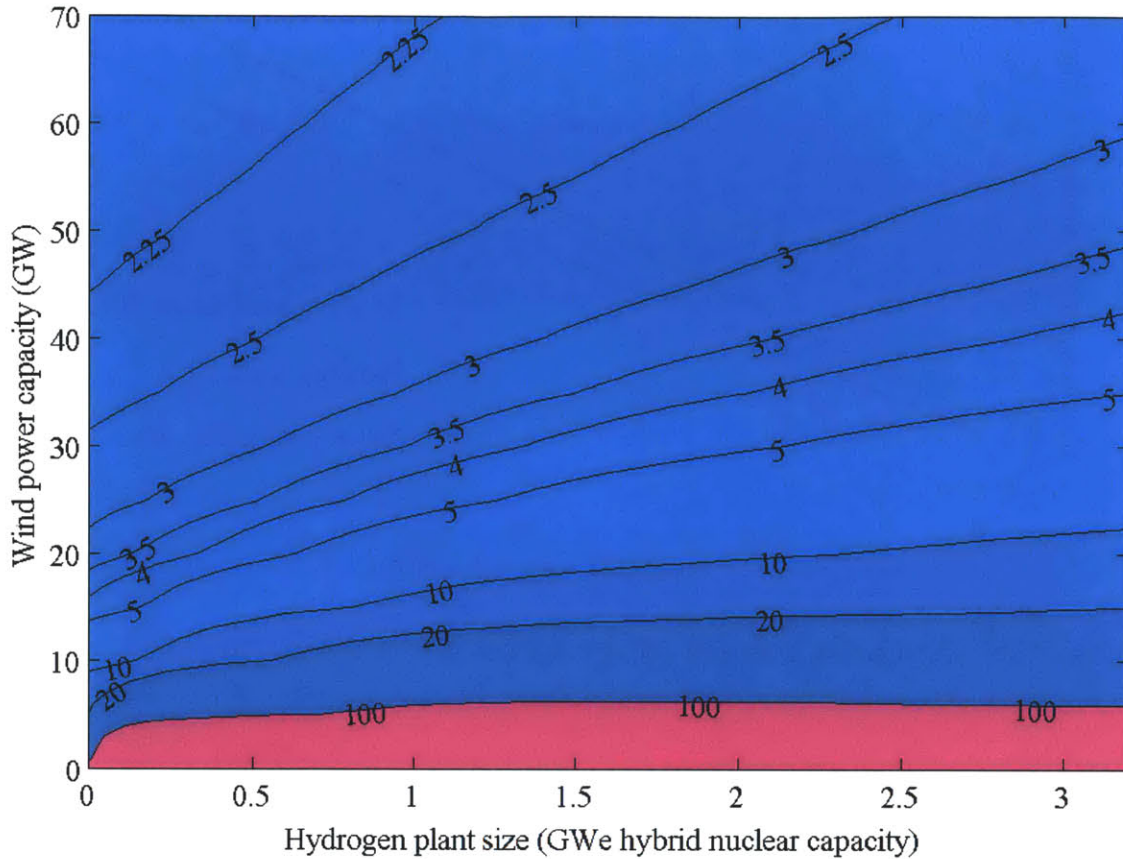


Figure 3-25: LCOH (\$ /kg) vs wind power and hybrid nuclear capacity

Comparison with steam methane reforming

The price of natural gas has a big impact on the price of hydrogen since more than 95% of the hydrogen produced today is based on the steam methane reforming (SMR) process. Hence if we want to invest in high temperature steam electrolysis to produce hydrogen, the higher the price of natural gas, the more justifiable is the construction of hydrogen production plants using HTSE.

The production cost of hydrogen in a steam methane reforming plant depends significantly on the size of the facility. In our case, a large plant is considered (above a few tens of thousands of MT per year).

Several correlations have been found in the literature [27, 13, 25]. The accuracy and precision of the results do not give complete satisfaction since they are all between five and seven years old. The cost given in the INL study is higher but refers to the

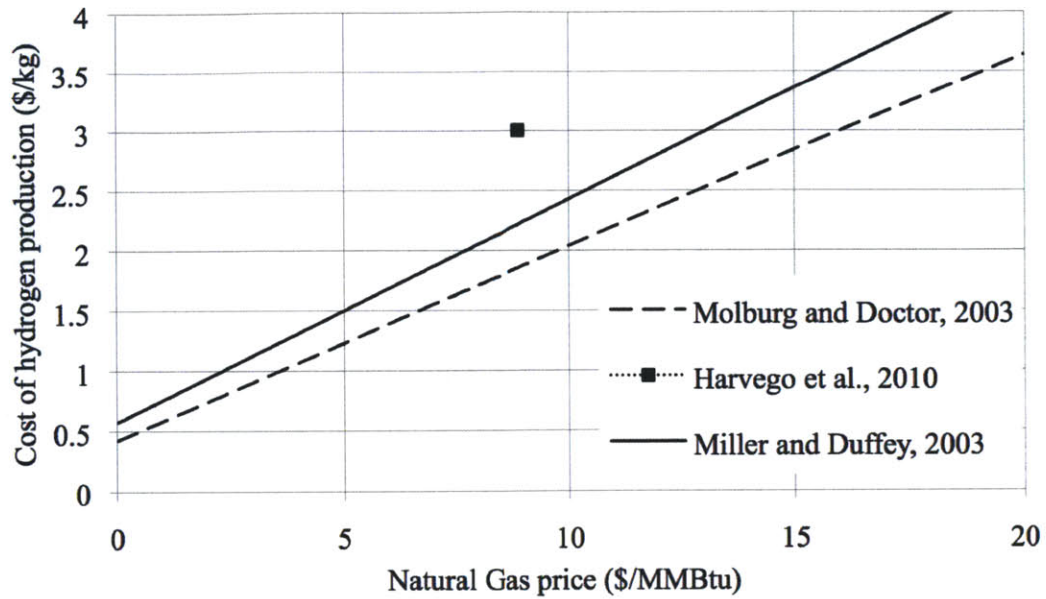


Figure 3-26: Correlation between NG price and hydrogen production cost (in 2010 US \$)

market price, therefore higher than the production cost (Figure 3-26).

In our case, if the cost of natural gas is \$13/MMBtu, the hydrogen price will be around \$3/kg. If the wind power capacity installed is 40 GW, a hybrid nuclear plant is competitive up to a size of 1.5 GW. Once again, it is seen that the natural gas price is a very important parameter for the competitiveness of the nuclear-hydrogen plant.

Cost of electricity

The grid-averaged cost of electricity, that is the cost of electricity generated by the different energy sources weighted by the electricity generation from those sources, is plotted in Figure 3-27.

The introduction of wind power raises the cost of electricity for large capacities, because the excess wind power is bought at a low price by the hydrogen plant owner. If too many wind turbines are present, since the excess electricity generated and sold does not cover the capital cost of the wind farms, the electricity generated by wind becomes more expensive and thus the grid electricity as well. The hydrogen plant reduces the cost of electricity because the fuel cells displace the expensive gas

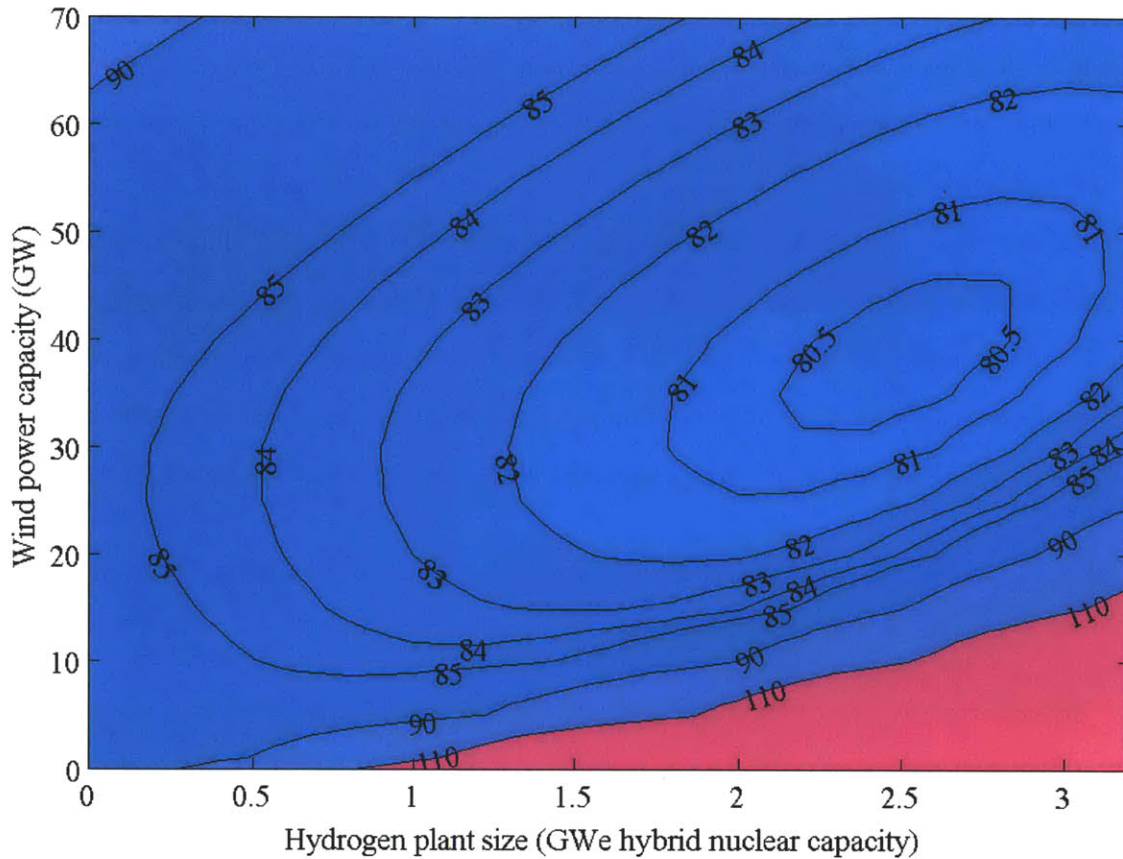


Figure 3-27: LCOE (\$ /MWh) vs wind power and hybrid nuclear capacity

turbines that are used a few hundred hours a year. However at some point gas turbines operating on natural gas are more economical than fuel cells, and the effect is reversed. That match point is about 700 hours of operation per year. The cost of electricity generated by the grid as a whole hence presents an optimum. That optimum for electricity is not optimal for hydrogen though, because the LCOH is high (about \$4/kg). This suggests deriving an optimum that takes into account both commodities.

Optimization

To evaluate the optimal wind power capacity and hydrogen plant size, one considers the point of view of a utility that owns both the entire generation fleet and the hydrogen plant. Such an actor would try to maximize its profit expressed by the difference between the sales revenue and the costs generated from both electricity and

hydrogen production. For such calculation, the price of electricity and hydrogen at which these commodities are sold is unknown. We decide instead and for simplicity to set them at a fixed value since we are here concerned by the relative profit yielded by the different cases.

The reference case taken here is the one when 1) hydrogen plant size = 2GW hybrid nuclear and 2) wind capacity = 50GW. In that case grid-average LCOE = \$81.7 /MWh and LCOH = \$2.84 /kg. They are the values considered as reference prices of electricity and hydrogen. The relative profit is thus the difference between the revenue (at the reference prices stated before) and the cost of production:

$$Profit_{rel} = Q_{elec} \times (\$81.7/MWh - LCOE_{grid}) + Q_{H_2} \times (\$2.84/kg - LCOH) \quad (3.7)$$

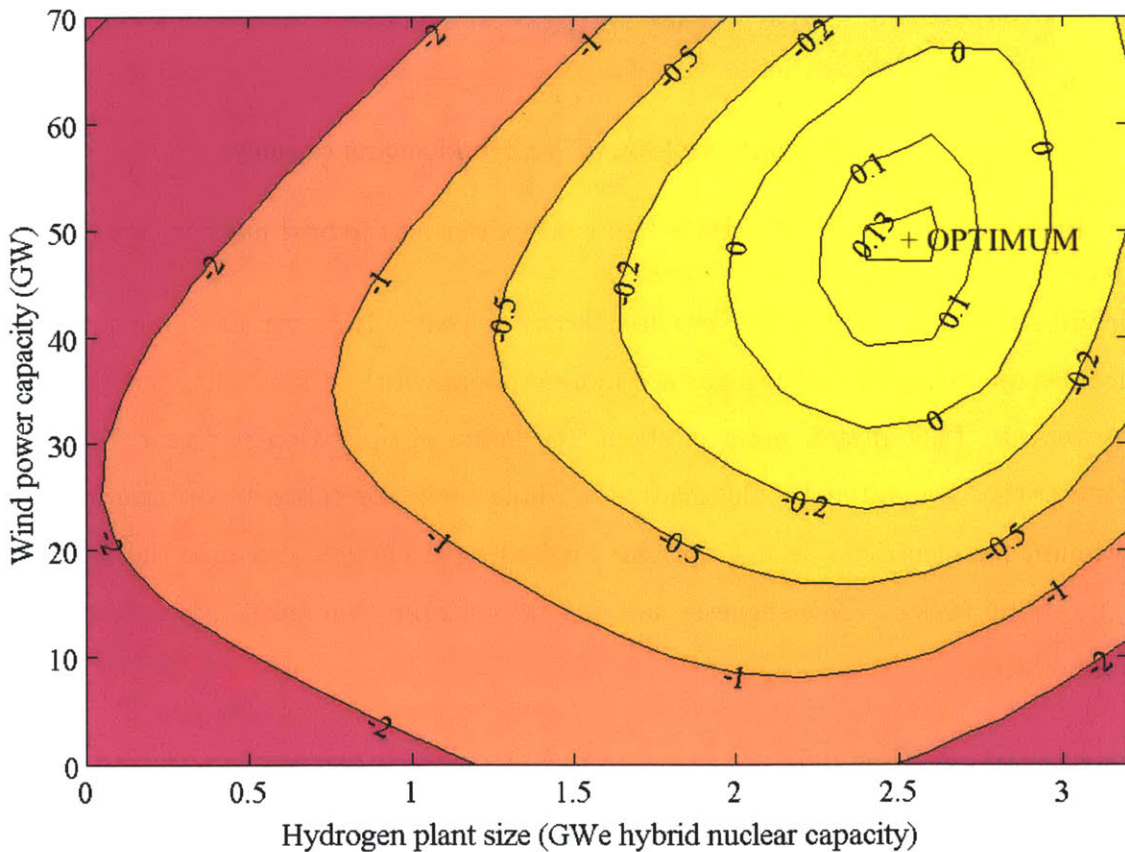


Figure 3-28: Relative total profit (billion \$ /yr)

The reference case appears logically on the contour 0 of Figure 3-28. One observes

an optimum for a hydrogen plant size of 2.5 GW hybrid nuclear capacity and for a wind power generation capacity of 50GW. It corresponds to a LCOH of about \$3.1 /kg, a grid-average LCOE of \$81 /kg. The net hydrogen production is 1.3 million MT /yr and the fuel cells are operated about 500 hrs a year. A total of 5.5 GWyr of excess wind power are converted to hydrogen every year.

3.5 Summary

The potential benefits of the introduction of a renewable-nuclear hybrid energy system in the grid are summarized in Table 3.13. Once again recall that the analysis is based on assumptions that are uncertain in the future: foremost an expensive natural gas price and a cost reduction factor of 1.5 for wind turbines. Without these assumptions, building a nuclear-renewables-hydrogen system is not relevant economically.

One can first notice that the system enables the presence of a large amount of wind energy in the grid (26% of the total electricity generated, see Figure 3-29), greater than what is observed anywhere today. Wind power is economically attractive. The cost of the electricity generated is significantly reduced by the hybrid system (5% cost reduction) because the expensive gas turbines formerly used a very limited time per year are replaced by fuel cells for peak power. Indeed, the fuel cells are equivalent to almost 30GW generation capacity.

The hydrogen production is large, and represents a significant part of a large market like the United States (9 million MT consumed per year today) or Europe. The cost of that hydrogen, \$3.1/kg, is high, which means that the steam methane reforming process will need to become more expensive to make the deployment of high temperature electrolysis competitive; typically it requires natural gas to be expensive. However several factors relative to the assumptions used can make that cost decrease. Looking at Figure 3-30, one notices that electricity purchases are responsible for more than half of the cost of production. We assumed a fixed cost of \$40/ MWh, but it could be lower if the wind turbine owners would accept a lower price for the sales of their

Table 3.13: Summary - system benefits

	Wind, nuclear, natural gas system	Wind, nuclear, natural gas system with HTE-FC
Grid-average LCOE	\$85.5 /MWh	\$80.9 /MWh
Optimal wind power capacity in the energy mix	25 GW 14% of the total electricity generation	50 GW 26% of the total electricity generation
Fuel cell peak electricity generation capacity	0	28.5 GW
Hydrogen plant size	0	2.5 GW of hybrid nuclear capacity
Net hydrogen production	0	1.3 million MT /yr
Hydrogen storage requirement	0	0.3 million MT /yr
Hydrogen transportation requirement	0	Two pipelines of 36-in diameter and 1,000 km length
LCOH	N/A	\$3.1 /kg
Levelized cost of hydrogen storage and transportation	N/A	Storage: \$0.2/kg Transportation: \$0.3/kg
Relative carbon emission	1	0.56

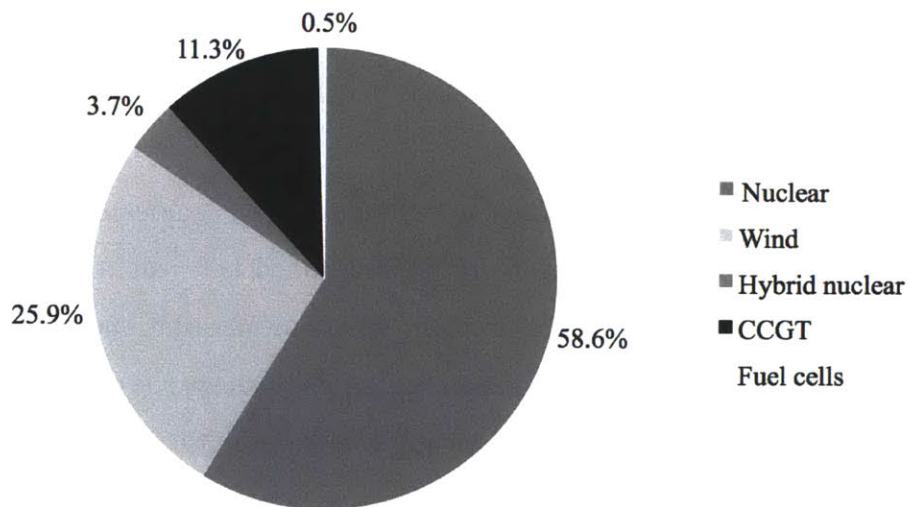


Figure 3-29: Electricity generation breakdown

excess electricity. The longer lifetime of the cells expected when they are occasionally operated in reverse and at high pressure could reduce the O&M costs significantly compared to our assumptions. Last but not least, the important savings generated by the elimination of the low-CF gas turbines in the grid could be incorporated in the cost of hydrogen to make it more attractive. While only 0.5% of the electricity is generated by these fuel cells, there are major capital savings. What the analysis shows is that the electricity game is much more important than the hydrogen game in terms of economic incentives to build the system in a regulated market for electricity.

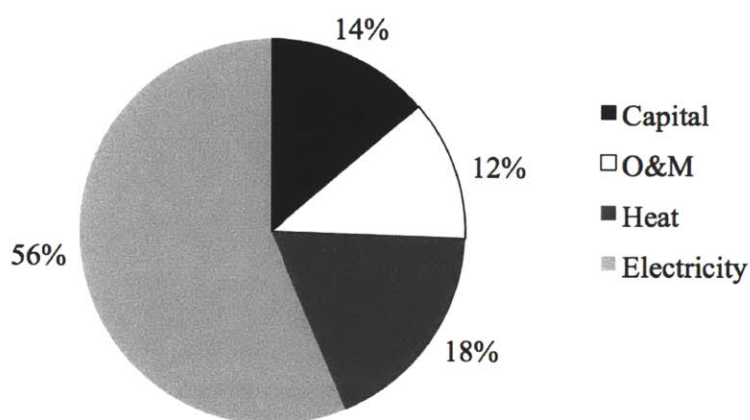


Figure 3-30: Hydrogen production cost breakdown

The storage requirement for hydrogen is important (300,000 MT /yr), which would probably require several underground storage facilities. Two 36-in diameter pipelines are required to ship the hydrogen product to industrial users that are located 1,000 km away from the Dakotas. The incremental costs due to storage and transportation are respectively \$0.2 and \$0.3 per kilogram of hydrogen.

Finally the environmental benefit of the system is large. The replacement of gas turbines by fuel cells and wind turbines cuts the greenhouse gas emission of the grid by 44%. 89% of the electricity is generated without carbon emission, which is outstanding.

Chapter 4

Economic analysis - deregulated market

In the previous economic analysis, we analyzed the benefits of introducing the nuclear-hydrogen plant in an electricity generation portfolio where wind energy (and clean energy technologies in general) represented most of the generating output. The standpoint we adopted was the one of a central planner who would own the entire generation fleet and who would meet the electricity demand while minimizing its generation cost. This situation is the one of a grid where a utility owns the entire generation capacity, which is the case in regulated electricity markets. In that case, the electricity prices are under the surveillance of the regulator (the state). Regulated electricity markets used to be dominant in the past, because the market characteristics (high investment costs and characteristics of the grid) favored the presence of a natural monopoly in the form of vertically integrated utilities [8].

However, for several reasons that are not the subject of this thesis, electricity markets began in the nineties to be deregulated. This happened in the United States, but also in Europe. The electricity generation activity became separated from the transmission and distribution activities by law. The idea is to provide to any investor the ability to build a generation plant and have access to the transmission lines to sell electricity. In practice the grid operators, responsible for the grid dispatch, collect every day the generation bids (prices and capacities) from the electricity producers

and assign generation schedules to them for the next day based on price minimization¹. From the point of view of the producers, the strategy is completely different. The goal is now to maximize profits.

In terms of economic analysis, we have now multiple investors who, theoretically, have little control on prices². The investment decision is taken while considering the prices as given. In the case of a nuclear-hydrogen plant, the investor looks at the prices to assess the opportunity of building the system and making a profit. This is the analysis carried out in this chapter.

4.1 Methodology

In this analysis one considers the investment in a nuclear-hydrogen plant to produce hydrogen and electricity. The electricity price is now the only signal that decides if the plant produces electricity or hydrogen. If the price is low, electricity is purchased from the grid and heat is diverted from the nuclear reactor to produce electricity by HTE. At time of high electricity price, electricity is produced by the HTE cells used in reverse as fuel cells and sold to the grid; hydrogen is consumed.

One notices here that the power generation from renewables is, as opposed to the regulated market case (chapter 3), not directly known. In fact, renewables penetration affect the prices. There are debates among experts about whether it raises the prices or on the contrary lowers them. We will discuss the effect more in detail later but it seems that the prices are more "peaky", i.e. lowest prices are lowered and highest prices are raised by the penetration of renewables. It makes therefore energy storage technologies like ours particularly interesting.

In order to be consistent with the regulated market case analysis, the economic assumptions and input data are kept as identical as possible. The electrical grid

¹The optimization process is more complicated in practice, because there are network constraints (line congestion), ramping constraints, start-ups and shutdowns, and thermal losses, for example, to consider. Furthermore there are different timescales: day-ahead and real time dispatch, to account for short-term generation changes in the grid (plant unavailability or wrong forecast of renewables generation).

²This is true if the producers are small and numerous; in short, in a case of perfect competition

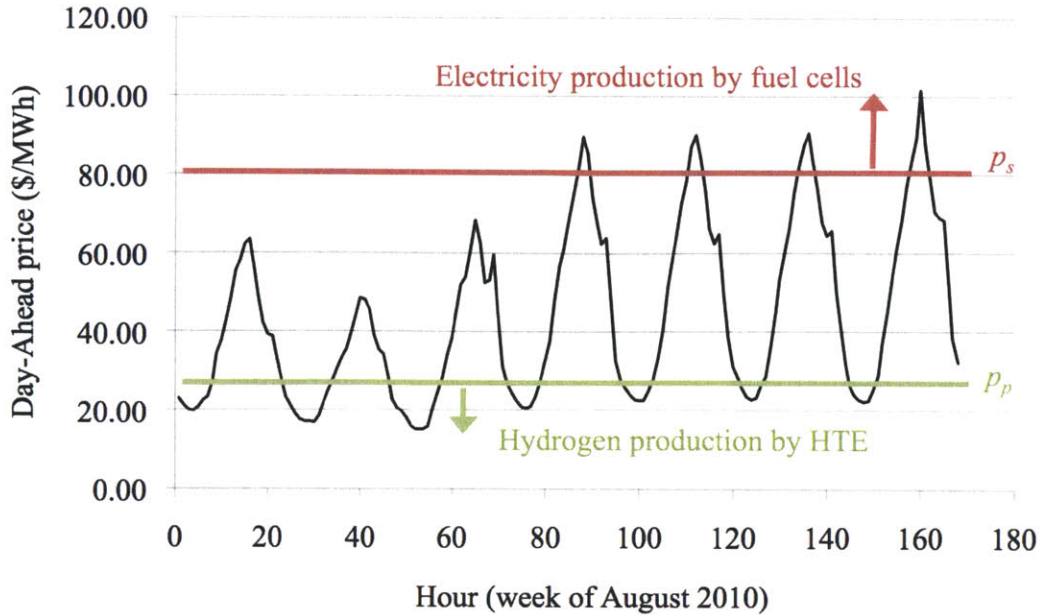


Figure 4-1: Operation modes of the hydrogen plant in a liberalized electricity market

considered is still the Midwest ISO. Day-ahead on a hourly basis have been collected [29] for the year 2010. The prices range from 0 to \$101/MWh and the average price is \$32/MWh.

The LCOH is calculated with the same assumptions as in the previous case, with the major difference that now the electricity is purchased at the market price, and not at the fixed price of \$40/MWh. A lower LCOH is therefore expected. Heat is purchased at a fixed price from nuclear, which makes sense because the nuclear unit runs at steady state and belongs to the nuclear-hydrogen plant. The other assumptions are summarized in Table 4.1.

It is assumed that the introduction of the system does not modify the prices of electricity. It is a reasonable assumption as long as the system is small compared to the size of the grid. It is the case here because the absorption and generation capacity of the system does not exceed a few gigawatts within a grid whose load varies between 40 and 97 GW (in 2009).

Table 4.1: Assumption for LCOH calculation

Capital cost	\$400 /kWe cell capacity
Purchase price of electricity	market price
Purchase price of heat	\$70/MWh electric = \$24.5/MWh thermal
O&M cost	\$8/ MWhe through the cells (degradation rate of the cells = 2% /1,000 hrs)
Lifetime of the plant	30 years
Construction time	3 years
Discount rate	7%

4.2 Results

4.2.1 Hydrogen production

The hydrogen production of a 300 MWe nuclear-hydrogen plant over one year was simulated. Such a plant has a maximal conversion rate of 4.63 GWe power to hydrogen (see chapter 2 for details). It is considered that it is always possible to buy such a quantity of power on the grid, without changing the price³.

The key parameter for hydrogen production is the maximal price at which electricity is purchased on the grid, p_p , because it determines when the plant will produce hydrogen or not. The higher it is the more often the plant will produce hydrogen, but also the higher the purchase price will be.

Figure 4-2 shows the total hydrogen production and cost of hydrogen vs p_p . One notices that for low p_p the hydrogen production is not high enough to recover the capital cost of the plant, resulting in a very high cost of hydrogen. For high p_p the cost of electricity becomes high and raises the cost of hydrogen production. In between there is an optimum point, a minimal cost of hydrogen. It occurs for a maximal purchase price of electricity p_p about \$30/ MWh. At this price the LCOH reaches \$1.5/kg, which is much lower than the LCOH obtained in the case of a regulated market (\$2.5/kg). Indeed, electricity is purchased at a average price of \$13.9/MWh instead of \$40/MWh.

³The average load is 62 GW and the minimal load 40 GW.

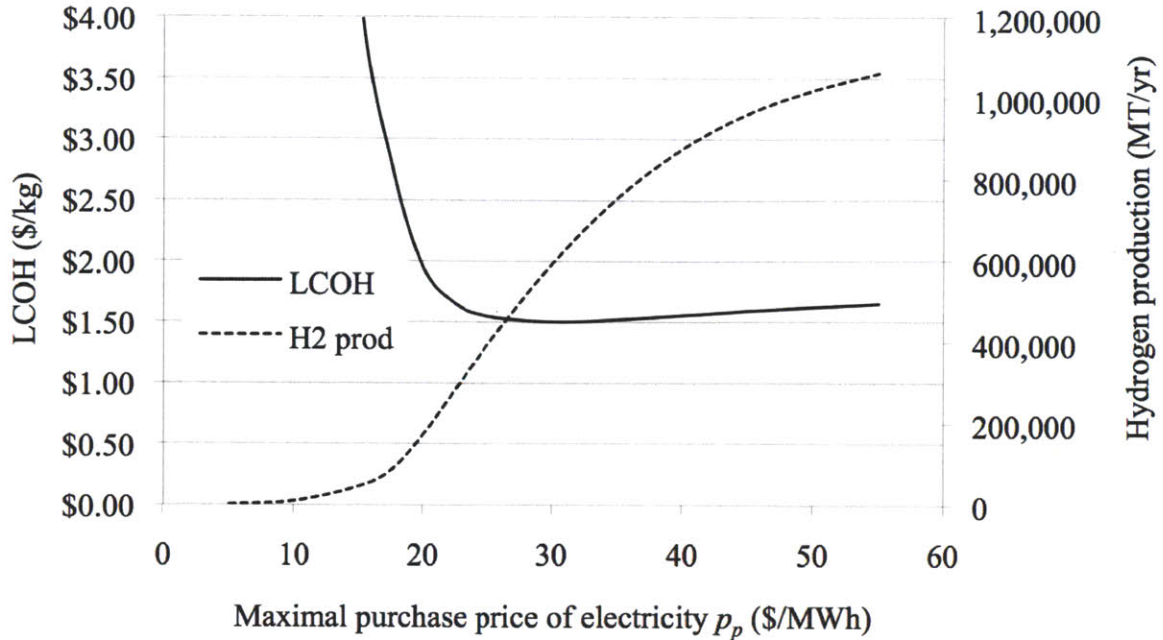


Figure 4-2: Hydrogen production by a 300MWe nuclear-hydrogen plant in a liberalized market

For the optimal $p_p = \$30/\text{MWh}$, the cell capacity factor is 52% and the LCOH breakdown is represented by Figure 4-3. Electricity is still the major cost contributor.

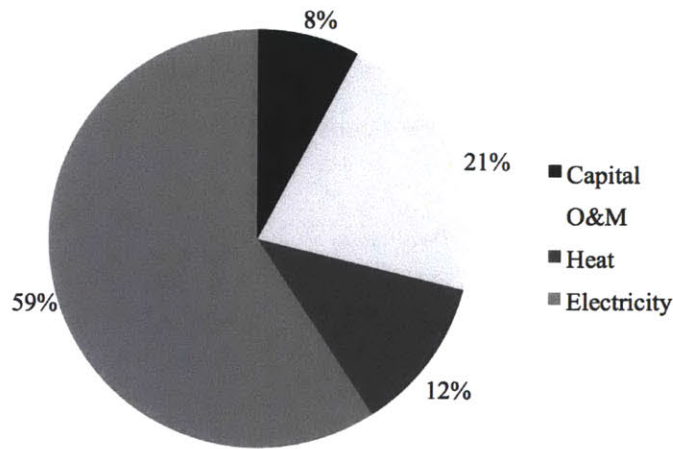


Figure 4-3: LCOH breakdown for the optimized case in a liberalized market

A hydrogen cost of \$1.5/kg by HTE is competitive with steam methane reforming if the natural gas cost is above \$5-7 /MMBtu (see Figure 4-4). Today's cost is \$4/MMBtu.

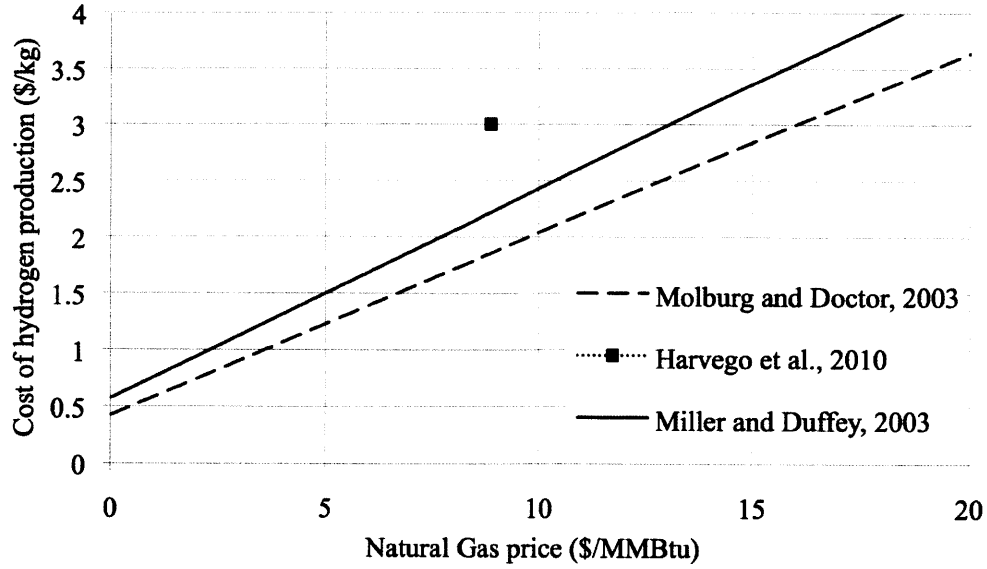


Figure 4-4: Impact of natural gas price on hydrogen production cost (steam methane reforming process)

4.2.2 Electricity production

Electricity production and sale is likely to occur if the electricity price reaches a minimal price p_s . This price is equal to the cost of burning one unit of hydrogen in fuel cells to convert it to electricity. The hydrogen value here is the market price of hydrogen p_{H_2} , because one considers that the hydrogen produced is sold on the market. Electricity production hence occurs if

$$p_{electricity} > p_s \quad (4.1)$$

with

$$p_s = \frac{p_{H_2}}{LHV_{H_2} \times \eta_{FC}} + C_{O\&M} \quad (4.2)$$

LHV_{H_2} is the Low Heating Value of hydrogen (120.1 MJ/kg), η_{FC} the fuel cell efficiency and $C_{O\&M}$ the operation and maintenance cost of producing electricity in the fuel cells.

The calculation gives $p_s = \$135/\text{MWh}$. It is higher than the maximal price in

Table 4.2: Assumptions for p_s calculation

p_{H_2}	\$1.70/kg
LHV_{H_2}	120.1 MJ/kg
η_{FC}	40%
$C_{O\&M}$	\$8/MWh (degradation rate = 2% / 1,000hrs)

the MISO grid in 2010, which means that with our assumptions the hydrogen plant owner does not have any interest in selling electricity from the fuel cells. It is different from the regulated market case, which compared the cost of generating electricity by different sources to dispatch the electricity generation among them. It was found that the LCOE for the fuel cells was lower than the LCOE for the gas turbines, allowing the fuel cells to operate up to 700 hours per year.

This conclusion is likely to change depending on the assumptions, and on the renewables penetration that changes the price profile. This is the object of the next two sections.

4.3 Sensitivity analyses

4.3.1 Cost of hydrogen

The sensitivity of the cost of hydrogen to different parameters is indicated by Figure 4-5. Four parameters are evaluated: the capital cost of the cells, the cell degradation rate, the cost of heat and the discount rate. The capital cost of the cells is the more important one, since a variation of 50% in the cost of the cells yields a variation of 19% in the final cost of hydrogen. It is worth noting that the cost of the cells affects the capital cost and the maintenance cost, because the cells must be replaced periodically due to their rapid degradation.

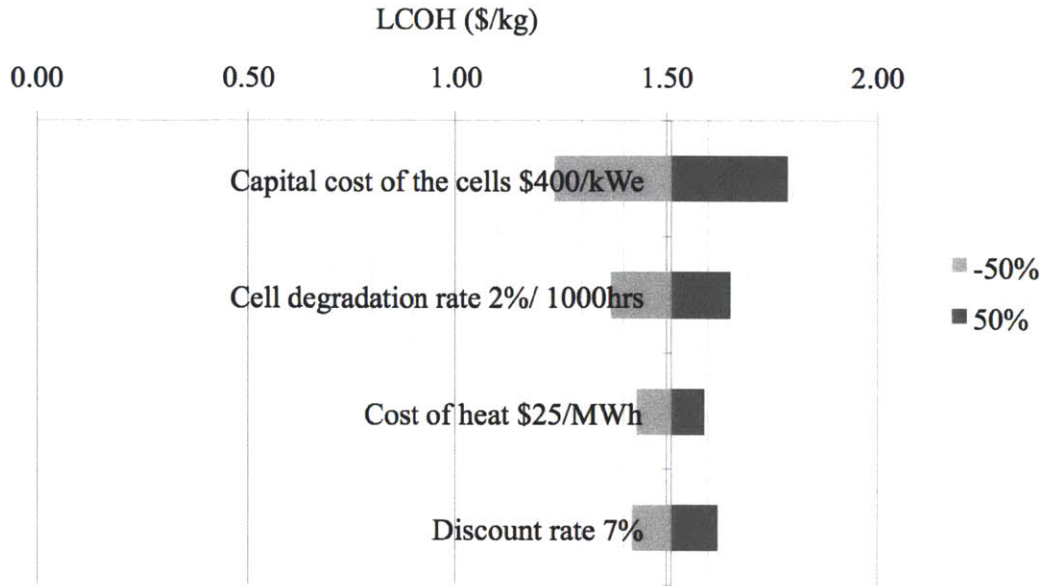


Figure 4-5: Sensitivity of the hydrogen cost to the assumptions as compared to the base case (\$1.51/kg)

4.3.2 Electricity production

The cost of the fuel cell electricity, as expressed by

$$p_s = \frac{p_{H_2}}{LHV_{H_2} \times \eta_{FC}} + C_{O\&M} \quad (4.3)$$

depends mainly on the price of hydrogen and on the fuel cell efficiency. The effect of these two parameters is plotted in Figures 4-6 and 4-7, corresponding to hydrogen prices of \$1.7 /kg and \$1.5 /kg, respectively. The cost of electricity generated is indicated as well as the subsequent operation time of the fuel cells (electricity production occurs when the cost is lower than the market price). In the first case electricity production occurs if the fuel cell efficiency is at least 55%. In the second case it occurs if it is greater than 50%.

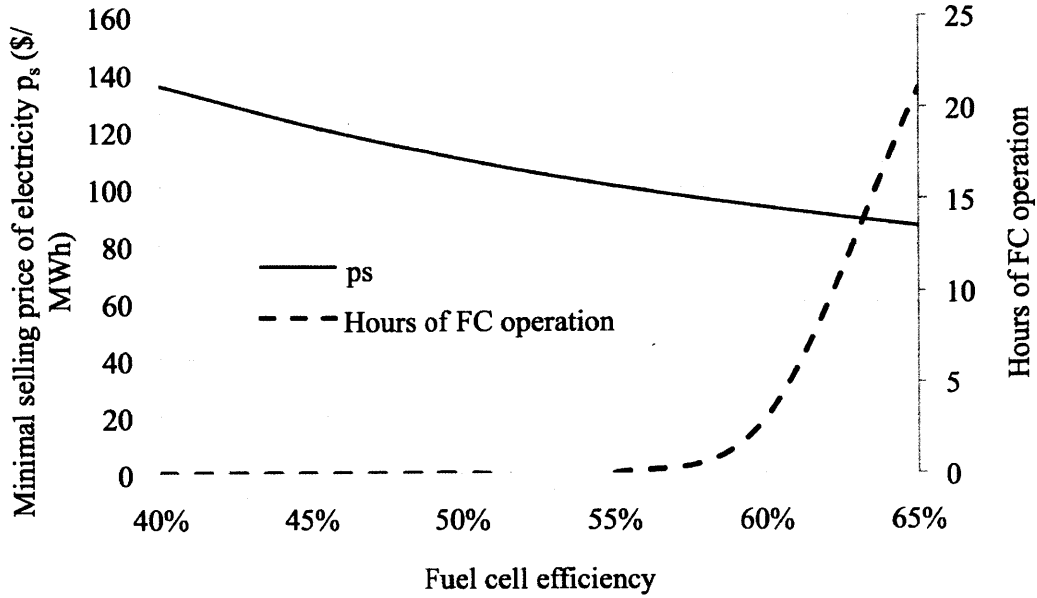


Figure 4-6: Fuel cell electricity cost and operation time for a price of hydrogen of \$1.7/kg

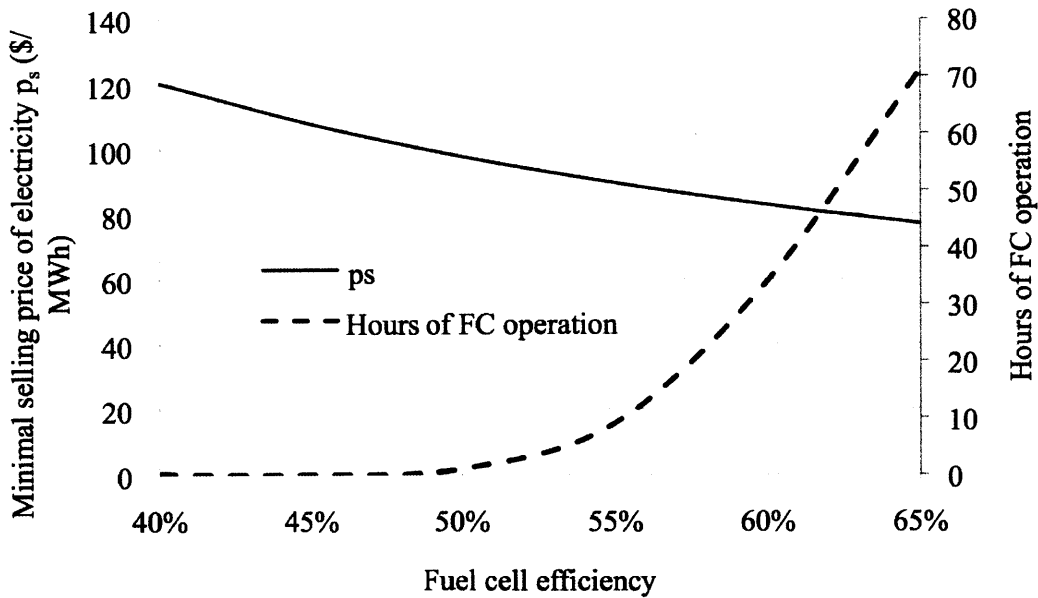


Figure 4-7: Fuel cell electricity cost and operation time for a price of hydrogen of \$1.5/kg

4.4 Perspectives

Other parameters are likely to favor the introduction of a nuclear-renewable energy system in a liberalized electricity market.

First, in a scenario where renewables replace conventional fossil fuel power plants, prices are expected to become more "peaky". During off-peak hours, the low marginal cost of renewables makes prices fall, whereas during peak hours, unpredicted unavailability of renewables makes prices rise. In short, the price becomes more volatile because of this low cost but intermittent and somehow unpredictable source of energy. This volatility makes energy storage technologies in general even more relevant, because they profit from this price difference between peak and off-peak period.

It was planned to model quantitatively the effect on prices of a large penetration of renewables in the grid, but it turned out to be a difficult task that has not been fully resolved. Indeed, it is not only the result of a demand-supply equilibrium. The real-time market has to be considered in addition to the day-ahead market, to account for the effect of unpredicted variation of wind conditions on supply.

Second, energy storage technologies can avoid having other generating units shut down and start up within short timescales, which has a big impact on the operating costs of these units. For short time periods, it is more economical to run a generating unit (typically a fossil fuel plant) at minimal power output instead of shutting it down and restarting it. An energy storage technology, by providing an extra load to the grid, would allow this operation and could be paid by the other generating units or the grid operators for this service.

It should be noted that the prices in the MISO do not reflect the startup costs. The utilities submit their bids, marginal costs and startup costs, separately, and the startup expenses are paid separately by the grid operators. As a result the situation in the US does not favor energy storage technologies, since prices do not include the startup costs, costs that are reduced by the introduction of electricity conversion and storage.

4.5 Summary

The nuclear-hydrogen energy system would be able to produce cheap hydrogen if introduced in today's MISO electricity market, at a price of \$1.5 /kg for a reasonable

HTE cell price (\$400 /kWe cell capacity). For a nuclear unit of 300 MWe, about 600,000 MT of hydrogen could be produced each year.

Today's price profile in the MISO market does not give much opportunity for the plant to generate electricity from hydrogen in fuel cells at time of peak demand. The reason is a peak price that is not high enough (overcapacity in gas turbines?). This situation could change for more efficient fuel cells (> 50%), or if prices are "favorably" modified by a large penetration of renewable capacity in the grid. Renewables are expected to increase the volatility and the variations of prices, making energy storage more relevant. A suggested future task would be to study this effect to complete this economic study in a liberalized market.

Conclusion

Hydrogen production creates synergies between nuclear and renewable energy sources in a low-carbon economy.

Nuclear and renewable energy sources alone are unable to generate power that matches the demand versus time. Nuclear power is suitable for baseload electric demand, whereas renewables have an uncontrolled and intermittent generation pattern. Capacity factors mechanically decrease with increased capacity because of excess production at time of low demand for electricity, making the costs rise. Hence future grid systems face a major challenge when they want to limit the use of fossil fuel, because the alternative technologies don't have the capacity to match electricity supply with demand at low cost.

However, the production of hydrogen, by a combination of nuclear and renewables, opens new options. Hydrogen, produced at time of low power demand, can play the role of a energy storage media for later use at time of peak power demand.

The production process involves high temperature electrolysis, a clean technology which uses heat from nuclear and electricity from the grid (nuclear and/or renewables). It has a potential for very high efficiency and good economics because in this process low cost heat partially replaces high cost electricity to split water molecules. Pressurized hydrogen can be stored on site, in a dedicated underground storage facility. It can then be used in the high temperature cells used in reverse as fuel cells to produce electricity at time of peak power demand. Or it can be shipped by pipeline to industrial markets for hydrogen, for example to refineries or ammonia plants.

An energy storage system with hydrogen is not necessarily symmetric, as are other storage devices (pumped hydro for example). There is no reason that electricity stored

from times of excess production should economically match demand when production is low. Energy storage with hydrogen is not locked into symmetric operation, because hydrogen can be sold directly on the hydrogen market if it is more economical to do so.

The nuclear-hydrogen system has unique features compared to other storage technologies. It is a large scale system, because nuclear, renewables and high temperature cells make economic sense when they are big and numerous. Underground storage and associated pipelines for hydrogen are relatively cheap (typically between \$0.2 and \$0.3 /kg hydrogen, for a 1,000 km-long pipeline), so that several months of hydrogen production can be stored on site. The response time of the cells is very short, and the hydrogen facility can switch from one mode of production to another in less than one hour. Finally the power input and output are very large compared to the size of the nuclear unit that supplies heat (see Figure 5-1). For those reasons the system has very flexible use; it can serve for seasonal storage of electricity as well as for load following on the grid.

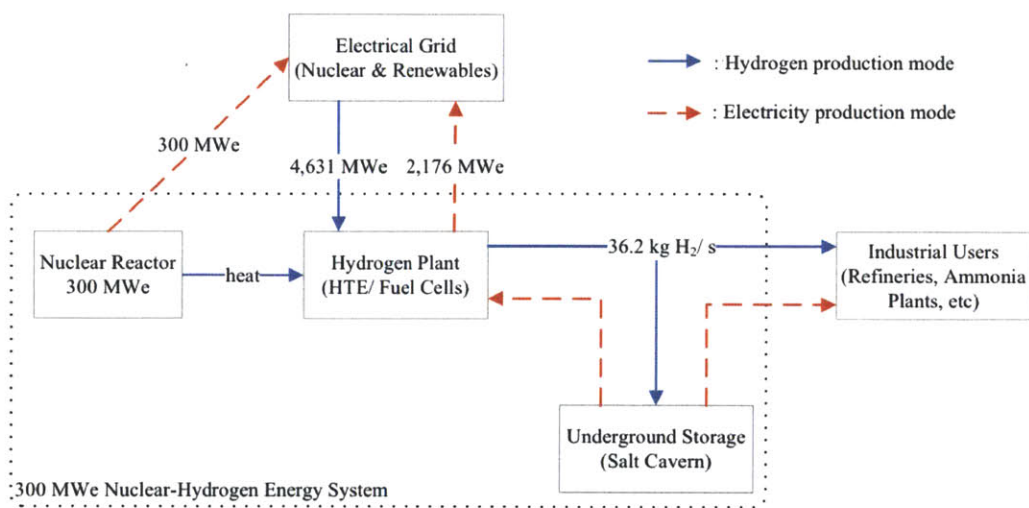


Figure 5-1: 300-MWe nuclear-hydrogen plant performance

Electricity storage enables one to fully utilize capital intensive nuclear and renewables - both with low operating costs. These are operating at their full capacities, whereas electrolysis and fuel cells are used part-time.

The techno-economic analysis performed in this thesis studied the introduction of a nuclear-renewable-hydrogen system in the Dakotas as a reference case. The Dakotas are probably the best location for on-shore wind in the United States, and present a favorable geology for underground storage of hydrogen (salt caverns). Interestingly, the Dakotas are located between Alberta (Canada) and Chicago, which are major consumption centers for hydrogen because of their petrochemical complexes. The ammonia plants of the Midwest are close as well. These concentrated production and consumption areas suit perfectly the use of pipelines to transport hydrogen at low cost.

The economic analysis was based on the calculation of the performance of the hydrogen plant, which involved a 1-D model of electrolysis cell. The entire hydrogen production plant, coupled to a PWR-type nuclear reactor, was designed and the efficiency computed. The efficiency is, as expected, very high, about 25% better than a classical water electrolysis plant.

The price of hydrogen and price of electricity produced by the system were the result of an economic analysis which determined under which conditions the system was economical. The first part of the analysis examined a future energy mix in which the shares of nuclear and wind are maximized, whereas fossil fuel use is kept as low as possible (regulated market approach). The optimization, including the introduction of the nuclear-hydrogen plant, concluded that this generation mix makes economical sense if the price of natural gas is high, around \$12-13 /MMBtu equivalent⁴, and if the wind turbine cost decreases by 33%. Interestingly, the power production by fuel cells at time of peak demand replaces gigawatts of gas turbines that would usually be used only a few hours per year and which hence would produce very expensive electricity. On the scale of the Midwest ISO grid, millions of dollars can be saved in this way per year.

The final cost of hydrogen was assessed by assuming the purchase of electricity at today's price (regulated market analysis). The production cost, \$1.5 /kg, is very

⁴includes hypothetical carbon tax

competitive because electricity is purchased at a low price at time of low demand (electricity is the major cost of hydrogen production). This cost assumes reasonable cost (\$400 / kWe installed) and performance (2% degradation per 1000 hours of operation, and efficiencies of the electrolysis and fuel cell respectively, of 90% and 50%) of the cells, goal achievable on the mid-term. The electricity produced by the fuel cell costs about \$100 / MWhe. This is high, but low enough to displace the most expensive power production units of the grid, and generate profits. The storage and pipeline transportation of hydrogen add an extra cost between \$0.2 and \$0.3 / kg hydrogen.

Future work should simulate the introduction of the system in a future deregulated market, where fossil fuel are constrained, and where competition occurs between actors. Indeed, our deregulated market analysis focused on today's MISO prices of electricity, where coal and gas represent the major sources of electricity. In a future grid with mostly nuclear and renewables, the price pattern will change and favor energy storage technologies, even more than what this thesis suggests.

Combination of nuclear with solar instead of wind could also be studied with the methodology presented in this thesis. Several other locations could be studied as well (Europe, Asia, Middle East...) and the differences evaluated to assess the most economical location for installation.

It is understood that the system might not be implemented for 10-20 years. Progress still needs to be made in high temperature electrolysis technology. However this thesis gives new and strong incentives for the development of cells that are able to operate in both directions - electrolysis as well as fuel cell mode - and under high pressure. This is the major advancement required to make the system possible - all the other technologies (nuclear, underground storage...) are proven and used worldwide. There are also significant benefits to be able to operate cells at over capacities when excess electricity is available. Once implemented this system could play a major role to help the owners and operators of electrical grids face the challenges

of carbon emission limitations and expensive fossil fuels in the mid- and long-term future.

Appendix A

MATLAB code for electrolyzer performance calculation

Thermodynamic data, taken from NIST [4]:

```
1 function [hg]=h_H(T)
2   %hydrogen gas enthalpy [kJ/kg] at T [kelvin] and 7 MPa
3
4   Tk=[200,250,300,350,400,450,500,550,600,650,700,750,800,850,900,950,
5     1000];
6   %saturation temperature in kelvin
7
8   h=[2562,3270,3990,4716,5444,6173,6901,7629,8358,9087,9818,10551,
9     11286,12023,12764,13508,14255];
10  %vapor saturation enthalpy in kJ/kg
11
12  % figure;
13  % plot(Tk,h);
14
15  if T<=1000
16    hg=interp1(Tk,h,T);
17  else
18    hg=13508+(14255-13508)*(T-950)/(1000-950);
19  end
```

```

1 function [hg]=h.HO(T)
2   %water steam enthalpy [kJ/kg] at T [kelvin] and 7 MPa
3
4   Tk=[273,323,373,423,473,500,550,558.98,559,573,623,673,723,773,823,
5       873,923,973,1023,1073,1123,1173,1223,1240,1260];
6   %saturation temperature in kelvin
7
8   h=[7,215,424,636,855,976,1220,1268,2773,2840,3017,3159,3288,3411,
9       3532,3651,3769,3888,4007,4129,4250,4373,4497,4539,4589];
10  %vapor saturation enthalpy in kJ/kg
11
12  %figure;
13  %plot(Tk,h);
14
15  if T<1200
16  hg=interp1(Tk,h,T);
17  else
18      hg=4539+(4589-4539)*(T-1240)/(1260-1240);
19  end

```

```

1 function [hg]=h.N(T)
2   %nitrogen gas enthalpy [kJ/kg] at T [kelvin] and 7 MPa
3
4   Tk=[200,250,300,350,400,450,500,550,600,650,700,750,800,850,900,950,
5       1000,1050,1100,1150,1200];
6   %saturation temperature in kelvin
7
8   h=[172,238,297,354,409,464,518,573,627,682,738,794,850,907,964,1022,
9       1081,1140,1199,1259,1319];
10  %vapor saturation enthalpy in kJ/kg
11
12  % figure;
13  % plot(Tk,h);
14

```

```

15 if T<=1200
16 hg=interp1(Tk,h,T);
17 else
18     hg=1259+(1319-1259)*(T-1150)/(1200-1150);
19 end

```

```

1 function [hg]=h_O(T)
2     %oxygen gas enthalpy [kJ/kg] at T [kelvin] and 7 MPa
3
4     Tk=[200,250,300,350,400,450,500,550,600,650,700,750,800,850,900,950,
5         1000];
6     %saturation temperature in kelvin
7
8     h=[141,203,256,307,357,407,457,507,558,609,661,714,767,820,874,928,
9         983];
10    %vapor saturation enthalpy in kJ/kg
11
12    % figure;
13    % plot(Tk,h);
14
15    if T<=1000
16    hg=interp1(Tk,h,T);
17    else
18        hg=928+(983-928)*(T-950)/(1000-950);
19    end

```

```

1 % Standard enthalpy of formation H2(g)
2 % at T (Kelvins) and 1 bar
3 % in kJ/mol
4 % from NIST WebBook
5
6 function H=Hf_H(T)
7

```

```

8  if ((T>=298)&&(T<=1100))
9
10     a=33.066178;
11     b=-11.363417;
12     c=11.432816;
13     d=-2.772874;
14     e=-0.158558;
15     f=-9.980797;
16     g=172.707974;
17     h=0;
18
19  end
20
21  if (T>1100)&&(T<2500)
22
23     a=18.563083;
24     b=12.257357;
25     c=-2.859786;
26     d=0.268238;
27     e=1.977990;
28     f=-1.147438;
29     g=156.288133;
30     h=0;
31
32  end
33
34  t=T/1000;
35  H= a*t + 0.5*b*t^2 +c*(t^3)/3 + d*(t^4)/4 - e/t + f -h;

```

```

1  % Standard enthalpy of formation H2O(g)
2  % at T (Kelvins) and 1 bar
3  % in kJ/mol
4  % from NIST WebBook
5
6  function H=Hf_H2O(T)

```

```

7
8  if (T>=500)&&(T<=1700)
9
10     a=30.09200;
11     b=6.832514;
12     c=6.793435;
13     d=-2.534480;
14     e=0.082139;
15     f=-250.8810;
16     g=223.3967;
17     h=-241.8264;
18
19  end
20
21  if (T>1700)&&(T<=6000)
22
23     a=41.96426;
24     b=8.622053;
25     c=-1.499780;
26     d=0.098119;
27     e=-11.15764;
28     f=-272.1797;
29     G=219.7809;
30     H=-241.8264;
31
32  end
33
34  t=T/1000;
35  H= a*t + 0.5*b*t^2 + c*(t^3)/3 + d*(t^4)/4 - e/t + f;

```

```

1  % Standard enthalpy of formation N2(g)
2  % at T (Kelvins) and 1 bar
3  % in kJ/mol
4  % from NIST WebBook
5

```

```

6 function H=Hf_N(T)
7
8 if (T>=100)&&(T<=500)
9
10     a=28.98641;
11     b=1.853978;
12     c=-9.647459;
13     d=16.63537;
14     e=0.000117;
15     f=-8.671914;
16     g=226.4168;
17     h=0;
18
19 end
20
21 if (T>500)&&(T<=2000)
22
23     a=19.50583;
24     b=19.88705;
25     c=-8.598535;
26     d=1.369784;
27     e=0.527601;
28     f=-4.935202;
29     g=212.3900;
30     h=0;
31
32 end
33
34 t=T/1000;
35 H= a*t + 0.5*b*t^2 +c*(t^3)/3 + d*(t^4)/4 - e/t + f -h;

```

```

1 % Standard enthalpy of formation O2(g)
2 % at T (Kelvins) and 1 bar
3 % in kJ/mol
4 % from NIST WebBook

```

```

5
6 function H=Hf_O(T)
7
8 if (T>=100) && (T<=700)
9
10     a=31.32234;
11     b=-20.23531;
12     c=57.86644;
13     d=-36.50624;
14     e=-0.007374;
15     f=-8.903471;
16     g=246.7945;
17     h=0;
18
19 end
20
21 if (T>700) && (T<=2000)
22
23     a=30.03235;
24     b=8.772972;
25     c=-3.9881133;
26     d=0.788313;
27     e=-0.741599;
28     f=-11.32468;
29     g=236.1663;
30     h=0;
31
32 end
33
34 t=T/1000;
35 H= a*t + 0.5*b*t^2 +c*(t^3)/3 + d*(t^4)/4 - e/t + f -h;

```

```

1 % Standard entropy of formation H2(g)
2 % at T (Kelvins) and 1 bar
3 % in J/(mol.K)

```

```

4 % from NIST WebBook
5
6 function S=Sf_H(T)
7
8 if (T≥298)&&(T≤1100)
9
10     a=33.066178;
11     b=-11.363417;
12     c=11.432816;
13     d=-2.772874;
14     e=-0.158558;
15     f=-9.980797;
16     g=172.707974;
17     h=0;
18
19 end
20
21 if (T>1100)&&(T≤2500)
22
23     a=18.563083;
24     b=12.257357;
25     c=-2.859786;
26     d=0.268238;
27     e=1.977990;
28     f=-1.147438;
29     g=156.288133;
30     h=0;
31
32 end
33
34 t=T/1000;
35 S= a*log(t) + b*t +c*(t^2)/2 + d*(t^3)/3 - e/(2*t^2) + g;

```

```

1 % Standard entropy of formation H2O(g)
2 % at T (Kelvins) and 1 bar

```

```

3 % in J/(mol.K)
4 % from NIST WebBook
5
6 function S=Sf.H2O(T)
7
8 if (T>=500)&&(T<=1700)
9
10     a=30.09200;
11     b=6.832514;
12     c=6.793435;
13     d=-2.534480;
14     e=0.082139;
15     f=-250.8810;
16     g=223.3967;
17     h=-241.8264;
18
19 end
20
21 if (T>1700)&&(T<=6000)
22
23     a=41.96426;
24     b=8.622053;
25     c=-1.499780;
26     d=0.098119;
27     e=-11.15764;
28     f=-272.1797;
29     g=219.7809;
30     h=-241.8264;
31
32 end
33
34
35 t=T/1000;
36 S= a*log(t) + b*t +c*(t^2)/2 + d*(t^3)/3 - e/(2*t^2) + g;

```

```

1  % Standard entropy of formation O2(g)
2  % at T (Kelvins) and 1 bar
3  % in J/(mol.K)
4  % from NIST WebBook
5
6  function S=Sf_O(T)
7
8  if (T≥100)&&(T≤700)
9
10     a=31.32234;
11     b=-20.23531;
12     c=57.86644;
13     d=-36.50624;
14     e=-0.007374;
15     f=-8.903471;
16     g=246.7945;
17     h=0;
18
19 end
20
21 if (T>700)&&(T≤2000)
22
23     a=30.03235;
24     b=8.772972;
25     c=-3.9881133;
26     d=0.788313;
27     e=-0.741599;
28     f=-11.32468;
29     g=236.1663;
30     h=0;
31
32 end
33
34 t=T/1000;
35 S= a*log(t) + b*t +c*(t^2)/2 + d*(t^3)/3 - e/(2*t^2) + g;

```

Derivation of the Gibbs free energy of formation of hydrogen:

```
1 % Standard Gibbs free energy of formation H2O(g)=>H2(g)+0.5*O2(g)
2 % at T (Kelvins) and 1 bar
3 % in kJ/mol
4 % from NIST WebBook
5
6 function G=DeltaR0_G(T)
7
8 G = 1*(Hf_H(T) - T*Sf_H(T)/1000)...
9     + 0.5*(Hf_O(T) - T*Sf_O(T)/1000)...
10    - 1*(Hf_H2O(T) - T*Sf_H2O(T)/1000);
```

Calculation of the enthalpy change across the cell:

```
1 % Gives the change in enthalpy carried by the species along the cell
2 %
3 % in J/sec
4 % T in kelvin
5 % Beware the units!!
6 %
7 % Ntot_St is the total molar flow rate (including any inert gas ...
   flows) per
8 % cell on the CO2/steam side in mol/s
9 % Ntot_airIn is the total molar flow rate (including any inert ...
   gas flows) per
10 % cell on the air sweep side in mol/s
11 %
12 % yH refers to H2
13 % yHO refers to H2O
14 % yN refers to N2
15 % yO refers to the molar fraction of O2 on the air sweep side
16 % 1 refers to pre-eletrolysis, equilibrium values (calculated before)
17 % 2 refers to post-eletrolysis, equilibrium values at T2
18
```

```

19 function En=H_prodI(Tin,Tout, i, Ntot_St, Ntot_airIn, yH1, yHO1 , ...
    yO1, yN1)
20
21 AreaOfCell = 225; % cm2
22 F=96485.3399; % Faraday constant (C/mol)
23
24 DeltaNO = i*AreaOfCell/(4*F);
25 yO2 = (yO1 + DeltaNO/Ntot_airIn)/(1+DeltaNO/Ntot_airIn);
26
27
28 Res= PostElecMolFrac(i,Ntot_St,yH1, yHO1);
29 yH2=Res(1);
30 yHO2=Res(2);
31
32 % The total molar flow rate is not modified in the CO2/steam side
33 % For the air sweep side:
34 Ntot_airOut = Ntot_airIn + DeltaNO;
35
36
37 % Hf free enthalpy of formation at T(K) , in kJ/mol
38 En= Ntot_St*(yH2*(Hf_H(Tout)) + yHO2*(Hf_H2O(Tout)) + ...
    yN1*(Hf_N(Tout)) )+...
39     -Ntot_St*(yH1*(Hf_H(Tin)) + yHO1*(Hf_H2O(Tin))+ ...
    yN1*(Hf_N(Tin)))+...
40     -Ntot_airIn*(yO1*(Hf_O(Tin)) +(1-yO1)*(Hf_N(Tin)))+...
41     Ntot_airOut*(yO2*(Hf_O(Tout)) + (1-yO2)*(Hf_N(Tout)));
42
43 En=En*1000; % to get the result in J/sec

```

Calculation of the point Nernst potential:

```

1 % Nernst Potential
2 % for T (Kelvin) and P (MPa)
3 % y mole fraction of H2, O2, H2O
4 % Result in volts

```

```

5
6 function V=V_nernst(T,P,yH,yO,yHO)
7
8 F=96485.3399; % Faraday constant (C/mol)
9 R= 8.314472; % Gas Constant (J/(K.mol))
10
11 V= (1000*DeltaR0_G(T)-R*T*log( ...
      (yHO/(yH*sqrt(yO)*sqrt(P/0.1)))))/(2*F);

```

Calculation of the integrated Nernst potential:

```

1 % V_nernst integrated over the cell
2 % for T (Kelvin) and P (MPa)
3 % y mole fraction of H2, O2, H2O
4 % Result in volts
5
6 function V=V_nernst_Int(Tin,Tout,P, yH1, yH2 , yO1, yO2, yHO1, yHO2)
7
8 % be careful of the units!
9
10 F=96485.3399; % Faraday constant (C/mol)
11 R= 8.314472; % Gas Constant (J/(K.mol))
12 L=0.15;
13
14 ΔX=0.001;
15
16 % yO depends on the inlet mass flow rate
17
18 X=0:ΔX:L;
19 yH=yH1+(yH2-yH1)*X/L;
20 yO=yO1+(yO2-yO1)*X/L;
21 yHO=yHO1-(yHO2-yHO1)*X/L;
22 T=Tin+(Tout-Tin)*X/L;
23
24 V=0;

```

```

25
26 for k=1:length(X)
27     V= V+ΔX*(V_nernst (T(k),P,yH(k),yO(k),yHO(k)));
28 end
29
30 V=V/L;

```

Calculation of the point operating potential (for reference):

```

1 % V_op
2 % for T (Kelvin) and i (A/cm2)
3 % Tin and Tout inlet and outlet temperature of the electrolyzer
4 % Result in volts
5 % ASR is the Area Specific Value of the cell (A.cm2)
6 % P pressure in MPa
7 % Ntot_St is the total molar flow rate (including any inert gas ...
   flows) per
8 % cell on the CO2/steam side (mol/s)
9 %
10 % yH refers to H2
11 % yHO refers to H2O
12 % yO refers to the molar fraction of O2 on the air sweep side
13 % 1 refers to pre-eletrolysis values at Tin
14 % 2 refers to post-eletrolysis values at Tout
15 %
16 % Ntot_airIn is the total molar flow rate (including any inert ...
   gas flows) per
17 % cell on the air sweep side (mol/sec)
18
19 function V=V_op.Eq(Tin,Tout,ASR, i,P, Ntot_St, Ntot_airIn, yH1, ...
   yHO1 , yO1)
20
21 AreaOfCell = 225; % cm2
22 F=96485.3399; % Faraday constant (C/mol)
23

```

```

24 DeltaNO = i*AreaOfCell/(4*F);
25 yO2 = (yO1 + DeltaNO/Ntot_airIn)/(1+DeltaNO/Ntot_airIn);
26
27 Res= PostElecMolFrac(i,Ntot_St,yH1, yHO1);
28
29 yH2=Res(1);
30 yHO2=Res(2);
31
32
33 V = V_op(Tin,Tout,ASR, i,P, yH1, yH2 , yO1, yO2, yHO1, yHO2);

```

Calculation of the integrated operating potential:

```

1 % V_op
2 % for T (Kelvin) and i (A/cm2)
3 % Tin and Tout inlet and outlet temperature of the electrolyzer
4 % Result in volts
5 % ASR is the Area Specific Value of the cell (A.cm2)
6 % P pressure in MPa
7
8 function V=V_op(Tin,Tout,ASR, i,P, yH1, yH2 , yO1, yO2, yHO1, yHO2)
9
10 L=0.15; % cm
11
12 Vasr=0;
13 ΔX=0.001;
14
15 X=0:ΔX:0.15;
16 T=Tin+(Tout-Tin)*X/L;
17
18 for k=1:length(X)
19     Vasr= Vasr+ΔX*(ASR - 0.463 + 3.973*(10^(-5))*exp(10300/T(k)));
20 end
21 Vasr=Vasr/L;
22

```

```

23 V= V_nernst_Int(Tin,Tout,P, yH1, yH2 , yO1, yO2, yHO1, yHO2) + ...
    i*Vasr;

```

Main calculation of V_{op} and T_{out} for the cell. The methodology is an iterative process which asks a guess for T_{out} at the first iteration.

```

1  % gives the operating voltage and the outlet temperature for one ...
    cell
2  %
3  % Tin inlet temperature (K)
4  % guess: guess for outlet temperature (K)
5  % i current density (A/cm2) ; requires 4 significant digits!!
6  %
7  % Ntot_St is the total molar flow rate (including any inert gas ...
    flows) per
8  % cell on the CO2/steam side in mol/s
9  % Ntot_airIn is the total molar flow rate (including any inert ...
    gas flows) per
10 % cell on the air sweep side in mol/s
11 %
12 % yH refers to H2
13 % yHO refers to H2O
14 % yN refers to N2
15 % yO refers to the molar fraction of O2 on the air sweep side
16 % 1 refers to pre-eletrolysis, equilibrium values (calculated before)
17 % 2 refers to post-eletrolysis, equilibrium values at T2
18
19 function ...
    Res=convi(Tin,guess,ASR,i,P,Ntot_St,Ntot_airIn,yH1,yHO1,yO1,yN1)
20
21 AreaOfCell = 225; % cm2
22 F=96485.3399; % Faraday constant (C/mol)
23
24 I=i*AreaOfCell;

```

```

25 W=V_op_Eq(Tin,guess,ASR, i,P, Ntot_St, Ntot_airIn, yH1, yHO1 , ...
    yO1)*I;
26 % electrical power supplied in watt per cell
27
28 H=H_prodI(Tin,guess, i, Ntot_St, Ntot_airIn, yH1, yHO1 , yO1, yN1);
29 % in J/sec
30
31 h=0.5; % temperature step in K
32
33  $\Delta=(H-W)/H$ ;
34
35 % convergence criteria 1%
36 while  $\Delta^2>0.005^2$ 
37      $\Delta_1=V\_op\_Eq(Tin,guess+h,ASR, i,P, Ntot\_St, Ntot\_airIn, yH1, \dots$ 
        yHO1 , yO1)*I-...
38     H_prodI(Tin,guess+h, i, Ntot_St, Ntot_airIn, yH1, yHO1 , ...
        yO1, yN1);
39      $\Delta_2=V\_op\_Eq(Tin,guess-h,ASR, i,P, Ntot\_St, Ntot\_airIn, yH1, \dots$ 
        yHO1 , yO1)*I-...
40     H_prodI(Tin,guess-h, i, Ntot_St, Ntot_airIn, yH1, yHO1 , ...
        yO1, yN1);
41     if  $\Delta_1^2<\Delta_2^2$ 
42          $\Delta=\Delta_1/H\_prodI(Tin,guess+h, i, Ntot\_St, Ntot\_airIn, yH1, \dots$ 
            yHO1 , yO1, yN1);
43         guess=guess+h;
44     else
45          $\Delta=\Delta_2/H\_prodI(Tin,guess-h, i, Ntot\_St, Ntot\_airIn, yH1, \dots$ 
            yHO1 , yO1, yN1);
46         guess=guess-h;
47     end
48
49 end
50
51 V=V_op_Eq(Tin,guess,ASR, i,P, Ntot_St, Ntot_airIn, yH1, yHO1 , yO1);
52
53 Tout=guess;

```

54

```
55 Res=[V,Tout]; % T outlet (K) and Operating Voltage
```

Calculation of the new molar fraction after electrolysis:

```
1 % Mole fractions of the two species after the electrolysis on ...
   the steam/H2
2 % side of the electrolyzer
3 %
4 % i is the current density (A/cm2)
5 % yH refers to H2
6 % yHO refers to H2O
7 % 1 refers to pre-electrolysis, equilibrium values (calculated before)
8 % 2 refers to post-electrolysis, equilibrium values at T2
9 % T is the electrolyzer inlet temperature in Kelvin
10 % Ntot is the total molar flow rate (including any inert gas ...
    flows) per
11 % cell on the CO2/steam side in mol/s
12
13
14 function Res = PostElecMolFrac(i,Ntot,yH1,yHO1)
15
16 AreaOfCell = 225; % cm2
17 F=96485.3399; % Faraday constant (C/mol)
18
19 DeltaNO = i*AreaOfCell/(4*F); % moles of O2 produced by electrolysis
20 DeltaNH = i*AreaOfCell/(2*F); % moles of H2 produced by electrolysis
21
22 yH2=yH1+DeltaNH/Ntot;
23 yHO2=yHO1-2*DeltaNO/Ntot;
24
25 Res = [yH2,yHO2];
```

This is the main code that should be run by the user:

```

1 % Main function for High Temperature Steam Electrolysis calculations
2 %
3 % Tin      : Electrolyzer inlet temperature (K)
4 % Tout_guess : guess for outlet temperature (K)
5 % ASR      : Area Specific Resistance (A.cm2)
6 % i        : current density (A/cm2) per cell
7 % The cell has an area of 225cm2
8 %
9 % Ntot_St   : total molar flow rate (including any inert gas ...
      flows) per
10 %           cell on the CO2/steam side (mol/s)
11 % Ntot_airIn : total molar flow rate (including any inert gas ...
      flows) per
12 %           cell on the air sweep (mol/s)
13 %
14 % Molar fractions:
15 % yH refers to H2
16 % yHO refers to H2O
17 % yN refers to N2
18 % yO refers to the molar fraction of O2 on the air sweep side
19 % 1 refers to pre-eletrolysis, equilibrium values (calculated before)
20 % 2 refers to post-eletrolysis, equilibrium values at T2
21
22 function ...
      HTSE_OneCell(Tin,Tout_guess,ASR,i,P,Ntot_St,Ntot_airIn,yH1,yHO1,
23      yO1,yN1)
24
25 AreaOfCell = 225; % cm2
26 F=96485.3399; % Faraday constant (C/mol)
27
28 if (Ntot_St*(yHO1))<(2*i*AreaOfCell/(4*F))
29     disp(' ');
30     disp('Oxygen starvation. Please increase oxygen atoms in ...
      input streams or reduce current density');
31     return
32 end

```

```

33
34 if (yH1+yHO1+yN1)≠1
35     disp(' ');
36     resp = input('Sum of the molar fractions non equal to 1. Lets ...
                 normalize? (yes type 1) ');
37     if resp== 1
38         ntot=yH1+yHO1;
39         yH1=yH1/ntot;
40         yHO1=yHO1/ntot;
41         yN1=yN1/ntot;
42         disp(' ');
43     else return
44     end
45 end
46
47 Res1=PostElecMolFrac(i,Ntot_St,yH1,yHO1);
48 yH2=Res1(1);
49 yHO2=Res1(2);
50
51
52 Res2=convi(Tin,Tout_guess,ASR,i,P,Ntot_St,Ntot_airIn,yH1,yHO1,yO1,
53           yN1);
54
55 Vop=Res2(1);
56 Tout=Res2(2);
57
58 DeltaNO = i*AreaOfCell/(4*F);
59 Ntot_airOut = Ntot_airIn + DeltaNO;
60 yO2 = (yO1 + DeltaNO/Ntot_airIn)/(1+DeltaNO/Ntot_airIn);
61
62 disp(' ');
63 disp('---RESULTS---');
64 disp(' ');
65 disp(' ');
66 disp(['Electrolyzer inlet temperature: ', num2str(Tin), ' K']);
67 disp(['Electrolyzer outlet temperature: ', num2str(Tout), ' K']);

```

```

68 disp(' ');
69 disp(['Cell operating voltage : ', num2str(Vop) , ' V']);
70 disp(['Cell current density : ', num2str(i) , ' A/cm2']);
71 disp(['Area of cell : ', num2str(AreaOfCell) , ' cm2']);
72 disp(['Cell power requirement : ', num2str(Vop*225*i) , ' W']);
73 disp(' ');
74 disp(' H2/Steam stream');
75 disp(' Electrolyzer inlet');
76 disp([' Molar flow rate at the inlet: ', num2str(Ntot_St), ' ...
mol/s']);
77 disp(' Molar fraction at the inlet for ');
78 disp([' H2: ', num2str(yH1)]);
79 disp([' H2O: ', num2str(yHO1)]);
80 disp([' N2: ', num2str(yN1)]);
81 disp(' Electrolyzer outlet');
82 disp([' Molar flow rate at the outlet: ', num2str(Ntot_St), ' ...
mol/s']);
83 disp(' Molar fraction at the outlet for ');
84 disp([' H2: ', num2str(yH2)]);
85 disp([' H2O: ', num2str(yHO2)]);
86 disp([' N2: ', num2str(yN1)]);
87 disp(' ');
88 disp(' Air stream');
89 disp(' Electrolyzer inlet');
90 disp([' Molar flow rate at the inlet: ', num2str(Ntot_airIn), ...
' mol/s']);
91 disp(' Molar fraction at the outlet for ');
92 disp([' O2: ', num2str(yO1)]);
93 disp([' N2: ', num2str(1-yO1)]);
94 disp(' Electrolyzer outlet');
95 disp([' Molar flow rate at the outlet: ', ...
num2str(Ntot_airOut), ' mol/s']);
96 disp(' Molar fraction at the outlet for ');
97 disp([' O2: ', num2str(yO2)]);
98 disp([' N2: ', num2str(1-yO2)]);

```

And below, a more user-friendly code to be run by the user, which asks for the desired inputs:

```

1 % Main function for HTSE calculations
2 %
3 % Tin      : Electrolyzer inlet temperature (K)
4 % Tout_guess : guess for outlet temperature (K)
5 % ASR      : Area Specific Resistance (A.cm2)
6 % i        : current density (A/cm2) per cell
7 % The cell has an area of 225cm2
8 %
9 % Ntot_St   : total molar flow rate (including any inert gas ...
      flows) per
10 %           cell on the CO2/steam side (mol/s)
11 % Ntot_airIn : total molar flow rate (including any inert gas ...
      flows) per
12 %           cell on the air sweep (mol/s)
13 %
14 % Molar fractions:
15 % yH refers to H2
16 % yHO refers to H2O
17 % yN refers to N2
18 % yO refers to the molar fraction of O2 on the air sweep side
19 % 1 refers to pre-eletrolysis, equilibrium values (calculated before)
20 % 2 refers to post-eletrolysis, equilibrium values at T2
21
22 function HTSE_OneCell_Fancy
23
24 Tin = input('Electrolyzer inlet temperature (K): ');
25 Tout_guess = input('Guess for electrolyzer outlet temperature ...
      (K): ');
26 ASR = input('ASR (Ohm.cm2): ');
27 disp('Cell area (cm2): 225');
28 i = input('Cell current density i (A/cm2): ');
29 P = input('Pressure (MPa): ');

```

```
30 Ntot_St = input('Total molar flow rate on H2/steam side (mol/s): ');
31 yH1 = input('Initial molar fraction of H2: ');
32 yHO1 = input('Initial molar fraction of H2O (steam): ');
33 yN1 = input('Initial molar fraction of N2: ');
34 Ntot_airIn = input('Total molar flow rate on air sweep side ...
    (mol/s): ');
35 yO1 = input('Initial molar fraction of O2 on air sweep aide: ');
36
37
38 HTSE_OneCell(Tin, Tout_guess, ASR, i, P, Ntot_St, Ntot_airIn, yH1, yHO1, yO1,
39     yN1)
```


Appendix B

Statoil alkaline electrolyzers

Statoil (who merged with Norsk Hydro in 2007), is a manufacturer of alkaline electrolyzers for industry. It is the leader in the fabrication of large generation units of hydrogen from electricity.

The largest product sold by this company has the following features [16].

- Hydrogen production rate: $485 \text{ Nm}^3/\text{h}$ ($1046\text{kg}/\text{day}$)
- Works at atmospheric pressure, but pressurized electrolyzers are under development
- Electric consumption: $4.3 \text{ kWh}/\text{Nm}^3$ (hence 2.086 MW electric consumption at maximal production rate)
- Floor area: $4 \times 13.5 \text{ m}^2$
- Variability of production from 20% to 100%
- Overhaul every 7 to 10 years

The electricity-to-hydrogen efficiency of such electrolyzer is then 70%.

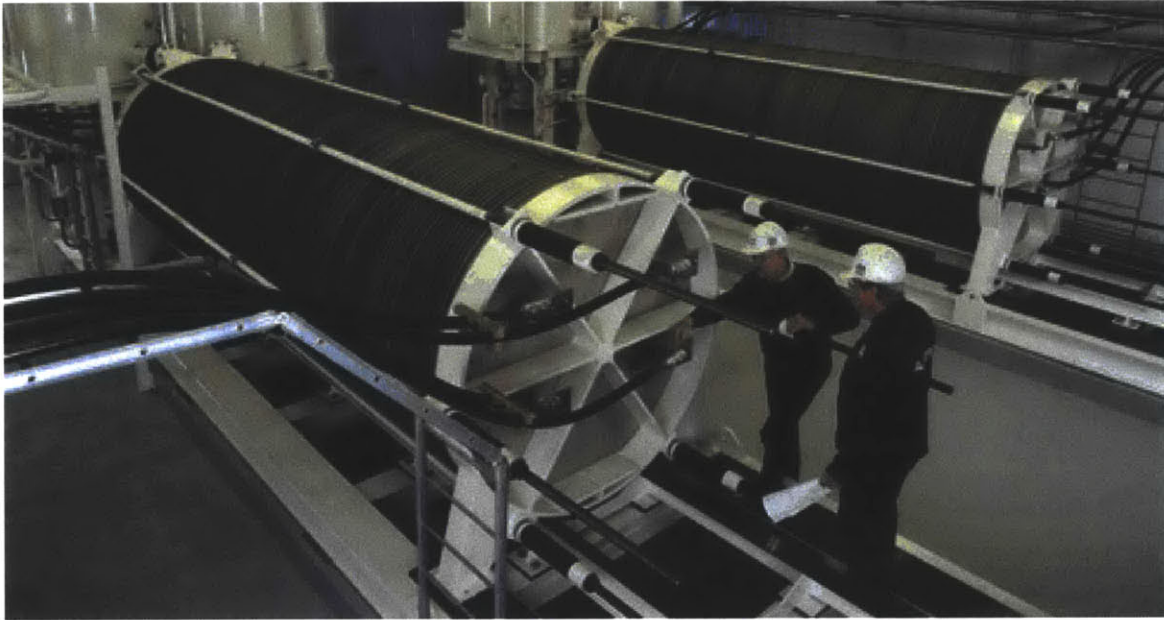


Figure B-1: Statoil alkaline electrolyzer (courtesy of Statoil Hydrogen)

References and Bibliography

- [1] Cooling water issues and opportunities at u.s. nuclear power plants. Technical Report INL/EXT-10-20208, Idaho National Laboratory, December 2010.
- [2] Integrating renewable electricity on the grid. Technical report, American Physical Society Panel on Public Affairs, 2010.
- [3] Elmar Achenbach. Response of a solid oxide fuel cell to load change. *Journal of Power Sources*, 57(1-2):105 – 109, 1995.
- [4] NIST chemistry webbook. <http://webbook.nist.gov/chemistry/>.
- [5] Federal Energy Regulatory Commission. Electric power markets - Midwest. <http://www.ferc.gov/market-oversight/mkt-electric/midwest.asp>, 2010.
- [6] Charles W. Forsberg. Future hydrogen markets for large-scale hydrogen production systems. *International Journal of Hydrogen Energy*, 32, 2007.
- [7] M. J. Gradassi. Economics of gas-to-liquids manufacture. In *2nd International Conference on Refinery Processing*, Houston, TX, June 26-30 1999. American Institute of Chemical Engineers.
- [8] Jean-Pierre Hansen. *Introduction a l'economie de l'energie (Introduction to energy economics)*. Ecole Polytechnique, 2009.
- [9] Geoffrey Haratyk and Charles W. Forsberg. Nuclear-renewables energy system for hydrogen and electricity production. *Nuclear Technology*, accepted for publication.
- [10] Geoffrey Haratyk and Charles W. Forsberg. Integrating nuclear and renewables for hydrogen and electricity production. In *ANS summer meeting*, San Diego, CA, June 13-18 2010.
- [11] Geoffrey Haratyk and Charles W. Forsberg. Incentives for reversible hydrogen electrolyzer-fuel cells for peak electricity. In *ANS summer meeting*, Hollywood, FL, June 26-30 2011.
- [12] E. A. Harvego. Private communication, June 2010.

- [13] E. A. Harvego, M.G. McKellar, M. S. Sohal, J. E. O'Brien, and J.S. Herring. System evaluation and economic analysis of a nuclear reactor powered high-temperature electrolysis hydrogen-production plant. *Journal of Energy Resource Technology*, 132(2):76, 2010.
- [14] A. Hauch, S. H. Jensen, S. D. Ebbesen, and M. Mogensen. Durability of solid oxide electrolysis cells for hydrogen production. In *Risø International Energy Conference*, pages 327–338, Roskilde (Denmark), May 22-24 2007.
- [15] J. Stephen Herring, James E. O'Brien, Carl M. Stoots, G.L. Hawkes, Joseph J. Hartvigsen, and Mehrdad Shahnam. Progress in high-temperature electrolysis for hydrogen production using planar SOFC technology. *International Journal of Hydrogen Energy*, 32(4):440 – 450, 2007.
- [16] Statoil Hydrogen. www3.statoil.com/hydrogentechnologies/svg03816.nsf.
- [17] Minnkota Power Cooperative Inc. Infinity hourly historical outputs. www.minnkota.com, 2009.
- [18] Sren Hjgaard Jensen, Xiufu Sun, Sune Dalgaard Ebbesen, Ruth Knibbe, and Mogens Mogensen. Hydrogen and synthetic fuel production using pressurized solid oxide electrolysis cells. *International Journal of Hydrogen Energy*, 35(18):9544 – 9549, 2010.
- [19] J. D. Jorgenson. *2008 Minerals Yearbook: Iron Ore*. U.S. Geological Survey, 2010.
- [20] R. Knibbe, M. L. Traulsen, S. D. Ebbesen, and M. Mogensen. Solid oxide electrolysis cells: degradation at high current densities. *Journal of the electrochemical society*, 2010.
- [21] Ruth Knibbe, Marie Lund Traulsen, Anne Hauch, Sune Dalgaard Ebbesen, and Mogens Mogensen. Solid oxide electrolysis cells: Degradation at high current densities. *Journal of The Electrochemical Society*, 157(8):1209 – 1217, 2010.
- [22] W. Leighty. Running the world on renewables: Hydrogen transmission pipelines and firming geologic storage. *International Journal of Energy Research*, 32(5):408–426, 2008.
- [23] Gilbert N. Lewis and Ronald T. Macdonald. Concentration of H² isotope. *Journal of Chemical Physics*, June 1933.
- [24] K. Maize and R. Peltier. The U.S. gas rebound. *Power Magazine*, January 2010.
- [25] A.I. Miller and Romney B. Duffey. Sustainable and economic hydrogen co-generation from nuclear energy in competitive power markets. June 24-26 2003.
- [26] MIT. *The future of natural gas - An interdisciplinary MIT study*. 2010.

- [27] John C. Molburg and Richard D. Doctor. Hydrogen from steam-methane reforming with CO₂ capture. In *20th annual international Pittsburgh coal conference*, Pittsburgh, PA, September 15-19 2003.
- [28] OECD/IEA/NEA. *Projected costs of generating electricity - 2010 edition*. 2010.
- [29] Midwest Independent System Operator. Market reports. www.midwestmarket.org/home/, 2009.
- [30] J. E. OBrien, M. G. McKellar, C. M. Stoots, G. L. Hawkes, and J. S. Herring. Analysis of commercial-scale implementation of HTE to oil sands recovery. Technical report, Idaho National Laboratory, September 2006.
- [31] J. E. OBrien, C. M. Stoots, J. S. Herring, M. G. McKellar, E. A. Harvego, M. S. Sohal, and K. G. Condie. High temperature electrolysis for hydrogen production from nuclear energy - technology summary. Technical Report INL/EXT-09-16140, Idaho National Laboratory, February 2010.
- [32] R. Rivera-Tinocco, C. Mansilla, C. Bouallou, and F. Werkoff. Hydrogen production by high temperature electrolysis coupled with an EPR, SFR or HTR: techno-economic study and coupling possibilities. 1(3), 2008.
- [33] B. Roberts. Capturing grid power. *Power and Energy Magazine, IEEE*, 7(4):32-41, 2009.
- [34] M. S. Sohal, J. E. OBrien, C. M. Stoots, J. S. Herring, J. J. Hartvigsen, D. Larsen, S. Elangovan, J. D. Carter, V. I. Sharma, and B. Yildiz. Critical causes of degradation in integrated laboratory scale cells during high-temperature electrolysis. Technical Report INL/EXT-09-16004, Idaho National Laboratory, May 2009.
- [35] J. W. Tester, E. M. Drake, M. J. Driscoll, M. W. Golay, and William A. Peters. *Sustainable energy: choosing among options*. MIT press, 2005.
- [36] Bilge Yildiz and Mujid S. Kazimi. Efficiency of hydrogen production systems using alternative nuclear energy technologies. *International Journal of Hydrogen Energy*, 31(1):77 - 92, 2006.